Aston University

If you have discovered material in AURA which is unlawful e.g. breaches copyright, (either yours or that of a third party) or any other law, including but not limited to those relating to patent, trademark, confidentiality, data protection, obscenity, defamation, libel, then please read our Takedown Policy and contact the service immediately

GENETIC AND ENVIRONMENTALLY DERIVED VARIATION IN THE CELL WALL COMPOSITION OF *MISCANTHUS* AND IMPLICATIONS FOR THERMO-CHEMICAL CONVERSION

Edward Matthew Hodgson

Doctor of Philosophy

Aston University

December 2008

This copy of the thesis has been supplied on the condition that anyone who consults it is understood to recognise that its copyright rests with its author and that no quotation from the thesis and no information derived from it may be published without proper acknowledgement.

Aston University

GENETIC AND ENVIRONMENTALLY DERIVED VARIATION IN THE CELL WALL COMPOSITION OF *MISCANTHUS* AND IMPLICATIONS FOR THERMO-CHEMICAL CONVERSION

Edward Matthew Hodgson

Doctor of Philosophy

December 2008

THESIS SUMMARY

Fifteen *Miscanthus* genotypes grown in five locations across Europe were analysed to investigate the influence of genetic and environmental factors on cell wall composition. Chemometric techniques combining near infrared reflectance spectroscopy (NIRS) and conventional chemical analyses were used to construct calibration models for determination of acid detergent lignin (ADL), acid detergent fibre (ADF), and neutral detergent fibre (NDF) from sample spectra. The developed equations were shown to predict cell wall components with a good degree of accuracy and significant genetic and environmental variation was identified. The influence of nitrogen and potassium fertiliser on the dry matter yield and cell wall composition of *M. x giganteus* was investigated. A detrimental affect on feedstock quality was observed to result from application of these inputs which resulted in an overall reduction in concentrations of cell wall components and increased accumulation of ash within the biomass.

Pyrolysis-gas chromatography-mass spectrometry (Py-GC-MS) and thermo-gravimetric analysis (TGA) and was used to further characterise feedstock properties and compositional differences between *Miscanthus* genotypes and significant genotypic differences were observed. This indicates that genotypes other than the commercially cultivated *M. x giganteus* have potential for use in energy conversion processes and in the bio-refining of chemicals. *Miscanthus* biomass appeared to provide a good feedstock for fast-pyrolysis. The yields and quality parameters of the pyrolysis liquids produced from *Miscanthus* compared favourably with that produced from SRC willow and produced a more stable pyrolysis liquid with a higher lower heating value (LHV). Heating value and stability of pyrolysis liquids was observed to be more influenced by ash concentration than lignin. Overall, genotype had a more significant effect on cell wall composition than environment. This indicates good potential for dissection of this trait by QTL analysis and also for plant breeding to produce new genotypes with improved feedstock characteristics for energy conversion.

Keywords: Lignocellulosic; Biomass; NIRS; Fast-pyrolysis; Bio-oil.

This thesis is dedicated to the memory of

Dr John Hastie

and

Mr James Daley

"Your memory remains undiluted and your influence still strong,

but your presence has been sorely missed

in the days that you've been gone."

ACKNOWLEDGEMENTS

I would like to acknowledge and thank my supervisors Dr Iain Donnison, Professor Tony Bridgwater, and Dr John Clifton-Brown for their advice and support throughout the project.

Particular acknowledgement should be made to those people involved in the European Miscanthus Improvement (EMI) project without whom this research would not have been possible: Lewandowski, I.; Clifton-Brown, J. C.; Andersson, B.; Basch, G.; Christian, D. C.; Jorgensen, U.; Jones, M. B.; Riche, A. B.; Schwarz, K. U.; Tayebi, K.; Teixeira, F.; Kjeldsen, J. B.; Mortensen, J. V.; Riche, A. B.

I would also like to thank the members of the SUPERGEN bioenergy consortium and members of the Institute of Grassland and Environmental Research for their council and support throughout the project: Bio-Energy Research Group, Aston University: Dr Romani Fahmi, Dr Daniel Nowakowski, Jurgen Sitzman, Miss Emma Wylde, Dr Guozhan Jiang, Dr Elma Gyftopoulou, Miss Emily Wakefield, and Mr Rob Fenton. Rothamsted Research, Harpenden: Dr Iain Shield, Mrs Nicola Yates, Mr Andrew Riche, and Mr Tim Barraclough. Leeds University: Professor Jenny Jones, Dr Toby Bridgman, Professor Alan Williams, and Dr Andrew Ross. Institute of Grassland and Environmental Research*, Aberystwyth: Dr Jessica Adams, Dr Rob Hatch, Dr Kerrie Farrar, Dr David Bryant, Dr Steve Bowra, Dr Sue Lister, Miss Ruth Sanderson, Dr Simon Thain, and Dr Gordon Allison.

Miscellaneous fellows of distinction: Mr Edward Heywood, Andrew and Helen Rowlatt, Master Dennis Whiffin, Dr Kris Coupland, Mr Jonathan Martin, Mr Christopher Guest, Mr Chris Clark, Dr David Hedley, Dr Laura Jones, Dr Richard Matthews, Dr Martin Daley, Mr Geoff Capes, Bethesda Softworks, and Mrs M. P. Hodgson.

**It should be noted that the Institute of Grassland and Environmental Research has now become part of the Institute of Biological, Environmental, and Rural Sciences (IBERS), a department of Aberystwyth University.*

LIST OF CONTENTS

THESIS SUMMARY 2
ACKNOWLEDGEMENTS 4
LIST OF CONTENTS 5
LIST OF TABLES 9
LIST OF FIGURES 11

1. INTRODUCTION 12

2. BACKGROUND 14

2.1. Climate change and energy generation 14

2.1.1. Status of energy production and consumption in the UK 15

2.2. Biomass as a renewable resource 17

2.2.1. The C_3 and C_4 photosynthetic pathways 19

2.3. Biomass composition 22

2.3.1. The plant cell wall 22
2.3.2. Monocots versus *dicots 26*

2.4. *Miscanthus* as an energy crop 27

2.4.1. Agronomy 27

2.5. Biomass conversion to fuels and chemicals 28

2.5.1. Bio-chemical conversion pathways 29
2.5.2. Thermo-chemical conversion pathways 30

2.6. Fast-pyrolysis of lignocellulosic biomass 32

2.6.1. Properties and utilisation of pyrolysis liquid as a fuel 34
2.6.2. Pyrolysis based bio-refinery 35

2.7. Thermo-chemical conversion quality parameters for lignocellulosic feedstocks ..36

2.7.1. Lignocellulosic biomass as a feedstock for combustion 36
2.7.2. Lignocellulosic biomass as a feedstock for fast-pyrolysis 37
2.7.3. Miscanthus as a feedstock for thermo-chemical conversion 38

2.8. Identifying and harnessing the genetic potential of *Miscanthus* 39

2.8.1. High throughput screening techniques 39
2.8.2. Marker assisted selection and identification of candidate genes 40

3. MATERIALS AND METHODS 42

3.1. Plant material 42

3.1.1. *European Miscanthus improvement (EMI) project* 42

3.1.2. *Nitrogen and Potassium fertiliser field trial experiment at Rothamsted Research* 43

3.1.3. *EMI field trial plots at Rothamsted Research* 44

3.1.4. *Sample preparation* 44

3.2. Feedstock characterisation 45

3.2.1. *Moisture content* 45

3.2.2. *Ash* 45

3.2.3. *Acid detergent lignin (ADL)* 45

3.2.4. *Neutral detergent fibre (NDF)* 45

3.2.5. *Acid detergent fibre (ADF)* 45

3.2.6. *Cellulose and hemicellulose* 46

3.2.7. *Near infrared spectroscopy (NIRS)* 46

3.2.8. *Higher and lower heating values of Miscanthus biomass* 46

3.2.9. *Thermo-gravimetric analysis (TGA)* 47

3.2.10. *Pyrolysis gas chromatography - mass spectrometry (Py-GC-MS)* 49

3.3. Fast pyrolysis experiments: Aston bench-scale (150 g hr^{-1}) fast-pyrolysis system. 50

3.4. Pyrolysis product characterisation 50

3.4.1. *Mass balance calculation* 50

3.4.2. *Non-condensable gases* 50

3.4.3. *Water content* 51

3.4.4. *Molecular weight distribution* 51

3.4.5. *Pyrolysis liquid stability* 52

3.4.6. *Liquid injection gas chromatography - mass spectrometry* 52

3.4.7. *Ultimate analysis and determination of heating values from pyrolysis liquids* 52

3.5. Statistical analysis 53

4. GENOTYPIC AND ENVIRONMENTALLY DERIVED VARIATION IN THE CELL WALL COMPOSITION OF *MISCANTHUS*. 54

4.1. Chapter introduction 54

4.1.1. The EMI project: key results and conclusions 54

4.2. Materials and methods 55

4.2.1. Plant material 55

4.2.2. Development of NIRS calibration for determination of cell wall composition 56

4.3. Results and discussion 58

4.3.1. Determination of cell wall composition by NIRS 58

4.3.2. Genotypic and environmental variation in cell wall composition 62

4.3.3. Implications of cell wall composition on feedstock quality 65

4.4. Chapter conclusions 66

5. INFLUENCE OF NITROGEN AND POTASSIUM FERTILISER ON CELL WALL COMPOSITION OF *MISCANTHUS X GIGANTEUS* AND RESULTANT IMPACTS ON FAST-PYROLYSIS LIQUID QUALITY. 68

5.1. Introduction 68

5.2. Materials and methods 68

5.2.1. Fertiliser application field trials 68

5.2.2. Fast pyrolysis trials at Aston University, UK. 69

5.2.3. Cell wall composition analyses 70

5.3. Results and discussion 70

5.3.1. Influence of fertiliser treatment on cell wall composition 70

5.3.2. Resultant impacts on fast-pyrolysis liquid quality 75

5.3.3. Influence of fertiliser treatment on dry matter yield 79

5.4. Chapter conclusions 79

6. CHARACTERISATION OF *MISCANTHUS* SPECIES AND GENOTYPES BY THERMOGRAVIMETRY AND PYROLYSIS GAS-CHROMATOGRAPHY MASS-SPECTROMETRY 81

6.1. Chapter introduction 81

6.2. Materials and methods 81

6.3. Results and discussion 82

6.3.1. Variation in cell wall composition 82

6.3.2. Thermogravimetric analysis 84

6.3.3. Py-GC-MS characterisation 86

6.4. Chapter conclusions 91

7. INFLUENCE OF GENOTYPIC VARIATION IN CELL WALL COMPOSITION OF *MISCANTHUS* ON THE QUALITY OF PYROLYSIS LIQUIDS PRODUCED UNDER FAST-PYROLYSIS CONDITIONS 92

7.1. Introduction 92

7.2. Materials and methods 92

7.2.1. Feedstock selection and characterisation 92

7.2.2. Fast-pyrolysis experiments 93

7.3. Results and discussion 98

7.3.1. Dry matter yields of selected genotypes 98

7.3.2. Feedstock characterisation 98

7.3.3. Fast-pyrolysis products 99

7.3.4. Molecular weight distribution and stability of pyrolysis liquids 102

7.3.5. Pyrolysis liquid composition 105

7.3.6. Comparison of pyrolysis liquids produced from Miscanthus and other feedstocks ... 108

7.4. Chapter conclusions 112

8. SUMMARY OF CONCLUSIONS 114

9. RECOMMENDATIONS FOR FURTHER RESEARCH 116

10. BIBLIOGRAPHY 118

LIST OF TABLES

Table 1.1 Energy ratios of candidate energy crops based on conversion by combustion 12
Table 2.1 Overview of cell wall fractions and components [32].....23
Table 2.2 Approximate composition of typical monocot and dicot cell walls. 26
Table 2.3 Process conditions and typical product yields of fast-pyrolysis and gasification 32
Table 2.4 Physical properties of pyrolysis liquids and mineral oils. 35
Table 3.1 *Miscanthus* species and genotypes used in the EMI field trials. 42
Table 3.2 Fertiliser treatments applied in the field trial experiment conducted at Rothamsted Research.....43
Table 3.3 Details of harvests taken over the 2005/2006 growing season.....44
Table 4.1 EMI samples analysed, listed by country and trial site. 55
Table 4.2 Calibration and cross validation statistics for developed equations. 58
Table 4.3 Lignin concentration of *Miscanthus* species and genotypes harvested in autumn 1999. 59
Table 4.4 Lignin concentration of *Miscanthus* species and genotypes harvested in winter 2000. 60
Table 4.5 Hemicellulose concentration of *Miscanthus* species and genotypes harvested in autumn 1999. 60
Table 4.6 Hemicellulose concentration of *Miscanthus* species and genotypes harvested in winter 2000. 61
Table 4.7 Cellulose concentration of Miscanthus species and genotypes harvested in autumn 1999. 61
Table 4.8 Cellulose concentration of *Miscanthus* species and genotypes in winter 2000.....62
Table 4.9 Results of analyses of variance performed on cell wall compositional data. 63
Table 5.1 Treatments selected for fast-pyrolysis trials and cell wall composition analysis. 69
Table 5.2 Mean lignin concentrations of *M. x giganteus* stem and leaf material by fertiliser treatment and harvest time.....72
Table 5.3 Mean cellulose concentrations of *M. x giganteus* stem and leaf material by fertiliser treatment and harvest time.....73
Table 5.4 Mean hemicellulose concentrations of *M. x giganteus* stem and leaf material by fertiliser treatment and harvest time. 74
Table 5.5 Comparison of the results of cell wall and thermogravimetric analyses, with fast-pyrolysis product yields achieved from *Miscanthus* biomass grown under different fertiliser treatments. 75

Table 5.6 Comparison of results of cell wall composition analyses with characteristics of fast-pyrolysis liquids produced from *Miscanthus* biomass grown under different fertiliser treatments. 76
Table 5.7 Mean dry matter yields of *M. x giganteus* grown under five different fertiliser treatments at Rothamsted Research, Harpenden, UK. 79
Table 6.1 Cell wall composition of *Miscanthus* species and genotypes in the November and February harvests. 82
Table 6.2 Thermogravimetric analysis and apparent activation energies of *Miscanthus* species and genotypes in the November and February harvests. 85
Table 6.3 Key marker compounds identified by Py-GC-MS analysis of *Miscanthus* species and genotypes. 87
Table 7.1 Species, genotype, and lignin concentration of EMI genotypes harvested in February 2006 showing genotypes selected for fast-pyrolysis experiments 93
Table 7.2 Cell wall composition and ash concentration of genotypes selected for fast-pyrolysis. 99
Table 7.3 Feedstock characteristics, operating conditions, product yields and mass balances achieved in the fast-pyrolysis of *Miscanthus* genotypes. 100
Table 7.4 Molecular weight distribution of pyrolysis liquid before and after aging as determined by gel permeation chromatography. 103
Table 7.5 Key marker compounds identified by GC-MS analysis of fast-pyrolysis liquids produced from *Miscanthus* genotypes. 106
Table 7.6 Influence of feedstock type and composition on fast-pyrolysis product yields and characteristics of the liquid product. 109

LIST OF FIGURES

Figure 2.1 Global average near-surface temperatures between 1850 and 2005 [6] 14
Figure 2.2 UK CO_2 emissions by end use in 2005 [9] 15
Figure 2.3 Utilisation of heat energy by end use in 2005 [9] 16
Figure 2.4 UK electricity generation mix in 2006 [9] 16
Figure 2.5 Carbon dioxide fixation and reduction in C_3 photosynthesis [18] 19
Figure 2.6 Simplified outline of C_4 pathway coupled with C_3 fixation of Carbon dioxide 20
Figure 2.7 Secondary cell wall structure and organisation 24
Figure 2.8 Lignin biosynthesis pathway 25
Figure 2.9 Conversion pathways, processes, products and markets [49]. 29
Figure 2.10 Main processes, intermediate energy carriers and final energy products from the thermo-chemical conversion of biomass [48] 30
Figure 2.11 Schematic diagram of a bubbling fluid bed fast-pyrolysis system [49]. 33
Figure 2.12 Conceptual diagram of a pyrolysis based bio-refinery [66] 36
Figure 3.1 Annotated example of a derivative ($d\alpha/dt$) curve from TGA 48
Figure 4.1 Locations of EMI project trial sites and predicted harvestable *Miscanthus* yields across Europe 56
Figure 5.1 Mean concentrations of lignin, cellulose, and hemicellulose in stem material for all treatments over the growing season 71
Figure 5.2 Mean concentrations of lignin, cellulose, and hemicellulose (g kg^{-1}) in leaf material for all treatments over the growing season. 71
Figure 6.1 Example chromatogram of *M. x giganteus* from PY-GC-MS analysis 86
Figure 6.2 Mean amounts and standard deviations of key markers identified in *Miscanthus* genotypes at both harvest times 89
Figure 7.1 Schematic diagram of the bench scale rig used for fast-pyrolysis of *Miscanthus* biomass. 94
Figure 7.2 Schematic diagram of the bench scale reactor unit used for fast-pyrolysis of *Miscanthus* biomass 95
Figure 7.3 Schematic diagram of the biomass feeder unit 96

1. INTRODUCTION

Due to the rise in demand for renewable energy, dedicated biomass energy crops such as *Miscanthus* are becoming more widely cultivated across Europe, predominantly for use as a feedstock for thermo-chemical conversion. *Miscanthus* is a rhizomatous perennial C_4 grass originating from south-east Asia. Key attributes which make *Miscanthus* an attractive energy crop include high dry matter yields, high efficiency of light, nutrient, and water use, minimal requirements of agronomic inputs, and few problems with pests and pathogens when grown under UK conditions [1]. In addition, when used as a feedstock for combustion, *Miscanthus* has a high energy ratio (output:input) compared to other candidate energy crops currently being considered for use in the UK (Table 1.1).

Table 1.1 Energy ratios of candidate energy crops based on conversion by combustion
Table adapted from Powlson *et al.* (2003) [1]. The energy ratios for the crops listed were calculated on the basis of the harvested biomass being converted by direct combustion. Energy ratios were defined as the energy available from the product: energy expended in producing it, expressed as x:1 (output:input).

Energy crop	Energy ratio (x)
Miscanthus	37.5
Switchgrass	35.4
SRC Willow	22.2
Reed canary grass	18.0

Currently, the *Miscanthus x giganteus* hybrid is the main genotype used for commercial production of lignocellulosic biomass. However, other *Miscanthus* species and genotypes have been shown to provide improved biomass yields and feedstock characteristics in terms of thermo-chemical conversion [2-4]. However, at present there is a lack of knowledge regarding the composition of the cell wall and the range of variation between *Miscanthus* species and genotypes. This represents a major barrier to accurate assessment of the suitability of *Miscanthus* genotypes to prospective conversion pathways, and the breeding of new varieties with improved energy conversion traits.

Therefore, this research had two key objectives: Firstly, to determine the extent of genetic and environmentally derived variation in the cell wall composition of *Miscanthus*, and secondly to investigate the influence this variation may have on conversion by combustion and pyrolysis. These objectives may be broken down into the following research targets:

- Development of a high-throughput screening tool for rapid analysis of *Miscanthus* cell wall composition.
- Assessment of the range of genetic and environmentally derived variation in the cell wall composition of *Miscanthus* and implications for thermo-chemical conversion.
- Assessment of the effect of harvest time on the cell wall composition of *Miscanthus* and implications for thermo-chemical conversion.
- Assessment of the influence of fertiliser treatment on the cell wall composition of *Miscanthus* and implications for thermo-chemical conversion.
- Assessment of the influence of genetic and environmentally derived variation in *Miscanthus* cell wall composition on conversion by fast-pyrolysis and the quality of the product liquid.

2. BACKGROUND

2.1. Climate change and energy generation

Climate change represents one of the most serious and urgent issues humanity has ever had to face. Over the last forty years or so, climate change has been a controversial topic and a centre of fierce debate. Whilst systems of climate modelling have been subject to intense scrutiny and are subject to inherent uncertainties, it is becoming clear that human activities have had a significant role in influencing the global climate through emissions of greenhouse gases. Research has highlighted that drastic changes to the global climate are likely to occur if levels of greenhouse gas emissions continue to increase unchecked [5, 6]. Approximately 290 billion tonnes of carbon has been released into the atmosphere since 1751, primarily through the use of fossil fuels [7]. Around half of these emissions have occurred since the mid 1970s, and in 2002 resulted in a peak in estimated CO_2 emissions from fossil fuels of approximately 6975 million metric tonnes [7]. In 2001 atmospheric CO_2 concentrations were estimated as being almost double that of pre-industrial times [6], and were projected to increase by a further 50% by 2050, rising on average by an estimated 0.4% per annum [5].

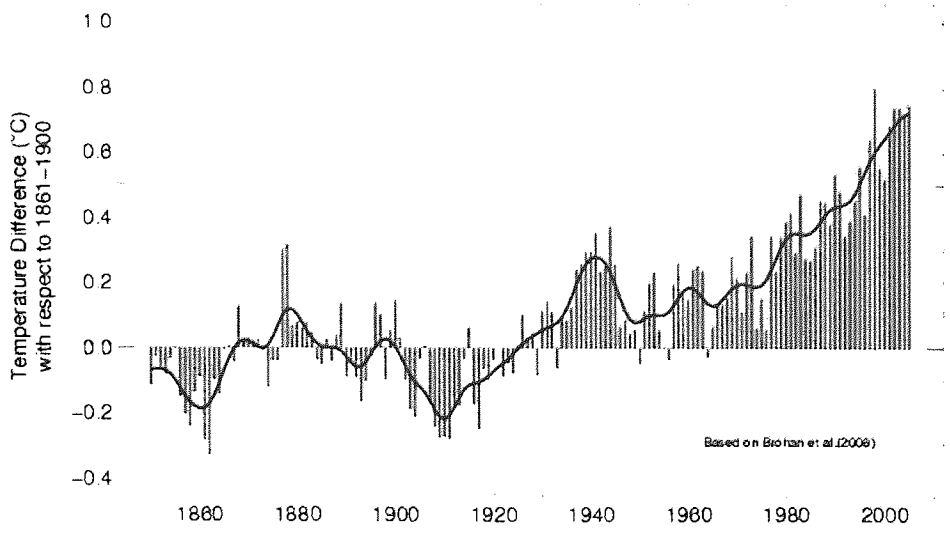

Figure 2.1 Global average near-surface temperatures between 1850 and 2005 [6]
Figure shows the change in global average near-surface temperature from 1850-2005 relative to the average temperature between 1862 and 1900. The individual annual averages are shown as red bars and the blue line represents the smoothed trend [6].

As a result of this increase in atmospheric concentrations of CO_2 and other greenhouse gases, global near-surface temperatures have shown a steady increase (Figure 2.1), rising by 0.2°C per decade over the last 30 years [6].

The Kyoto protocol came into effect in 2005, setting targets for the reduction of CO_2 emissions for all signatory countries. The stipulations of first commitment period (2008-2012) oblige member countries to reduce their emissions to a minimum of 5% below their 1990 levels by means of emissions trading, joint implementation, and utilisation of the clean development mechanism [8]. In March 2007, the European council approved a climate change and energy package requiring EU countries to reduce their greenhouse gas emissions by at least 20% by 2020 based on their 1990 levels [9]. In addition, EU countries were set a target of establishing a minimum 20% renewable energy share by 2020, with biofuels contributing at least 10% [9].

2.1.1. Status of energy production and consumption in the UK

CO_2 emissions from energy generation in the UK are predominantly derived from the production of heat (including electrical heaters), followed by emissions from transport and electricity generation respectively [9] making these end uses primary targets for emissions reduction and renewable energy strategies (Fig 2.2). Heat generation contributes almost half the CO_2 emissions produced from energy generation, equating to 71 million tonnes of carbon, predominantly derived from natural gas, and coal in the case of electrical heating systems [9].

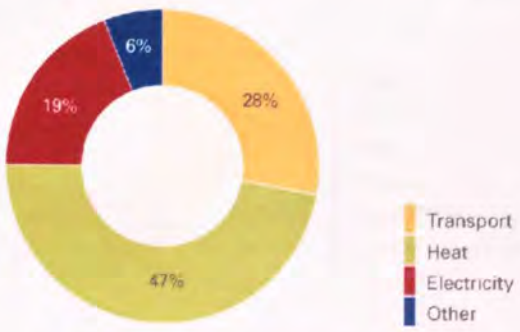

Figure 2.2 UK CO_2 emissions by end use in 2005 [9]

The bulk of the heat energy produced is utilised for space and water heating, which combined account for 71% of the total heat energy consumed (Figure 2.3) [9]. The key methods highlighted for reducing emissions from heat generation in the 2007 UK White Paper centred around improving overall energy efficiency, increasing use of combined heat and power (CHP) systems, and increasing the proportion of heat generated from less carbon-intensive renewable energy sources such as biomass [9].

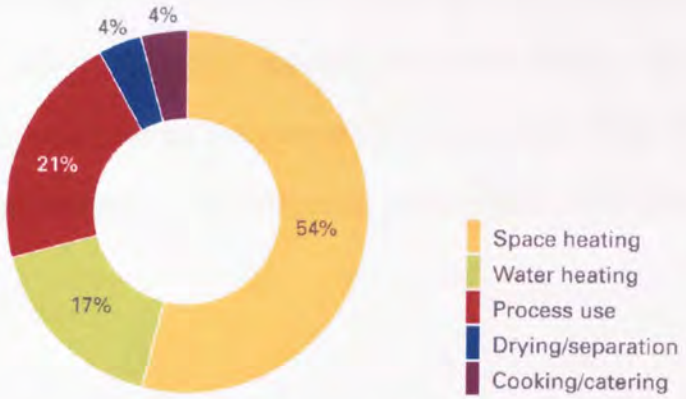

Figure 2.3 Utilisation of heat energy by end use in 2005 [9]

A total of 96% of the energy consumed in the UK is derived from non-renewable sources, namely coal, gas, oil, and nuclear derived power [9, 10]. In terms of electricity generation, 73% of the total electricity generated in the UK derives from coal and natural gas (Figure 2.4) and it is anticipated that fossil fuels will still play a major role in UK energy generation in 2020. The UK government has set a target of increasing the share of renewable electricity generation to 20% by 2020 [9].

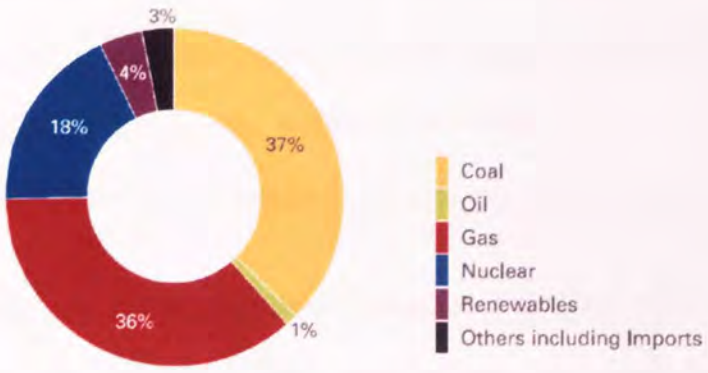

Figure 2.4 UK electricity generation mix in 2006 [9]

In addition to concerns regarding climate change, security of supply is also a major driver in reducing reliance on fossil fuel resources. The UK is fortunate to have a domestic reserve of fossil fuels, however as these resources deplete and demand continues to increase, it is likely that reliance on imported fuel resources will increase. Current projections estimate that by 2020, 60-80% of fuels utilised in UK energy generation will derive from imports [9, 11], a substantial proportion of which are likely to be derived from less stable parts of the world [9]. Therefore, in order to reduce emissions and improve security of supply, it is necessary to increase utilisation of domestically sourced renewable energy resources. The main technologies currently available for the generation of renewable energy include: on/offshore wind farms, wave and tidal stream, solar-thermal, photo-voltaics (PV), and energy generation from biomass.

2.2. Biomass as a renewable resource

Biomass constitutes one of the most abundant sources of renewable energy and refers to all organic matter derived from green plants (algae, trees and crops). Solar energy captured via photosynthesis is stored within the chemical bonds created throughout growth. This stored chemical energy can be released and utilised by breaking the bonds between adjacent carbon, hydrogen and oxygen molecules through processes of digestion, combustion or decomposition [12].

Terrestrial biomass resources can be categorised into three broad strata:

1. Wastes (agricultural residues, municipal solid (organic) waste (MSW), landfill gases)
2. Standing forests (Trees, shrubs, and forest residues)
3. Energy crops (short rotation woody crops; grasses; starch, sugar and oil crops)

In 2001, lignocellulosic (woody) materials constituted the major biomass energy source, predominantly derived from energy crops, forest products and residues, which collectively comprised approximately 64% of the global energy derived from biomass, with 24% being

derived from MSW, 5% from agricultural residues, and approximately 5% from landfill gases [13]. Despite being derived from a variety of different sources with varying chemical composition, biomass feedstocks as a whole display a great degree of uniformity in many of their physical properties in comparison to fossil fuels such as coal and petroleum [14]. For example, the gross heating values of coal range from 20-30 GJ t^{-1}, whereas the gross heating values for almost all biomass feedstocks fall between 15-19 GJ t^{-1}. Agricultural residues and lignocellulosic materials display even greater uniformity, yielding gross heating values of 15-17 GJ t^{-1} and 18-19 GJ t^{-1} respectively [14].

There are several immediate environmental benefits which can be achieved through utilising biomass resources: Firstly, reducing reliance on non-renewable resources can improve sustainability of production and improve security of supply. Secondly, the utilisation of renewable biodegradable resources has far fewer problems in terms of waste disposal and environmental pollution compared with nuclear and fossil fuel based processes [15]. Thirdly, the cultivation of biomass crops provides an additional buffer to offset concentrations of atmospheric CO_2 through sequestration. The main focus of utilising biomass is to provide an adequate and efficient substitute for fuels and chemicals currently derived from fossil fuels. With reference to the UK, depletion of North Sea oil and natural gas reserves has increased reliance on imported fuels and reduced supply security, biomass and other forms of renewable energy are more attractive and economically viable than at any other time. The utilisation of domestically sourced resources for the production of fuels and chemicals would have profound benefits in terms of reducing emissions, improving security of supply, and in doing so create improved opportunities for the agricultural and forestry sectors [15, 16].

Energy crops cultivated for use as biomass fuel must display two key features in order to qualify as an economically viable fuel source, high biomass yields and good feedstock characteristics based on their intended conversion pathway. In terms of agronomy, crops must

display high light, water, nutrient use efficiency, and resistance to pest and pathogens, whilst presenting minimal problems in cultivation and harvesting [3]. For this purpose, those biomass crop species which utilise the C_4 photosynthetic pathway are best suited, as they are more efficient in converting solar energy, require fewer agrochemical inputs, and often have lower moisture content in the harvested material than the C_3 plant species which constitute the dominant flora in Western Europe [17].

2.2.1. The C_3 and C_4 photosynthetic pathways

Photosynthesis is the photochemical process by which plants, algae, and some bacteria use the reducing power generated by the light driven oxidation of water to convert CO_2 into organic compounds. Three key photosynthetic pathways are utilised by plants: C_3, C_4, and crassulacean acid metabolism (CAM) which occurs in xerophytes such as cacti and most succulents [18]. The majority of plants utilise the C_3 photosynthesis pathway where all of the photosynthetic reactions take place in the mesophyll cells which contain a single chloroplast type [19]. In the C_3 pathway CO_2 is accepted by the pentose sugar ribulose biphosphate (RuBP). Carboxylated RuBP is converted by RuBP-carboxylase/oxygenase (Rubisco) to two molecules of a 3-carbon compound, phosphoglyceric acid (PGA) (hence C_3 photosynthesis). PGA is subsequently converted through phosphorylation and reduction by the products of the light reaction (ATP and NADPH) to produce triose phosphate (TP) (Fig. 2.5) which is then used in the biosynthesis of organic compounds [19].

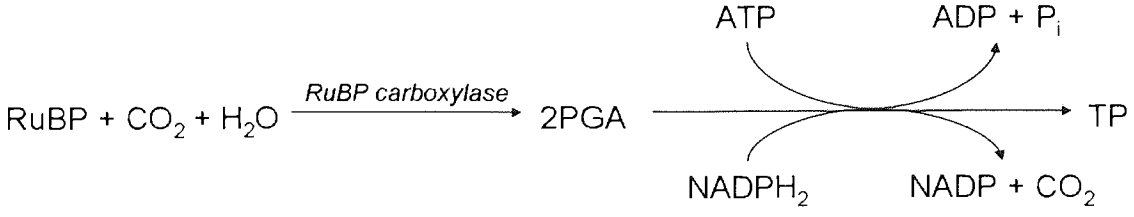

Figure 2.5 Carbon dioxide fixation and reduction in C_3 photosynthesis [18]

The main limitation of C_3 photosynthesis is that RuBP will also accept O_2 which represents a competitive inhibitor to CO_2 fixation. The acceptance of O_2 by RuBP leads to the production of phosphoglycolate which cannot be utilised in the carbon reduction cycle. As a result phosphoglycolate must be recycled into PGA via an additional pathway known as photorespiration, expending energy (ATP and NADPH) and resulting in a loss of carbon [18, 19]. This causes an overall reduction in photosynthetic efficiency and ultimately causes a reduction in biomass accumulation (dry matter yield) [17].

The C_4 photosynthesis pathway represents an adaptation of the C_3 pathway rather than a completely different photochemical process. A simplified diagram of the C_4 pathway is shown in Fig.2.6.

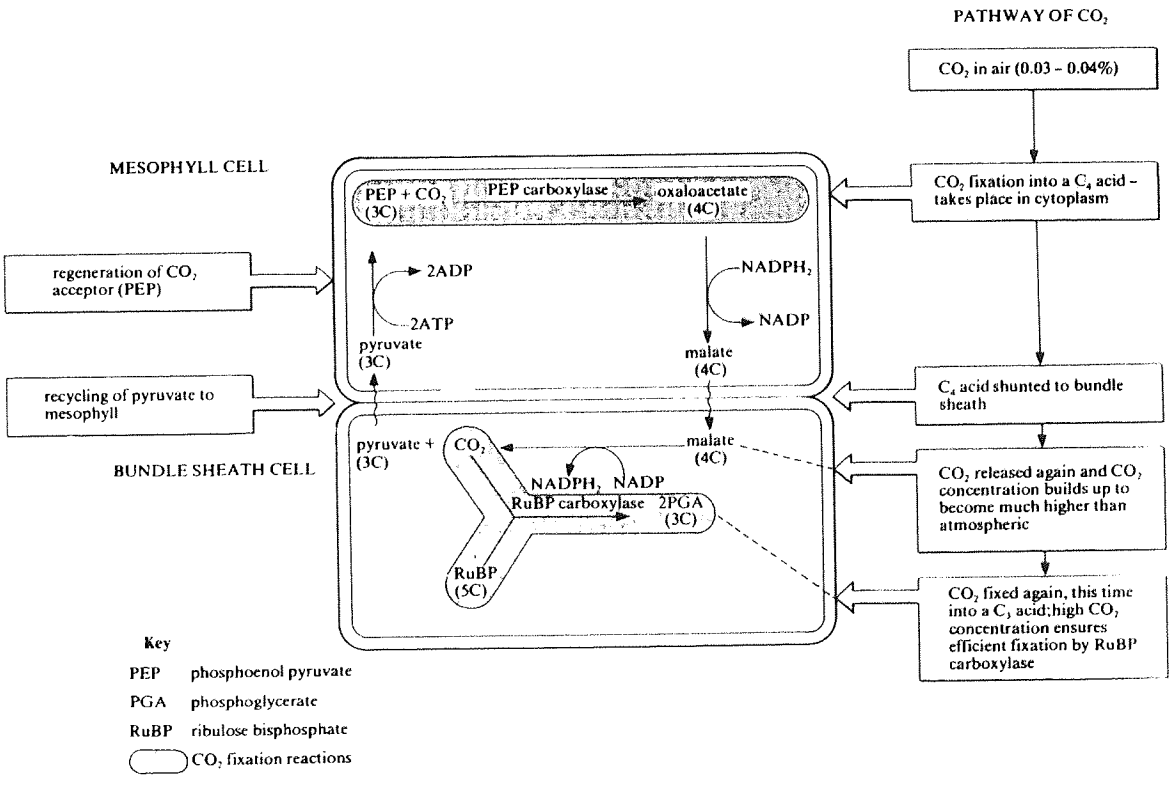

Figure 2.6 Simplified outline of C_4 pathway coupled with C_3 fixation of Carbon dioxide
Transport of CO_2 from air to bundle sheath cell is shown, together with final fixation of carbon dioxide into the C_3 acid PGA [18].

C_4 photosynthesis overcomes the limitations of the C_3 pathway by two main physiological and biochemical adaptations. Firstly, C_4 plants have a different leaf anatomy referred to as the 'Kranz anatomy' where two different types of cell are utilised in photosynthesis, each containing their own type of chloroplast (mesophyll and bundle sheath). Secondly, phosphoenolpyruvate (PEP) is employed as the initial CO_2 acceptor which has a higher affinity for CO_2 than RuBP, and as PEP does not accept O_2, photorespiration does not occur [18]. The first product of C_4 photosynthesis is the 4-carbon dicarboxylic acid oxaloacetate which is converted to malate or aspartate and shunted through plasmodesmata in the cell walls to the chloroplasts of the bundle sheath cells (Hatch-Slack pathway) where it is converted into CO_2, H_2, and pyruvate [18, 19]. Once CO_2 becomes available in the chloroplasts of the bundle sheath cells, fixation by RuBP proceeds as in the conventional C_3 pathway. Three different C_4 types have been identified which differ according to the decarboxylation mechanism employed in the chloroplasts of the bundle sheath cells [19]. The descriptions given in the text and in Fig. 2.6 refer to the most studied NADP-ME (malic enzyme) type.

Due to the fact that O_2 is excluded and CO_2 is made available in concentrations up to ten times atmospheric levels [19, 20] the Rubisco operates with much greater efficiency than in C_3 plants. The net result is that the maximum efficiency for the conversion of intercepted light into biomass is ~40% higher in C_4 plants compared to C_3 plants [21]. In C_4 photosynthesis each molecule of CO_2 has to be fixed twice, therefore the energy consumed is greater than in C_3 [18]. However, in the hot semi-arid climates where the majority of C_4 species evolved, higher temperatures and longer periods of high light-intensity more than off-set the additional energy consumed during photosynthesis, but growth may be limited by the lower temperatures and shorter periods of high light-intensity prevalent in northern temperate regions [20, 22, 23]. Naturally, this may reduce their effectiveness in terms of cultivation as a biomass energy crop in the cooler climates of North - Western Europe.

Compared to other C_4 crop varieties *Miscanthus* displays exceptional adaptability to temperate climates, lower temperatures still present limitations to growth, but dry matter yields remain relatively high compared to other candidate C_3 energy crops such as short-rotation coppice willow and poplar [1, 17, 24, 25].

2.3. Biomass composition

Biomass is chiefly composed of three cell wall components: cellulose, hemicelluloses, and lignin. The relative proportions of these cell wall components, and the manner in which the lignin binds the cellulose and hemicelluloses (holocellulose) within the material, constitutes a major factor in determining which conversion pathway to which the biomass material is suited. The composition and relative proportion of cell wall components within the biomass material also affects the range of products which may be recovered from conversion processes [26, 27].

2.3.1. The plant cell wall

Plant cell walls are composed of two to three layers which differ in structure and organisation: the middle lamella, the primary cell wall, and the secondary cell wall [28-31]. The middle lamella is deposited soon after cell division and creates a boundary layer between adjacent cells [32]. The primary cell wall is deposited once the cell plate is complete and continues to be deposited throughout cell growth and expansion [28-34]. The primary cell wall is typically only 0.1–10 μm thick, however its composition is of key importance for biomass accumulation through controlling cell growth [30, 32]. The cell wall of many cell types is limited to these two layers [28, 29, 32], for example parenchyma and collenchyma [30]. Certain specialized cells develop a secondary cell wall which is deposited once cell elongation has ceased and cell differentiation commences [30, 32]. The secondary cell wall comprises at least 50% of all cell wall mass [34] and is deposited internally to the primary cell wall and varies in morphological and chemical structure depending on cell type and function [30, 32].

For example, many secondary cell walls contain lignin that increases the wall strength, particularly important in cells such as xylem [30]. The composition of the secondary cell wall is of considerable importance in the context of biomass production and conversion [30]. A graphical representation of secondary cell wall structure and organisation is shown in Fig. 2.7. All cell wall layers are primarily composed of long cellulose chains bound in a crystalline lattice structure to form a series of microfibrils. Cellulose comprises the greatest proportion of the cell wall and constitutes 40-50% of the dry matter [12]. Cellulose is composed of linear chains of β1-4 linked glucose units [29] with a molecular weight of around 100,000 [12]. These cellulose microfibrils are embedded within a gel-like matrix composed of pectic polysaccharides, glycoproteins, and hemicelluloses, which collectively form the bulk of the cell wall [28-32, 34]. The hemicellulosic fraction comprises somewhere in the order of 20-40% of the dry biomass [12] and the composition of this fraction varies greatly according to plant species and cell type [32]. An overview of cell wall components is shown in Table 2.1.

Table 2.1 Overview of cell wall fractions and components [32]

Phase	Fraction	Components
Microfibrillar	Cellulose	β1,4-glucan
Matrix*	Pectins	rhamnogalacturonan I arabinan galactan arabinogalactan I homogalacturonan rhamnogalacturonan II
	Hemicelluloses	xylan glucomannan mannan galactomannan glucuronomannan xyloglucan callose (β1,3-glucan) Mixed linkage glucans (β1,3-β1,4) arabinogalactan II
	Proteins	extensin arabinogalactan-proteins others, including enzymes
	Phenolics	lignin ferulic acid others e.g. *p*-coumaric acid, truxillic acid

* *components are not always found in all cell walls*

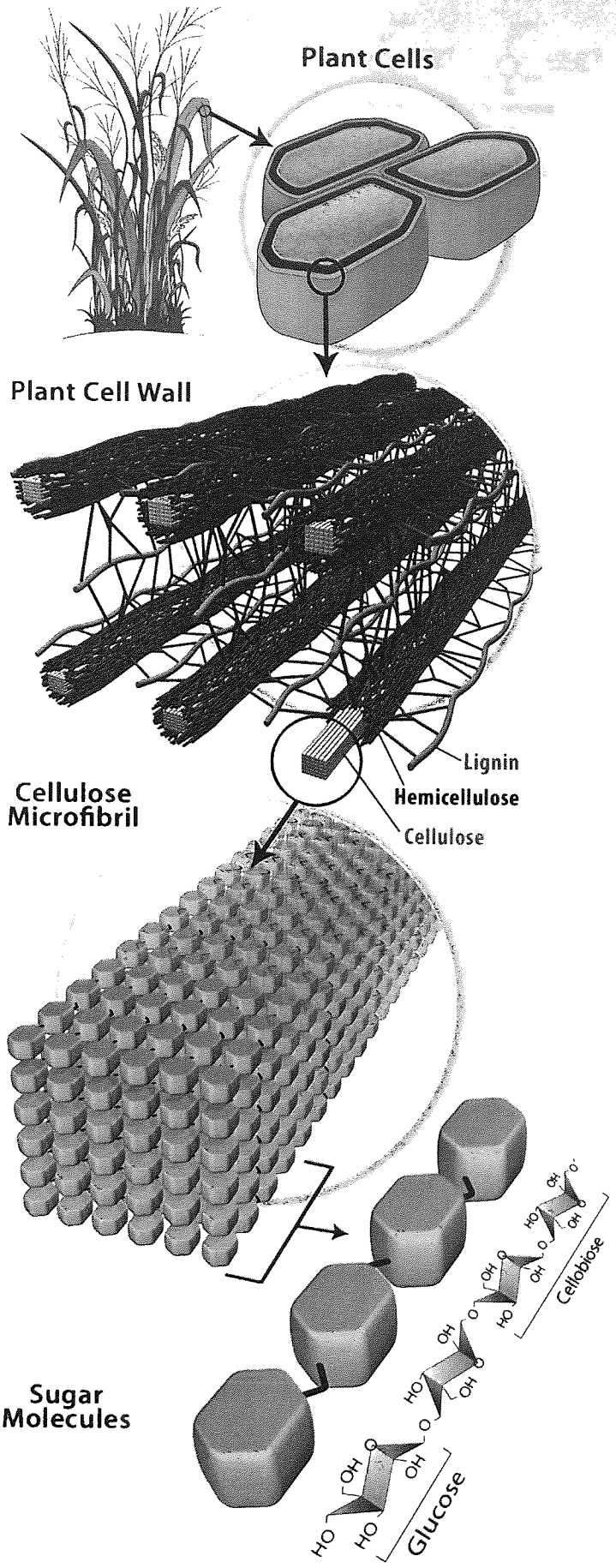

Figure 2.7 Secondary cell wall structure and organisation
Adapted from [35]

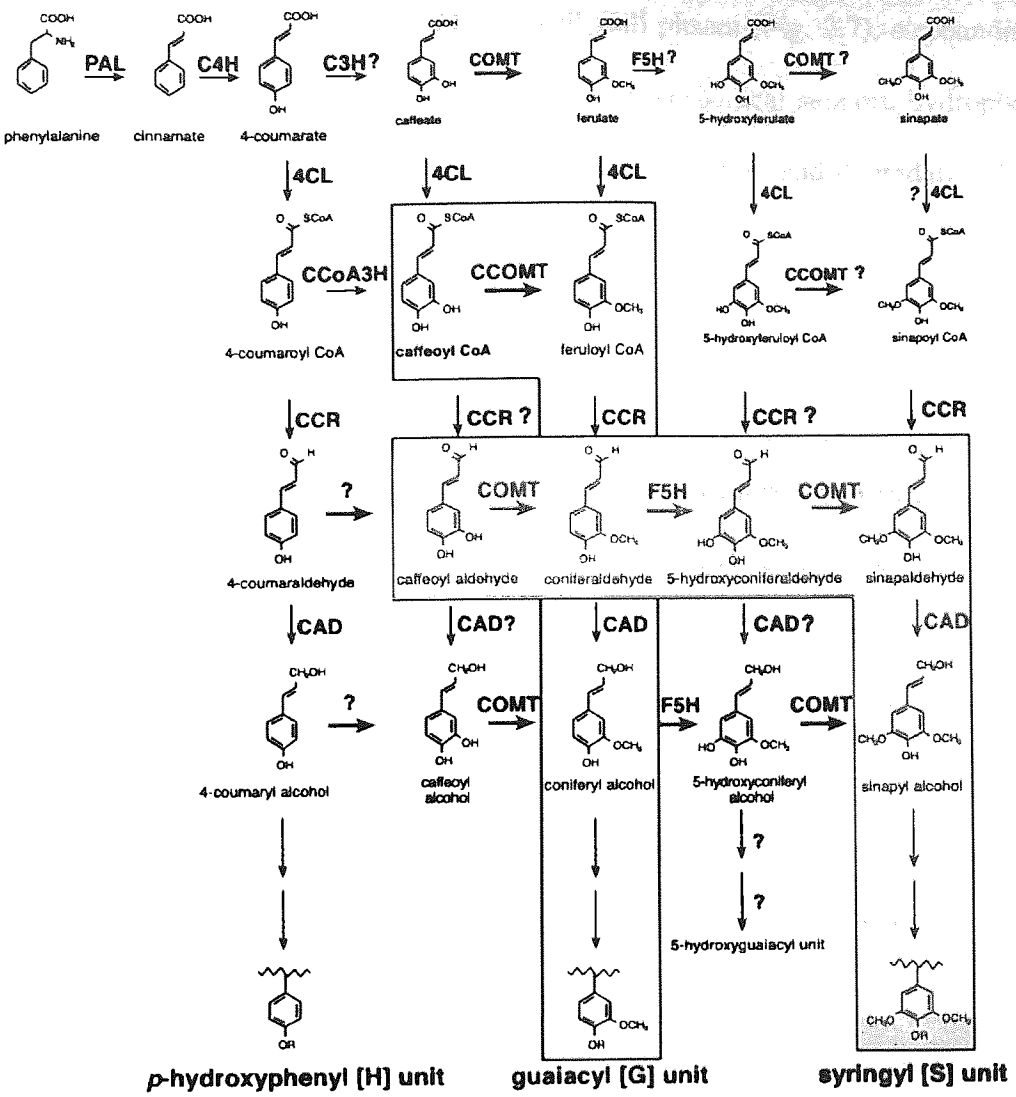

Figure 2.8 Lignin biosynthesis pathway
Adapted from [36]

The lignin fraction of the cell wall is also known to vary in proportion and chemical composition between species and cell types [37]. Lignification occurs in the final stages of cell differentiation once cell elongation has ceased and represents a key distinguishing feature of secondary cell walls [29, 30, 32] [32]. Lignin is a complex phenylpropanoid polymer which predominantly derives from the oxidative condensation of three *p*-hydroxycinnamyl alcohol monomers: *p*-coumaryl, coniferyl and sinapyl alcohols (Fig. 2.8) [37]. These monolignols produce the lignin 'sub units' *p*-hydroxyphenyl (H), guaiacyl (G), and syringyl (S), respectively [36-40]. These three sub units represent the key building blocks of the lignin polymer. Lignin deposition occurs in spaces within the carbohydrate matrix and bonds with the hemicelluloses to form a strong hydrophobic meshwork [32, 39]. This meshwork provides

cohesion between the matrix and microfibrillar cell wall phases (Fig. 2.7), surrounding and cementing the cell wall components to confer improved mechanical support, hydrophobicity to water-conducting vessels, and improved resistance to infection and degradation [32, 36, 39].

2.3.2. *Monocots* versus *dicots*

Flowering plants are classified into two subdivisions: monocotyledons and dicotyledons (monocots and dicots). Trees and herbaceous plants are examples of dicots, and grasses, cereals and palms are examples of monocots. Many differences have been observed in the cell wall composition of the primary and secondary cell walls of monocots and dicots as shown in Table 2.2 [34]. In general, the cellulose composition of the primary cell wall is similar for both monocots and dicots, however, a higher cellulose content has been observed in the secondary cell walls of dicots [34, 41]. Far greater differences have been observed between monocots and dicots in the total content and composition of the hemicellulosic fraction of both cell walls [30, 31, 33, 34, 41, 42].

Table 2.2 Approximate composition of typical monocot and dicot cell walls.
Approximate composition of cell wall components is expressed as a percentage of the dry weight. Table adapted from Vogel (2008) [34].

Component		Primary wall		Secondary wall	
		Monocots	Dicots	Monocots	Dicots
Cellulose		20-30	15-30	35-45	45-50
Hemicelluloses	Xylans	20-40	5	40-50	20-30
	Mixed linkage glucans	10-30	0	-	0
	Xyloglucan	1-5	20-25	-	-
	Mannans and glucomannans	-	5-10	-	3-5
Lignin		-	-	7-10	20

The total lignin content and composition of the secondary cell wall has also been observed to differ between taxa [34, 41]. Both monocot and dicot lignin is primarily composed of guaiacyl (35-49%) and syringyl (40-61%) sub units, however monocot lignin has also been identified as containing small but significant concentrations of the *p*-hydroxyphenyl sub unit (4-15%) which has only been identified at trace levels in dicot lignin [34]. The observed differences between the cell wall composition of grasses and dicots are likely to influence their properties

in terms of their use as feedstocks for energy conversion pathways, and also the types and ranges of products that can be derived within a bio-refinery.

2.4. *Miscanthus* as an energy crop

Miscanthus is a rhizomatous perennial C_4 grass species originating from the tropical / sub tropical regions of south-east Asia [43]. At present, this crop is receiving considerable interest in terms of its use as a feedstock for thermo-chemical conversion processes. Due to the occurrence of inter-specific hybridisation within the genus a range of hybrid cultivars have been exploited, the majority of which are sterile [44]. One such hybrid is *M.* x *giganteus* which has been widely cultivated across Europe, predominantly for commercial production of lignocellulosic biomass as a feedstock for combustion. The genotype was originally collected from Japan and cultivated extensively in Denmark where it was re-classified as *Miscanthus sinensis* (horticultural pseudonym 'Giganteus') and distributed across Europe [45]. When cultivated in suitable conditions *Miscanthus* produces high yields of lignocellulosic material which has good potential for the production of energy and fibre. The productive lifecycle/rotation length of *Miscanthus* is estimated to be 10-15 years, maturing after three, with both stem and leaf material harvested annually [46].

2.4.1. Agronomy

Key characteristics which make *Miscanthus* an attractive candidate species for energy production include its ability to be grown with minimal agrochemical inputs compared with other biomass crop varieties. In addition, *Miscanthus* also displays characteristics of good light, water, and nutrient use efficiency, and dry matter yields of up to 40 t ha^{-1} have been reported when grown in favourable conditions [3].

The start of the *Miscanthus* growing season is initiated on the date of the latest spring frost and ended by the first frost in autumn. The effect of ambient temperature on the absolute leaf

extension rate varies greatly between genotypes, however, as low temperatures strongly inhibit leaf expansion / canopy closure rate, a general threshold for growth could be around 5-10°C [23]. Direct planting of rhizomes or rhizome cuttings represents the most feasible technique for large-scale establishment of *Miscanthus* stands. Rhizomes / rhizome pieces are planted at 10-20cm soil depth, the planting depth depending on the site and soil conditions. In the cooler northern European climates deeper planting depths (>20 cm) were found to be necessary to improve winter survival rates, especially in the first year [47].

In addition to influencing factors of temperature and water availability, soil type and quality are key factors affecting the productivity of *Miscanthus*. Medium soil types such as sandy or silty loams (para-brown earth / brown earth) are most suitable for *Miscanthus* cultivation, provided they are well aerated, high in organic matter, and have a high moisture holding capacity. Very heavy clay soils which waterlog easily are not suited to *Miscanthus* growth. Generally speaking, most soils suitable for growing maize are more than likely suitable for growing *Miscanthus* [47], however *Miscanthus* has also been shown to perform respectably on marginal soils provided they are freely draining and of appropriate depth.

2.5. Biomass conversion to fuels and chemicals

A range of conversion pathways are currently available for the conversion of biomass to fuels and chemicals. The conversion processes used can be categorised into three key pathways: bio-chemical, thermo-chemical, and mechanical extraction [48]. The conversion pathway used is determined according to technical and economic parameters of the biomass feedstock and the conversion system used e.g. matching feedstock characteristics to process specifications. A flow diagram illustrating the key conversion pathways, processes, and products is illustrated in Fig 2.9 adapted from Bridgwater (2007) [49]

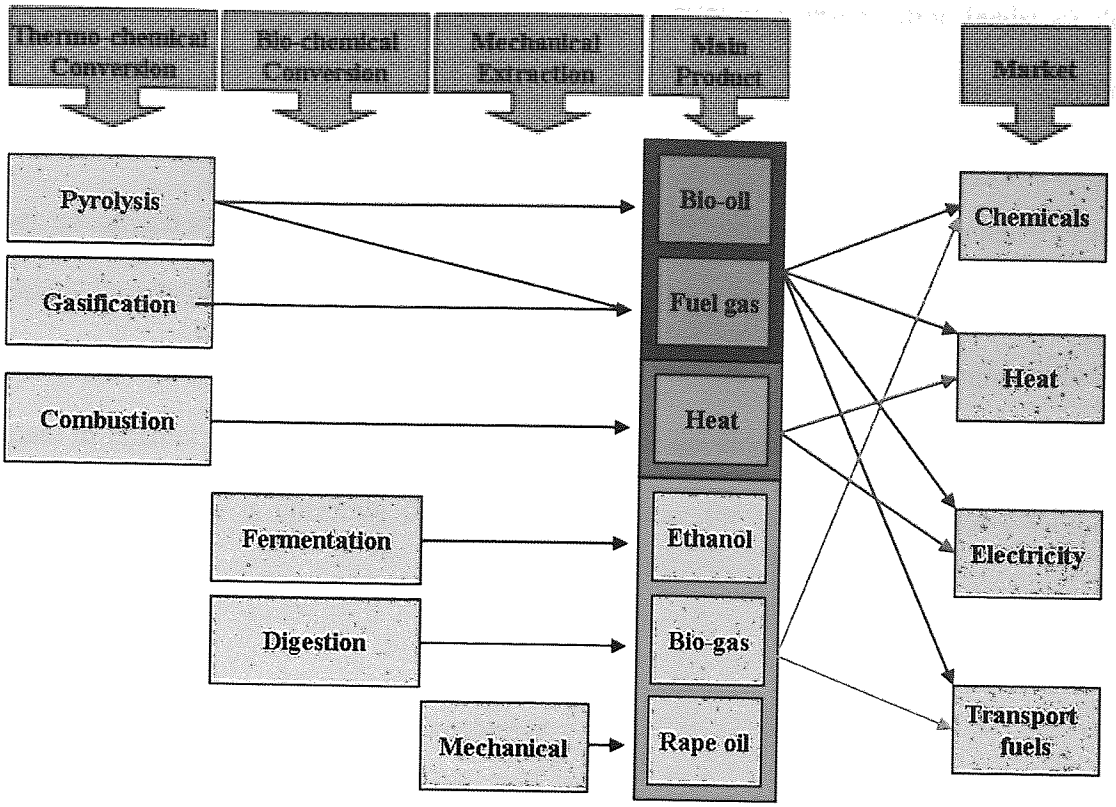

Figure 2.9 Conversion pathways, processes, products and markets [49].

2.5.1. Bio-chemical conversion pathways

Within the bio-chemical conversion pathway two key processes are currently used: Anaerobic digestion (AD), and fermentation. Anaerobic digestion converts the organic matter directly into gaseous products, collectively referred to as biogas. Biogas is primarily composed of a mixture of methane and carbon dioxide with small amounts of other gases such as hydrogen sulphide [13, 50]. The process is best suited to utilising material with a high moisture content, and operates by utilising bacteria in an anaerobic environment to convert the biomass material into a gaseous product which may be used directly as a fuel source or as a feedstock for subsequent processes.

Fermentation as a means of producing ethanol, primarily for transportation fuels, has been used commercially in various countries for a number of years, mainly from sugar crops such as sugar cane, sugar beet, and starchy crops such as wheat and maize. However, there is

growing interest in the utilisation of lignocellulosic material as a fermentation feedstock due to concerns about the use of food crops for the production of fuels. Broadly speaking, this process involves the utilisation of enzymes to breakdown starch or holocellulose to simple sugars which can subsequently be converted to ethanol by yeasts [13]. The efficiency of this process is largely dependant on the enzyme mixtures used in the saccharification process and the cell wall composition of the feedstock used. At present, conversion of lignocellulosic biomass to ethanol is largely inefficient and still under development [51], therefore thermo-chemical conversion is currently the favoured pathway for conversion of lignocellulosic feedstocks.

2.5.2. Thermo-chemical conversion pathways

A general outline of thermo-chemical conversion processes and products is illustrated in Figure 2.10. Within the category of thermo-chemical conversion, four separate processes may be employed to convert the biomass material into desired products: direct combustion; pyrolysis; gasification; and liquefaction. Until recently, liquefaction was considered uneconomical due to the feeding systems and reactors involved being of greater complexity than those required for gasification and pyrolysis [13, 48].

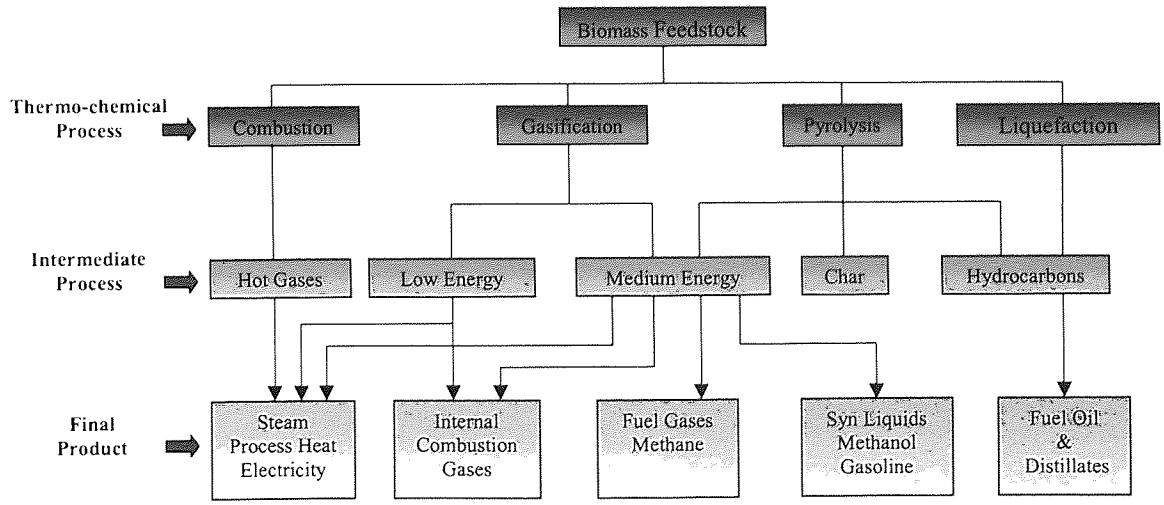

Figure 2.10 Main processes, intermediate energy carriers and final energy products from the thermo-chemical conversion of biomass [48]

Direct combustion constitutes the most basic method of converting chemical energy locked within the biomass to produce heat and power. Biomass heating has been identified as the most effective form of bioenergy, both in industrial and commercial applications [16]. The technologies available for this purpose range from simple stoves and boilers to steam turbines and turbo-generators [48]. The overall efficiencies of these technologies are relatively low, usually around 15% for small scale plants and around 30% for larger or more recently constructed facilities [52]. Potentially, any form of biomass may be burned, however this is only practicable if the material has a moisture content of less than 50%, either in its harvested state or after drying prior to combustion. Biomass with a moisture content of 50% or higher is best converted using bio-chemical methods such as anaerobic digestion [48]. Direct combustion represents the most basic biomass conversion process and the lowest risk to potential investors as the technology is widely available [16, 52].

Co-firing biomass material in coal fired power stations represents the most common industrial scale utilisation of lignocellulosic biomass in Europe, predominantly due to high overall electrical efficiency achieved as a result of the economies of scale of existing plants, and the low investment cost required in modifying existing facilities to allow for biomass utilisation [51]. Co-firing has also been made more attractive in the UK as a result of policy directives such as the renewables obligation (ROCs) [53]. At present, biomass only represents a 5-10% share of the total thermal input, but facilities are being developed which can extend this share up to 40% [51].

The pyrolysis conversion process may be simply defined as thermal decomposition of a material under anoxic or limited oxygen conditions, and represents the foundation of all combustion and gasification processes. Differences between pyrolytic processes, and the products they yield, arise from variation in parameters of temperature, heating rate, and gas

residence time used during the conversion process [52]. The gasification process is designed to maximise the gaseous output, and involves conversion of biomass feedstocks into a mixture of combustible gases by partially oxidising the biomass under temperatures of 800-900°C and allowing a long gas residence time within the reactor [48]. Fast-pyrolysis processes are designed to maximise the liquid output and use lower reaction temperatures (~500°C), very high heating and heat transfer rates, and a very short gas residence time typically less than 2 seconds [52, 54]. Pyrolysis vapours produced are rapidly cooled and condensed to produce the liquid product at efficiencies of up to 70% [13]. Table 2.3 displays the key differences between gasification and fast-pyrolysis processes, and the percentage yields of gaseous, solid (char), and liquid products, adapted from Bridgwater (2003) [52].

Table 2.3 Process conditions and typical product yields of fast-pyrolysis and gasification

Process:	Key features:	Liquid (%)	Char (%)	Gas (%)
Fast pyrolysis	Moderate temperature (~500°C) Short residence time	75	12	13
Gasification	High temperature (~800°C) Long residence time	5	10	85

2.6. Fast-pyrolysis of lignocellulosic biomass

Fast-pyrolysis is a technology currently receiving considerable interest as a means of producing liquid fuels and a range of speciality and commodity chemicals [54]. The main advantage of fast-pyrolysis is the production of a liquid product which can be easily and economically transported and stored [55] thereby de-coupling the handling of solid biomass from utilisation. Pyrolysis liquid represents a low cost liquid biofuel with a positive carbon balance [56] capable of providing a substitute for mineral fuel oils with potential to be used in small to large scale (co-firing) power generation systems [55-58]. A number of different reactors and system configurations have been developed for the fast-pyrolysis of biomass. The most common reactor types include bubbling fluid bed, circulating fluid bed, and ablative reactors [49, 52, 54]. Bubbling fluid bed reactors constitute the most popular design due to

their ease of operation and scale-up [54]. A schematic diagram of a bubbling fluid bed fast-pyrolysis system is shown in Figure 2.11.

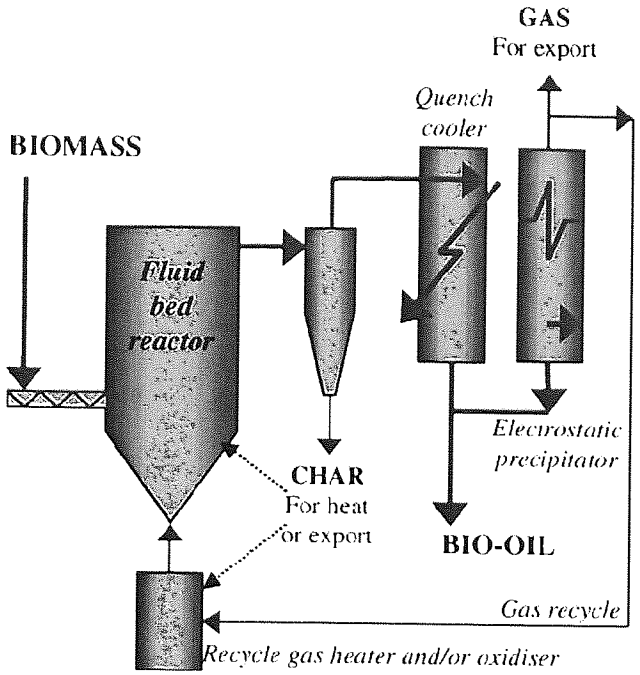

Figure 2.11 Schematic diagram of a bubbling fluid bed fast-pyrolysis system [49].

In a bubbling fluid bed fast-pyrolysis system, the reactor bed is composed of an inert heat transfer medium (typically quartz sand) which is fluidised by a flow of inert gas (typically nitrogen). Biomass is fed into the reactor and injected directly into the fluidised bed where it is rapidly heated to around 500°C. The produced vapours leave the reactor through a cyclone which separates the bulk of the solids and char. Vapours continue into a condensation system consisting of a quench column and an electrostatic precipitator where all condensable gases are rapidly cooled and condensed to form a liquid. Non-condensable gases pass out of the electrostatic precipitator and are either collected or may be recycled, along with the char, to provide heat for the reactor unit. The heat required for the pyrolysis process typically equates to around 15% of the energy of the feedstock, as the char and gas combined contain around 30% of the energy in the feedstock these by-products are sufficient to fuel the energy requirements of the pyrolysis process [49]. Pyrolysis liquid yields, based on the dry weight of biomass fed, range from around 70-75% for wood [52] and 55-65% for grasses [49].

2.6.1. *Properties and utilisation of pyrolysis liquid as a fuel*

Pyrolysis liquid, commonly referred to as 'bio-oil', constitutes a micro-emulsion of the intermediate degradation products of the plant cell wall polymers cellulose, hemicellulose, and lignin [49]. The elemental composition of the pyrolysis liquids approximates to that of the biomass feedstock used [49, 54, 57, 59]. Unlike petroleum fuels, biomass derived pyrolysis oils contain a high concentration of oxygenated compounds, the amount and distribution depending on the biomass feedstock used and the severity of the pyrolysis process (temperature, gas residence time, and heating rate) [52, 57]. The oxygen content represents the primary source of differences between properties and behaviour of pyrolysis liquids compared to petroleum fuels [57]. A high oxygen concentration causes pyrolysis liquids to be very polar and increases the amount of water that can be held in solution [59]. The water content of pyrolysis liquids is a mixed blessing, whilst detrimental to the heating value and combustion rate [57, 59], a higher water content reduces viscosity thereby improving flow characteristics [57]. A higher water content has also been associated with lower emissions of NO_x and has also been observed to provide a more uniform temperature profile in the cylinder of a diesel engine [57].

One of the main barriers to the commercial utilisation of pyrolysis liquid is its incompatibility with conventional fuels. Table 2.4 compares the properties of biomass derived pyrolysis liquids with conventional light and heavy fuel oils. The oxygen content, corrosivity, and instability of pyrolysis liquids is significantly higher than that of conventional fuel oils and has around half the lower heating value (LHV) [52, 56] (Table 2.4).

The phase stability greatly affects the duration for which pyrolysis liquids can be stored. Only partial decomposition of the biomass occurs during fast-pyrolysis and polymerisation and

condensation reactions continue to occur in the liquid during storage [60]. The effects of 'aging' include an increase in viscosity, density, and water content, and a decrease in molecular homogeneity and heating value [60-62]. However, a number of physio-chemical and catalytic upgrading processes have been developed to upgrade pyrolysis liquids into a form more similar to conventional fuels, most notably by hot-vapour filtration, solvent addition, or deoxygenation through hydrogenation or zeolite cracking [48, 49, 52, 57, 63, 64].

Table 2.4 Physical properties of pyrolysis liquids and mineral oils.
The table compares physical properties of pyrolysis liquids with those of light and heavy fuel oils. Table adapted from Chiaramonti *et al.* (2007) [65].

Analysis	Unit	Pyrolysis liquids	Light fuel oil	Heavy fuel oil
Carbon	% wt	32-48	86.0	85.6
Hydrogen	% wt	7-8.5	13.6	10.3
Nitrogen	% wt	<0.4	0.2	0.6
Oxygen	% wt	44-60	0	0.6
Sulphur	% wt	<0.05	<0.18	2.5
pH		2-3	Neutral	-
Water	% wt	20-30	0.03	0.1
Solids	% wt	<0.5	0	0.2-1.0
Ash	% wt	<0.2	0.01	0.03
Density	kg dm^3 at 15°C	1.10-1.30	0.89	0.94-0.96
Viscosity	cSt at 40°C	15-35	3-8	351 (50°C)
Flash point	°C	40-110	60	100
Pour point	°C	-10 to -35	-15	21
LHV	MJ kg^{-1}	13-18	40.3	40.7
Phase stability		Unstable	Stable	Stable

2.6.2. Pyrolysis based bio-refinery

In addition to direct utilisation of pyrolysis liquids as a fuel, there is considerable potential for development of a pyrolysis based bio-refinery to produce a broad range of products from pyrolytic conversion of biomass feedstocks. A conceptual diagram of a pyrolysis based bio-refinery and the range of products which may be refined is shown in Figure 2.12 [66].

Products which may be refined from biomass derived pyrolysis liquids includes sugars, agri-chemicals, food flavourings, adhesives, fuel additives, and emission reduction agents [66]. However, the range, quantity, and quality of achievable products depends greatly on the type and composition of the biomass feedstock used [59, 63, 66-71].

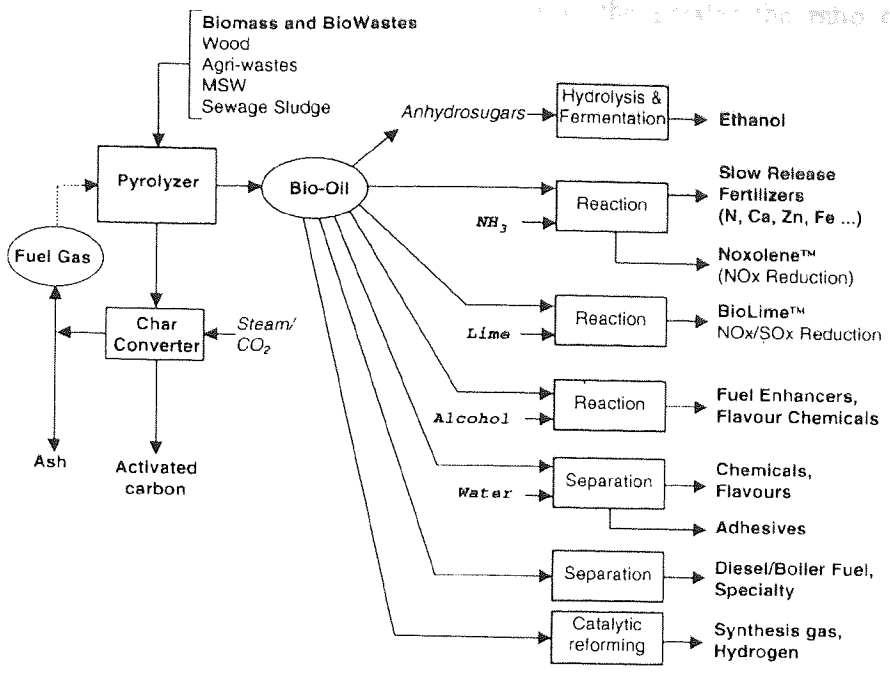

Figure 2.12 Conceptual diagram of a pyrolysis based bio-refinery [66]

2.7. Thermo-chemical conversion quality parameters for lignocellulosic feedstocks

Quality parameters for lignocellulosic feedstocks are greatly dependant on the conversion method used and the intended end use of the converted product. Therefore, biomass feedstock quality criteria differ according to whether the intended conversion route is by combustion or pyrolysis.

2.7.1. Lignocellulosic biomass as a feedstock for combustion

When lignocellulosic biomass is to be used as a feedstock for thermo-chemical conversion, heating value is the most important quality parameter. Variation in heating value of biomass feedstocks predominantly derive from variation in cell wall composition and concentrations of moisture and ash [3]. The oxygen concentration of a material has a strong effect on its heating value when combusted. For example, heating value has been shown to decrease almost linearly as oxygen concentration increases [72]. It has been suggested that the proportion of lignin contained within the material can be used as an indicator of its heating value [73, 74]. Lignin has a lower oxygen concentration (<300 g kg^{-1}) than holocellulose (>500 g kg^{-1}), and as a result the heating value of lignin (24,000 kJ kg^{-1}) is much higher than

that of holocellulose (15,000 kJ kg^{-1}) [72]. Therefore, the greater the ratio of lignin to holocellulose the higher the heating value of the biomass.

High moisture content in biomass causes a reduction of its heating value and an overall decrease of combustion efficiency. This is a result of inhibition of ignition and an increased volume of flue gas produced during combustion [48, 72]. This in turn reduces the overall combustion temperature leading to incomplete combustion of the feedstock and an increase in the evolution of harmful gases such as CO, NO_x and SO_2 [72]. Biomass ash has a relatively low melting point, the occurrence of ash melting during thermal processing results in the production of 'slag' which, when deposited inside combustion chambers or boilers, results in a reduction of heat transfer and an overall reduction in the efficiency of combustion [72]. In addition, high concentrations of alkali metals can lead to accumulation of corrosive chemicals (KCl and HCl) within the combustion equipment [48, 72]. Therefore, biomass feedstock quality criteria for combustion processes include high lignin to holocellulose ratio, high heating value, and low concentrations of moisture and ash.

2.7.2. Lignocellulosic biomass as a feedstock for fast-pyrolysis

For conversion via pyrolysis, feedstock quality criteria depend on whether the pyrolysis liquid product is to be used as a fuel or as an intermediate product in a bio-refinery. In both cases cell wall composition of the feedstock greatly influences the characteristics of the pyrolysis liquid and the range of products which can be subsequently refined [61, 71, 75-77]. The lignin concentration of the feedstock has both beneficial and detrimental effects in terms of pyrolysis liquid quality. For example, high lignin concentrations confer higher heating value to the product liquid [73, 74] and increased yields of phenolic compounds [68, 78], however high lignin feedstocks have also been observed to produce more viscous and unstable pyrolysis liquids [61, 63, 79].

The presence of high ash concentrations, or more specifically alkali metals, has also been shown to have a detrimental effect on product yields and pyrolysis liquid quality parameters. Ash is known to have a catalytic effect on thermal decomposition, higher ash concentrations giving rise to higher yields of char and gas at the expense of the liquid product yield [63, 67]. In addition, the presence of high ash concentrations in the feedstock has also been shown to confer poor thermal stability of the liquid product [61, 67, 79], and a reduction of its heating value due to increased yields of reaction water formed by catalytic cracking of vapours primarily through the increased production of char [59, 61, 67].

2.7.3. Miscanthus as a feedstock for thermo-chemical conversion

In comparison with other lignocellulosic biomass crops, *Miscanthus* has been shown to contain significantly lower concentrations of moisture and ash [72] which are favourable feedstock characteristics for both combustion and pyrolysis processes. A delay of the crop harvest by 3-4 months (to February/March) has been shown to reduce these concentrations further. The EMI field trials conducted by Lewandowski *et al.* (2003) [3] observed reductions in moisture content from 564 to 291 g kg^{-1} (fresh weight) and ash concentrations from 40 to 25 g kg^{-1} as a result of delaying harvest time. In terms of ash composition, *Miscanthus* has been observed to contain lower concentrations of N, K, Cl, and S in the harvested biomass than other energy crops. Delaying the harvest was also found to reduce concentrations of K from 9 to 4 g kg^{-1}, Cl from 4 to 1 g kg^{-1}, and N from 5 to 4 g kg^{-1}, respectively, on a dry matter (DM) basis [3]. Whilst delaying harvest time has been shown to improve combustion quality of the harvested biomass, a reduction in dry matter yield (17 to 14 t ha^{-1}) was also observed. However, the extent of these reductions varied greatly according to site specific factors such as climate, precipitation, and soil type [2, 3, 72]. The influence of agronomic practice (e.g. inorganic fertiliser application) is also likely to influence the dry matter yields and the levels of inorganics present in the harvested biomass. However the extent of this influence has not yet been fully investigated.

At present, there is a lack of knowledge regarding the extent of genetic and environmentally derived variation in cell wall composition within *Miscanthus*, and the influence this variation may have on feedstock quality in terms of conversion by combustion and fast-pyrolysis. In addition to research on agronomic practice, research into the influence of genotype would enable an assessment of the suitability of different *Miscanthus* genotypes to prospective conversion pathways.

2.8. Identifying and harnessing the genetic potential of *Miscanthus*

2.8.1. High throughput screening techniques

Detailed analysis of plant materials using conventional 'wet chemistry' techniques is often labour intensive, time consuming, and expensive. Near infrared reflectance spectroscopy (NIRS) and Fourier-transform infra red (FTIR) spectroscopy techniques represent rapid non-destructive alternatives to a complete analysis of material by conventional wet chemical analyses. NIRS represents a high throughput method for quantitative analysis of chemical composition in plant material which has been used extensively for many years in commercial analysis of animal feeds and forages. The advantage this method has over FTIR is that a greater amount of material can be scanned, therefore providing data which better represents the composition of the sample as a whole.

NIRS operates by measuring variations in the absorption of light by various chemical bonds in certain segments of the infrared spectral range (780 and 2500 nm). In order for NIRS to be used in quantitative measurement, a calibration must be created to map the NIR spectra to the compositional feature of interest (i.e. lignin, protein, nitrogen etc.). Procedures of this kind are collectively referred to as chemometrics. Chemometrics relies on statistical analysis of the relationship that exists between the mathematically transformed NIR spectra and the frequency of chemical bonds in an organic matrix [80]. The organic matrix being the compositional feature of interest which has previously been quantified by wet chemical

analysis. Once a calibration model has been created and verified, quantitative predictions of compositional features may be generated solely from sample spectra. Assessment of the precision (robustness) of calibrations is performed by assessing linearity and accuracy. Linearity is assessed using the coefficient of variation (R^2) which provides an indication of how much of the variation in the reference data is accounted for by the regression equation, and the standard error of calibration (SEC) represents the difference between predicted and reference values [80]. A calibration can be expected to perform with a satisfactory degree of accuracy if the R^2 value is in excess of 0.8, and the SE of prediction is lower than 1.3 x SEC [27]. The accuracy of a calibration can be assessed by cross validation, where the calibration equation is applied to subsets of data from the calibration set and the cross validation R^2 (R^2cv or 1-VR) and cross validation standard error (SECV) scrutinised in the same way as the calibration R^2 and SEC. The overall accuracy of a calibration is assessed when the model is applied to a completely independent sample set of the same type.

The ultimate aim of using this technology would be to utilise its potential as a screening tool to characterise genotypic variation in cell wall composition of energy crops, for the purposes of assessing biomass quality traits in a bio-refinery and to provide a rapid screening tool for plant breeding programmes.

2.8.2. Marker assisted selection and identification of candidate genes

Given the impact of cell wall composition on biomass quality, characterisation of the underlying genetic basis for variation in cell wall polymers would provide an alternative method of selecting *Miscanthus* genotypes with improved quality traits for breeding purposes. Molecular markers may be utilised to determine associations with quantitative trait loci (QTL) for a given trait (e.g. lignin content), and facilitate the identification of specific genes governing aspects of cell wall composition and structure [38, 42]. For the purposes of mapping, the *M x giganteus* genotype is not suitable owing to it being a sterile triploid hybrid.

Therefore, the diploid *M. sinensis* genotype is considered the most promising candidate for mapping, due to its high variability in chemical composition and its smaller genome size. A preliminary genetic linkage map of *M. sinensis* has already been generated by Atienza *et al.* (2002) [81] where an 'offspring cross' mapping strategy coupled with a random amplified polymorphic DNA (RAPD) assay produced the first genetic map of *M. sinensis*. The mapping family was created from a cross between two parent genotypes, one of which had previously been used in the EMI project. QTL identified in this study included those associated with flowering, plant height, and stem diameter traits [81]. The extension of this technology to map QTL's associated with cell wall quality traits in *Miscanthus* would constitute a valuable contribution to knowledge regarding its genetic constitution, improve selection efficiency and enhance breeding strategies.

3. MATERIALS AND METHODS

3.1. Plant material

All harvested material came from mature plants specimens (3 years old) (3.1.1 and 3.1.3.) with the exception of the later harvested Rothamsted EMI material (9 years old) (3.1.2.).

3.1.1. European Miscanthus improvement (EMI) project

The plant materials used for analyses (Chapter 4) comprised samples of 15 Miscanthus genotypes originating from EMI field trials harvested in autumn 1999 and winter 2000 (peak dry matter yield and delayed harvest respectively) from trial sites in England, Denmark, Sweden, Germany and Portugal. Species, genotypes and additional details are listed below in Table 3.1. At all field trial sites genotypes were planted using a randomised block design with three replications per genotype, except in Portugal where only two replicates were planted. Full details of experimental methodology used in the EMI project and detailed information on trial site conditions can be found in Clifton-Brown *et al.* 2001 [2].

Table 3.1 *Miscanthus* species and genotypes used in the EMI field trials.
Table includes *Miscanthus* species and genotypes used in the European *Miscanthus* Improvement (EMI) project listed by genotype identification code including provenance and acquisition details. Adapted from [2].

Code	Provenance	Details
Miscanthus x. giganteus		
EMI01	Larsen, Denmark	No. 16.05 in [82]
EMI02	Knoblauch, Hornum	No. 16.21 in [82]
EMI03	Hagemann, Berlin	No. 17.02 in [82]
EMI04	Griefswald Bot. Gnd.	No. 17.03 in [82]
Miscanthus sacchariflorus		
EMI05	Deuter, Germany	Matumura *et al.*, 1985
Miscanthus sinensis		
EMI06	Deuter, Germany	Hybrid selected in a M. sinensis population
EMI07	Deuter, Germany	Hybrid of two M. sinensis
EMI08	Deuter, Germany	Hybrid of M. sacchariflorus X M. sinensis
EMI09	Deuter, Germany	Hybrid of two M. sinensis
EMI10	Deuter, Germany	Hybrid of M. sacchariflorus X M. sinensis
EMI11	Brander, Denmark	Collected in Honshu, Japan in 1983, selected 1988
EMI12	Brander, Denmark	Collected in Honshu, Japan in 1983, selected 1988
EMI13	Brander, Denmark	Collected in Honshu, Japan in 1983, selected 1990
EMI14	Brander, Denmark	Collected in Honshu, Japan in 1983, selected 1990
EMI15	Andersson, Sweden	Collected Hokkaido, Japan in 1990

All material was received dried and milled, however to ensure sample homogeneity, all material used for analysis was prepared as described in section 3.1.4.

3.1.2. Nitrogen and Potassium fertiliser field trial experiment at Rothamsted Research

Field trials were carried out at Rothamsted Research (Harpenden, UK) as part of the Supergen Bioenergy Research project. The objectives of the experiment were to assess the impact of fertiliser application on dry matter yield, combustion and pyrolysis characteristics of the commercially cultivated hybrid *Miscanthus x giganteus*. The field trial was conducted using a randomised block design with 14 different fertiliser treatments applied to test plots of M. x giganteus grown from clonally propagated stock. The trial site was 84x82 m (0.69 ha) in total, and divided into 3 replicate blocks each containing 14 x 0.012 ha test plots. Fertiliser treatments were allocated at random to each test plot within each of the three replicate blocks as detailed in Table 3.2.

Table 3.2 Fertiliser treatments applied in the field trial experiment conducted at Rothamsted Research.

Table displays details of the 15 nitrogen and potassium fertiliser treatments applied to *M. x giganteus* grown from clonally propagated stock. Details include replicate plot numbers and levels of N, KCl, and K_2SO_4 applied expressed in kg ha^{-1}.

Treatment no.	N	KCl	K_2SO_4	Plot no.
1	0	50	0	02, 15, 33
2	50	100	0	01, 19, 41
3	50	0	0	03, 22, 38
4	50	0	50	04, 26, 36
5	50	50	0	05, 24, 29
6	50	0	100	07, 21, 39
7	100	50	0	13, 27, 42
8	150	100	0	06, 18, 31
9	150	0	100	09, 16, 32
10	150	0	0	10, 17, 37
11	150	50	0	11, 23, 35
12	150	0	50	12, 20, 34
13	200	50	0	14, 28, 40
14	200	50	0	08, 25, 30

The site was planted in 2002 and plant material sampled at 5 time points over the 2005-2006 growing season (Table 3.3). In the first three harvests material was separated into leaf and stem, but this was not performed for subsequent harvests due to senescent leaf loss. Sample material from each harvest was oven dried at 80°C and milled to <1 mm at Rothamsted Research prior to receipt.

Table 3.3 Details of harvests taken over the 2005/2006 growing season.
Table includes harvest number, date, and sample material received from the 2005/2006 growing season.

Harvest	Date	Sample material
1	03/11/05	Leaf and Stem
2	19/12/05	Leaf and Stem
3	01/02/06	Leaf and Stem
4	07/03/06	Stem
5	19/04/06	Stem

3.1.3. EMI field trial plots at Rothamsted Research

The EMI field trial site at Rothamsted Research (Harpenden, UK) was revisited over the 2005/2006 growing season. Samples of the 15 EMI genotypes were harvested in November 2005 and February 2006 to correspond with peak dry matter yield and delayed harvest respectively. Each plot was harvested separately and chipped using a rotary chaff-cutter. A 1kg sub-sample of chipped material was taken from each plot and prepared for analysis as described in 3.1.4. The plant material harvested at both times was used in thermogravimetry (TGA) and pyrolysis gas-chromatography mass-spectrometry (Py-GC-MS) experiments (Chapter 6). Plant material taken from the final harvest in February 2006 was also used in fast-pyrolysis experiments (Chapter 7).

3.1.4. Sample preparation

In order to provide consistent particle size and moisture content, all *Miscanthus* sample material was dried in a draught oven at 80°C for 24 h and milled using a 'Pulverisette 14' (Fritsch) mill operating at 18000 rpm with a 1 mm screen.

3.2. Feedstock characterisation

3.2.1. Moisture content

Sample dry matter (DM) or moisture content was determined gravimetrically, by measuring the difference in weight after drying in an air circulated oven at 102 ± 2 °C for 16 h.

3.2.2. Ash

Ash content of samples was determined by 'loss on ignition' after incineration in a muffle furnace at 550 °C for 5 h.

3.2.3. Acid detergent lignin (ADL)

Acid detergent lignin (ADL) content was determined using the Van Soest method [83]. ADL was determined gravimetrically by first obtaining the acid detergent residue, then treating it with 72 % sulphuric acid to solubilise cellulose and isolate crude lignin plus ash.

3.2.4. Neutral detergent fibre (NDF)

Neutral detergent fibre (NDF) was determined using the Gerhardt fibrecap system [84]. NDF is the fibre fraction regarded as cell wall and is the residue, corrected for ash, after refluxing the sample for 1 h in a neutral detergent solution.

3.2.5. Acid detergent fibre (ADF)

Acid detergent fibre (ADF) was determined using the Gerhardt fibrecap system [85]. ADF is defined as the loss on ignition of the dried residue remaining after digestion with an acid detergent solution.

3.2.6. Cellulose and hemicellulose

The cellulose and hemicellulose content of samples were derived from the predicted values generated for lignin, ADF and NDF analyses. Given that ADF consists of cellulose and lignin, and NDF comprises cellulose, hemicellulose and lignin, the cellulose and hemicellulose content of samples are calculated by the equations: Cellulose = ADF – ADL; Hemicellulose = NDF – ADF.

3.2.7. Near infrared spectroscopy (NIRS)

For the determination of cell wall fractions, samples were analysed using near infrared reflectance spectroscopy (NIRS) (absorbance) and prediction equations developed for lignin, ADF and NDF using data from spectral and wet chemical analyses. Biomass samples were analysed using a NIRSystems 6500 spectrophotometer, operating with WinISI^{TM} software (FOSS UK Limited, Warrington, UK). Samples were mixed thoroughly and scanned in small ring cells with a quartz glass window (50 mm diameter, 10 mm depth) held in place with a disposable cardboard backing. Samples were scanned over the NIR spectral range (400-2500 nm). Each individual sample was scanned 24 times and the results averaged to produce a mean spectrum with 1050 data points, collected at 2 nm intervals. All samples were scanned in duplicate and duplicate scans were averaged to produce one final spectrum for each sample.

3.2.8. Higher and lower heating values of Miscanthus biomass

Ultimate analysis of pyrolysis *Miscanthus* biomass was performed by MEDAC Ltd. (Surrey, UK). The relative percentage content of carbon, hydrogen, nitrogen, and sulphur was determined and the oxygen content calculated by difference and corrected for ash.

Higher heating values (HHV) were calculated from the results of the elemental analysis using the following equation proposed by Channiwala and Parikh, 2002 [86], where C, H, N, S, O

correspond to the percentage content of carbon, hydrogen, nitrogen, sulphur, and oxygen respectively as determined from the ultimate analysis:

$$HHV^{dry}\ (MJ\ kg^{-1}) = 0.3491C + 1.1783H + 0.1005S - 0.1034O - 0.015N - 0.0211Ash$$

This method was selected as the equation developed by Channiwala and Parikh (2002) represents a unified equation for predicting the HHV of solid, liquid, and gaseous fuels. Therefore, the same equation could be used consistently for predicting the HHV of both the solid biomass and the resulting pyrolysis liquid.

The lower heating value (LHV) was calculated from the HHV and hydrogen values using the following equation proposed by the Energy Research Centre of the Netherlands (ECN) [87]:

$$LHV^{dry}\ (MJ\ kg^{-1}) = HHV^{dry} - 2.442*(8.936H/100)$$

3.2.9. Thermo-gravimetric analysis (TGA)

TGA experiments were carried out using a Perkin-Elmer Pyris 1 thermogravimetric analyser. Samples were pyrolysed in nitrogen at a flow rate of 20 mL min^{-1} using the following temperature program: heat from 40–105°C at 10°C min^{-1}; hold at 105°C for 10 min; heat from 105-905°C at 10, 25, and 100°C min^{-1}; hold at 905°C for 15 min; cool from 905-105°C at 25°C min^{-1}.

A proximate analysis was performed on the TGA data to calculate the relative proportions (wt%) of moisture, volatiles, and char (ash + fixed carbon) for each sample. The moisture content was calculated from the mass loss which occurred between 40-105°C, the volatiles from the mass loss between 105-550°C, and the char from 550-900°C (Fig. 3.1). Ash content was determined gravimetrically as described in section 3.2.2.

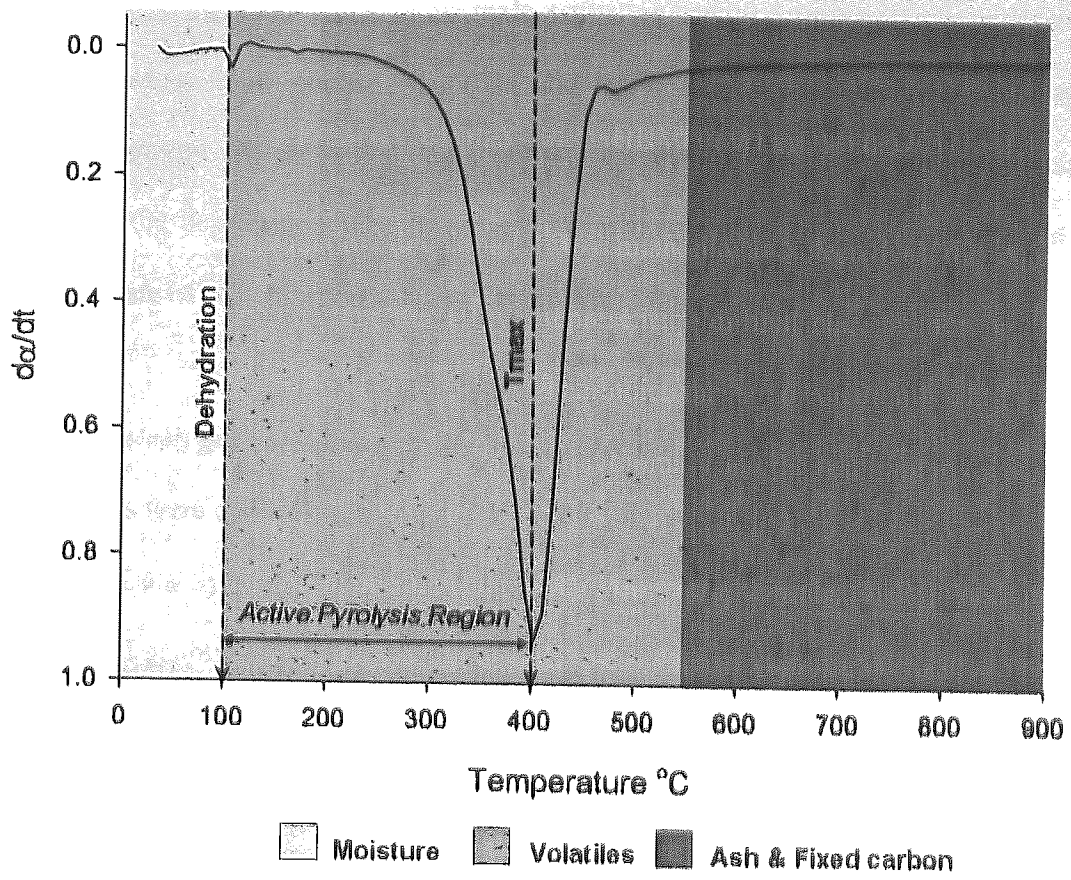

Figure 3.1 Annotated example of a derivative (dα/dt) curve from TGA
The figure displays an example derivative curve produced from TGA analysis of a *Miscanthus* genotype at a single heating rate (100°C min^{-1}). The figure includes the temperature ranges over which the proximate data was calculated and indicates the 'active pyrolysis region' from which the activation energies were calculated.

Activation energies were calculated for each genotype over the 'active pyrolysis region' which was defined as the degradation which occurred between dehydration and the temperature at which maximum evolution of products occurred (Tmax) as determined from the derivative curve (DTG) which is a function of mass-loss over time (Fig. 3.1). The kinetic analysis was performed according to the method suggested by Friedman *et al.* (1965) using the following equation [88]:

$$(-1/w_0)(dw/dt) = Ae^{-E/RT}f(w/w_0)$$

Where: w = weight of organic material; w_0 = total weight of sample; t = time (h^{-1}); Ae = pre-exponential factor; E = activation energy; R = gas constant; T = absolute temperature.

This method was selected on the basis that it was developed to predict activation energies for the main degradation process of complex polymers without any prior knowledge of the form

of the kinetic equation. It was identified that the use of multiple heating rates can aid in the development of equations to better estimate activation energy for the polymer under analysis. For this reason, three heating rates (10, 25, 100°C min^{-1}) were used to calculate mean activation energy for the main degradation process. The main degradation process was defined as the degradation which occurred from dehydration to the temperature at which maximum rate of volatilisation occurs (*T*max) (Fig. 3.1).

3.2.10. Pyrolysis gas chromatography - mass spectrometry (Py-GC-MS)

Experiments were carried out using a CDS 2000 pyroprobe and a CDS AS-2500 autosampler (Chemical Data Systems, US). Sub-samples from the 3 biological replicates of each of the five selected genotypes were used in the analysis. 0.5 ± 0.05 mg of sample was loaded into a quartz tube and heated to 500°C at a heating rate of 3000°C s^{-1} and held at 500°C for 10 seconds. The carrier gas used was Helium with a flow rate of 38 cm s^{-1}. An AutoSystem XL Gas Chromatograph (Perkin-Elmer, UK) fitted with a DB 1701 column (60 m x 25 µm with 0.25 µm film thickness) was used to separate vapours produced with a split ratio of 1:25. The oven program held the temperature at 45°C for 4 min then heated to 280°C at a rate of 4°C min^{-1}. The injector and detector temperatures were set at 280°C. Electron impact mass spectra were obtained using MS GOLD software (Perkin–Elmer, UK) at 70 eV, and the mass range from *m/z* 28–600 was scanned.

Data processing was performed using the National Institute of Science and Technology (NIST) Automated Mass spectral Deconvolution and Identification System (AMDIS, (v2.65) and compound identification was performed using the Perkin-Elmer NIST mass spectral library in combination with referenced data from the literature [89-93]. Data reported for key marker compounds is presented in data tables as 'amount' and is the area of the component peak relative to the total ion count (TIC) for the entire chromatogram expressed as a percentage.

3.3. Fast pyrolysis experiments: Aston bench-scale (150 g hr^{-1}) fast-pyrolysis system.

Fast-pyrolysis was performed using a bench scale 150 g hr^{-1} experimental rig with a fluidised bed reactor, designed and operated at Aston University (Birmingham, UK). The reactor consisted of a 316 stainless steel cylinder 26 cm in length and 4 cm in diameter. The heat transfer medium used for the fluidised bed was quartz sand. Approximately 150 g of quartz sand was used in the fluidised bed in a particle size range of 355-500 μm, and was fluidised by a flow of N_2 at a rate of approximately 6 L min^{-1}. The reactor was placed inside a furnace and all exposed parts of the reactor including the transition pipe were wrapped in insulating material. The furnace was set to maintain a constant reactor operating temperature of approximately 500°C. *Miscanthus* biomass in a particle size range of 250-355 μm was fed into the reactor using an entrained flow of N_2 from a feeder unit fitted with a rotary paddle stirrer. Full details of experimental set-up and operation of the fast-pyrolysis rig are described in section 7.2.

3.4. Pyrolysis product characterisation

3.4.1. Mass balance calculation

The mass balance was calculated as the sum of the differences in weight of all rig components pre and post pyrolysis processing plus the calculated weight of non-condensable gases produced expressed as a percentage of total amount of biomass fed on a dry matter basis.

Feed rate was calculated as the total amount of biomass fed over the whole run and expressed in g hr^{-1}. Pyrolysis temperature was calculated as the mean temperature (°C) in the reactor bed over the whole run as detected by two thermocouples: one in the reactor bed and one at the feeding tube outlet.

3.4.2. Non-condensable gases

Throughout the pyrolysis run samples of non-condensable gases were sent to the on-line GC system every 3 min. Analysis was performed using a CP-4900 micro gas chromatograph with

a thermal conductivity detector equipped with two columns (CP-molsieve 5A and CP-PoraPLOT) (Varian Chromatography Systems Inc., NE) using Helium (He) as the carrier gas. The molecular-sieve coated capillary column (CP-Molsieve 5A) was used for separation of carbon monoxide (CO), hydrogen (H_2), nitrogen (N_2), oxygen (O_2), and methane (CH_4). The CP-PoraPLOT column was used for the separation of carbon dioxide (CO_2), ethene (C_2H_4), Ethane (C_2H_6), Propene (C_3H_6) and Propane (C_3H_8). Varian Star Chromatography Workstation 6.0 software (Varian Chromatography Systems Inc., NE) was used for quantitative analysis of non-condensable gases produced during pyrolysis. Prior to each run columns were calibrated using a standard gas mixture of known composition.

3.4.3. Water content

The water content of pyrolysis liquids was determined by the Karl-Fischer (KF) titration method. All analyses were performed using a Metrohm 758 KFD Titrino instrument. Before each set of analyses the instrument was calibrated with HPLC-grade water and the system flushed between samples. Sub-samples of liquids were analysed in triplicate with the water content calculated automatically based on the weight of sample injected. All analyses were performed in triplicate.

3.4.4. Molecular weight distribution

The molecular weight distribution of pyrolysis liquid samples was determined by gel permeation chromatography (GPC). An integrated GPC system consisting of a PL-GPC50 unit (Polymer Laboratories, UK) fitted with a PLgel 3 µm MIXED-E 300 x 7.5 mm column and a refractive index detector was used for analyses. HPLC-grade tetrahydrofuran (THF) was used as the eluent with a flow rate of 1 ml min^{-1}. Prior to injecting samples, the instrument was calibrated using a series of polystyrene calibration standards with a molecular weight range of 162-19880 g mol^{-1}. Pyrolysis liquid samples were dissolved in HPLC-grade THF to a concentration of 0.01 g ml^{-1} and passed through a disposable 2 µm Millipore Millex-GN

nylon filter to remove any solids retained in the liquid fraction. Samples were injected using a PL-AS RT GPC auto-sampler (Polymer Laboratories, UK) and the weight average molecular weight (Mw), number average molecular weight (Mn), molecular weight at highest peak (Mp) and poly-dispersity (PD) values were calculated by Cirrus 3.0 software (Polymer Laboratories, UK) based on peak areas obtained by the refractive index signal and calibration curves generated for the calibration standards. All analyses were performed in duplicate.

3.4.5. Pyrolysis liquid stability

A sub-sample of pyrolysis liquid (oil pot 1) was subjected to accelerated aging by incubating at 80°C for 24 h. Aging which occurs at this time and temperature has been approximated to that which would occur after one year if the sample was stored at ambient temperature [94]. Sub-samples of fresh and aged pyrolysis liquids were analysed using gel permeation chromatography and the stability calculated by the following equation [79]:

$$\text{Stability index} = \frac{\text{Mw } aged - \text{Mw } Fresh}{\text{Mw } Fresh}$$

3.4.6. Liquid injection gas chromatography - mass spectrometry

A Perkin-Elmer AutoSystem XL Gas Chromatograph fitted with a DB 1701 column (30 m x 25 μm with 0.25 μm film thickness) preceded by a 10 m guard column was used for analyses. Pyrolysis liquid samples were dissolved in ethanol at a dilution of 1:10. 1 μl of pyrolysis liquid in ethanol was injected and a split ratio of 5:1 was used for all analyses. The oven program, mass spectral data collection, processing and interpretation was performed as described in section 3.2.10. Analyses were performed in duplicate.

3.4.7. Ultimate analysis and determination of heating values from pyrolysis liquids

Ultimate analysis of pyrolysis liquids collected in oil pot 1 was performed by MEDAC Ltd. (Surrey, UK). The relative percentage content of carbon, hydrogen, nitrogen, and sulphur was determined and the oxygen content calculated by difference and corrected for ash.

Higher heating values (HHV) and lower heating values (LHV) were calculated from the results of the elemental analysis using the equations as described in section 3.2.8 [86, 87]. Both the HHV and LHV values were subsequently corrected for the water present in the pyrolysis liquid as determined by the Karl-Fischer titration (% wt) (3.4.3). Conversion of the HHV and LHV values from a 'dry' to a 'wet' basis was performed using the following equations proposed by the Energy Research Centre of the Netherlands (ECN) [87]:

$$HHV^{wet}\ (MJ\ kg^{-1}) = HHV^{dry} * (1-H_2O/100)$$
$$LHV^{wet}\ (MJ\ kg^{-1}) = LHV^{dry} * (1-H_2O/100) - 2.442 * (H_2O/100)$$

3.5. Statistical analysis

All statistical analyses applied to data were performed using the Genstat statistical software package (9th edition, VSN International Ltd.). One-way and two-way analyses of variance (ANOVA) were used to identify significance differences in cell wall composition of *Miscanthus* genotypes within and between country groups for each harvest. Subsequently, the student Newman-Keuls multiple comparison analysis (P=0.05) was applied to the data to identify which genotypes were significantly different from each other within and between sites for each harvest. For ease of presentation, least significant differences (LSD) were used in tables to identify where significant differences were found to exist within the data and were expressed in the same units as the data described (e.g. g kg^{-1}). Correlation of data sets was performed in Microsoft Office Excel (2003) using the Pearson product moment correlation coefficient (R= -1.0 to 1.0) which reflects the extent of a linear relationship between two data sets.

4. GENOTYPIC AND ENVIRONMENTALLY DERIVED VARIATION IN THE CELL WALL COMPOSITION OF *MISCANTHUS*.

4.1. Chapter introduction

Fifteen *Miscanthus* genotypes grown in five locations across Europe were analysed to investigate the influence of genetic and environmental factors on cell wall composition. Chemometric techniques combining near infrared reflectance spectroscopy (NIRS) and conventional chemical analyses were used to construct calibration models for determination of acid detergent lignin (ADL), acid detergent fibre (ADF), and neutral detergent fibre (NDF) from sample spectra. Results generated were subsequently converted to lignin, cellulose and hemicellulose concentration and used to assess genetic and environmental variation in cell wall composition and to identify genotypes which display quality traits suitable for exploitation in a range of energy conversion systems.

4.1.1. The EMI project: key results and conclusions

This work represents a continuation of the research performed under the EU funded European Miscanthus Improvement (EMI) project [2, 72]. The primary objective of which was to evaluate the biomass production potential of fifteen *Miscanthus* genotypes under different environmental conditions. Field trials were conducted at five sites across Europe (Denmark, Sweden, UK, Germany, and Portugal) over a period of three years to investigate the potential for different *Miscanthus* genotypes to overcome several performance limitations inherent in the most widely planted clone, namely *M. x giganteus* Greef et Deuter. [45]. The EMI field trials identified that delaying the harvest time by 3-4 months (winter harvest), or until plants have fully senesced, may reduce moisture concentration from 564 to 291 g kg^{-1} and ash concentration from 40 to 25 g kg^{-1} [3]. Reductions were also observed in the dry matter concentration of alkali metals such as K (from 9-4 g kg^{-1}), Cl (from 4 to 1 g kg^{-1}), and N (from 5 to 4 g kg^{-1}) as a result of delaying the harvest [3]. However, a mean reduction in total

biomass dry matter yield was also observed to result from the delayed harvest time, reducing yield from 17 to 14 t ha^{-1} [2, 26, 72].

4.2. Materials and methods

4.2.1. Plant material

All plant material used for analysis was prepared as described in sections 3.1.1 and 3.1.4. Details of the analyses used were described in sections 3.2.1 - 3.2.7.

Due to adverse environmental conditions during establishment neither the *M. sacchariflorus* genotype planted in Sweden, nor the *M. x giganteus* genotypes (EMI01-04) planted in Denmark or Sweden survived the first winter [2], therefore no sample material for these genotypes was available for analysis. Details of replicate plots and total sample numbers are shown by country of origin in Table 4.1. The locations of trial sites are illustrated on the map in Figure 4.1 which also shows the predicted harvestable yield of *Miscanthus* adapted from Stampfl *et al.* (2007) [4].

Table 4.1 EMI samples analysed, listed by country and trial site.
The table displays the total number of replications and total number of samples received and analysed from the EMI trial sites.

Country	Trial site	Replicates	Samples
Denmark	Foulum	3	66
Sweden	Landskrona	3	60
England	Rothamsted	3	90
Germany	Hoenheim	3	90
Portugal	Evora	2	60
Total		14	366

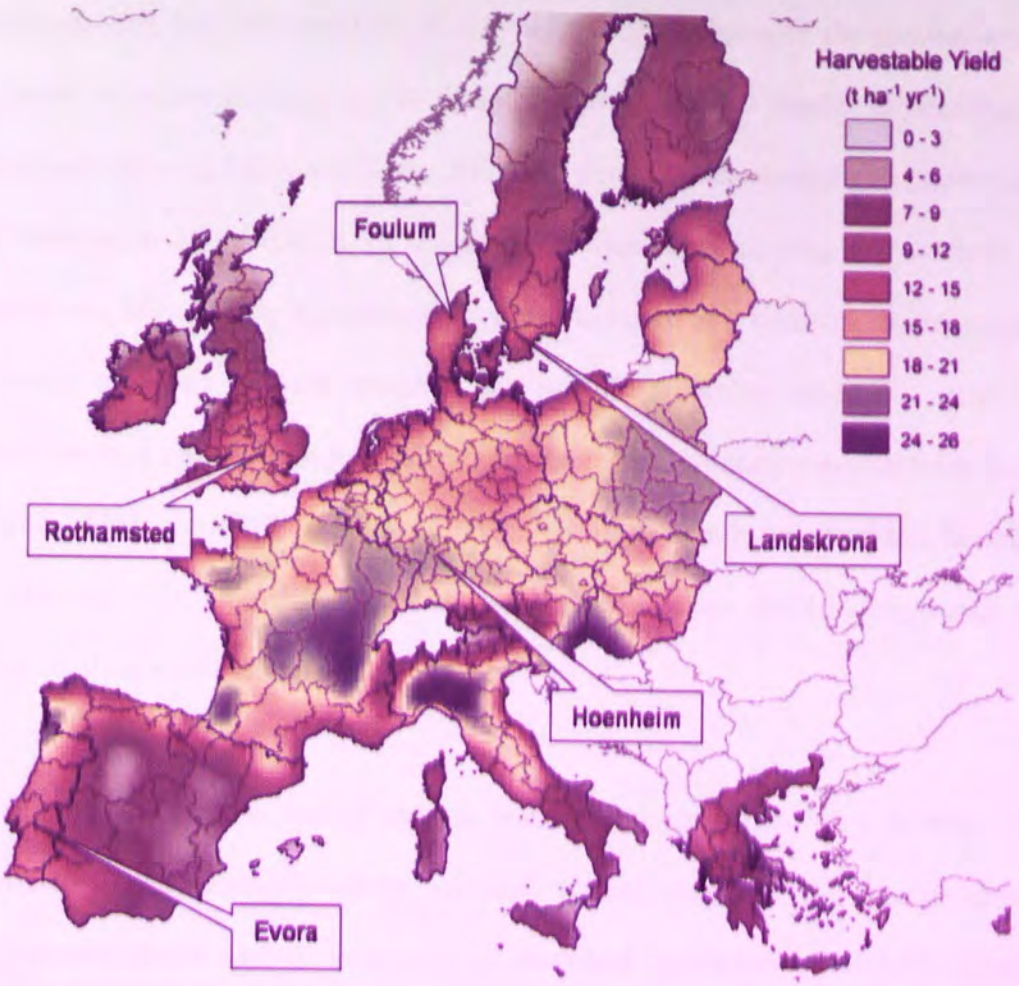

Figure 4.1 Locations of EMI project trial sites and predicted harvestable *Miscanthus* yields across Europe

The locations of field trial sites used in the European Miscanthus Improvement (EMI) project are indicated on a map illustrating the harvestable yield of *Miscanthus* (t ha^{-1} yr^{-1}) across Europe predicted using the GIS modelling system MISCANMOD. Adapted from Stampfl *et al.* (2007) [4].

4.2.2. Development of NIRS calibration for determination of cell wall composition

The WinISI™ software was used to define an appropriate population for the selection of samples for the calibration set. The mean spectrum for each genotype and country was calculated and a principle component analysis (PCA) was performed on the spectra. PCA loading-scores were calculated for the population (all samples from the 5 countries) producing a 3-D plot displaying global H (GH) distances of each sample spectrum. The global H distance is defined as the distance of every sample from the centre of the spectral hypersphere. The neighbourhood H (NH) distances were then calculated for each sample spectrum, NH distance defined as the distance between each sample and its neighbour.

Sample selection was performed by identifying those samples with the greatest number of neighbours within an NH limit of 1.0. Samples with the greatest number of neighbours were retained, and all neighbours within this NH limit were eliminated until all samples had been either selected or eliminated. A 76 sample calibration set combining spectra from all five countries was identified by this selection process and used as a basis for the development of calibration equations. In the development of the calibration equation, only spectral information from the 1100-2500 nm region was included. Calibration models were developed for lignin, ADF, and NDF using ISI-NIRS2 Version 4.00 software (Infrasoft International, Port Matilda, USA) utilising modified partial least squares (mPLS) regression for the generation of the calibration equations.

To minimise effects from factors such as particle size, scatter, packing density, moisture concentration, and multi-collinearity, standard normal variate (SNV) and de-trend (DT) transformations were applied to spectra as described by Barnes *et al.* [95]. During the development of the calibration, two different mathematical treatments were applied to the data i.e. 1,4,4,1 and 2,6,4,1. The first number indicates the order of the derivative (1 being the first derivative, 2 being the second), the second number is the gap in data-points over which the derivative was calculated, and the third and fourth numbers refer to the number of data-points used in the smoothing of the 1^{st} and 2^{nd} derivative.

Cross validation was used to select the optimum number of factors for the equation, as described by Stone [96]. Inclusion of too few factors may result in a loss of prediction accuracy whereas inclusion of too many factors increases the likelihood that the equation may 'over-fit' the data. Validation errors were combined to give a standard error of cross validation (SE_{cv}) and the optimum number of factors for each equation was determined by identifying the number which gave the lowest SE_{cv} value. The mathematical treatments used

in the final calibration equations were those which generated the lowest calibration standard error (SE_c), the lowest SE_{cv}, and the highest calibration and cross validation R^2 value (R^2_{cv}).

4.3. Results and discussion

4.3.1. Determination of cell wall composition by NIRS

The calibration and cross validation statistics for each of the developed equations are shown in Table 4.2. The mathematical treatment 1,4,4,1 was selected for use in equations developed for the prediction of lignin (ADL % DM) and ADF (% DM), whereas 2,6,4,1 was selected for use in the equation developed for the prediction of NDF (% DM). The mathematical treatments utilised in equations were selected on the basis of the standard error of cross-validation (SE_{cv}), which provides an indication of the accuracy of prediction for equations developed using the 76 sample calibration set. The model developed for the prediction of ADF (% DM) yielded standard error of calibration (SEC) and SECV values of 1.21 and 1.74 respectively, and coefficient of determination (R^2) and coefficient of determination for cross-validation (R^2_{cv}) values of 0.95 and 0.90 respectively (Table 4.2). The model developed for the prediction of NDF (% DM) resulted in SEC and SECV values of 1.05 and 1.36 respectively, and R^2 and R^2_{cv} values of 0.96 and 0.93 respectively (Table 4.2). A good relationship was observed between NIRS predicted and actual laboratory ADF and NDF (%DM) for the 76 samples used for calibration.

Table 4.2 Calibration and cross validation statistics for developed equations.
The table displays the mathematical treatments applied and number of factors used in the equations developed for acid detergent fibre, neutral detergent fibre, and acid detergent lignin. The R^2 statistics and standard errors of correlation (SE_c) and cross-validation (SE_{cv}) statistics are also included.

Variate	Treatment	Factors	SE_c	R^2	SE_{cv}	R^2_{cv}
ADF	1,4,4,1	8	1.21	0.95	1.74	0.90
NDF	2,6,4,1	7	1.05	0.96	1.36	0.93
ADL	1,4,4,1	5	0.58	0.82	0.69	0.75

The calibration model developed for the prediction of lignin (% DM) in *Miscanthus* samples yielded the lowest R^2 and R^2_{cv} values of all the equations developed, 0.82 and 0.75

respectively (Table 4.2). However, the R^2 and standard error (SE_c) values from the statistical analysis on the calibration equations indicated that the lignin, ADF, and NDF concentrations of *Miscanthus* samples were predicted with a good degree of accuracy, based on all R^2 and R^2_{cv} values being higher than 0.8, and SECV values being within the standard control limits suggested by Sanderson *et al.* [27]. The lignin, ADF, and NDF concentrations for all 366 EMI samples were therefore predicted using the developed equations. The cellulose and hemicellulose concentration of samples were derived by subtracting corresponding values from the predicted values generated for lignin, ADF, and NDF (3.2.6). The results for lignin, hemicellulose, and cellulose concentrations (g kg^{-1}) are displayed in Tables 4.3-4.8, including the results of the analyses of variance performed on the data to identify where significant genotypic and environmental differences in cell wall composition were found to exist within the data.

Table 4.3 Lignin concentration of *Miscanthus* species and genotypes harvested in autumn 1999.

Values are reported in g kg^{-1} on a dry matter basis as determined by the NIRS calibration. The table includes the means, standard deviations and the results of analyses of variance performed on all genotypes within and between countries including levels of significance where identified. Least significant differences (LSD) are reported in g kg^{-1} on a dry matter basis.

Genotype	Denmark	Sweden	England	Germany	Portugal	Mean	SD	df	$P\leq$	LSD
EMI01			82.4	86.8	88.5	85.9	3.1	2	n/s	
EMI02			92.6	94.7	82.0	89.8	6.8	2	n/s	
EMI03			93.3	93.5	82.8	89.9	6.1	2	n/s	
EMI04			84.8	93.8	87.0	88.5	4.7	2	n/s	
EMI05	79.7		86.8	90.1	92.6	87.3	5.6	3	**	10.4
EMI06	88.6	80.7	81.7	74.3	78.7	80.8	5.2	4	**	6.9
EMI07	80.2	66.9	80.6	72.2	85.2	77.0	7.4	4	**	13.4
EMI08	78.2	73.8	60.4	79.6	74.4	73.3	7.6	4	**	13.4
EMI09	64.8	73.0	69.6	66.3	75.8	69.9	4.6	4	***	2.8
EMI10	79.0	78.6	72.9	80.1	72.5	76.6	3.6	4	n/s	
EMI11	88.6	77.0	85.9	80.9	75.4	81.6	5.7	4	n/s	
EMI12	86.3	73.6	81.7	76.6	70.3	77.7	6.4	4	**	9.7
EMI13	81.1	75.1	73.5	73.7	71.1	74.9	3.8	4	n/s	
EMI14	78.9	78.9	76.7	79.2	69.9	76.7	3.9	4	n/s	
EMI15	83.7	85.0	80.7	78.5	71.8	79.9	5.2	4	**	6.7
Mean	80.8	76.3	80.2	81.4	78.5					
SD	6.6	5.0	8.7	8.6	7.4					
Df	20	18	28	28	28					
$P\leq$	***	***	***	***	***					
LSD	9.6	7.7	14.0	13.1	8.5					

SD= standard deviation; df = degrees of freedom; *** $P\leq0.001$; ** $P\leq0.05$; n/s = no significant difference ($P\geq0.05$); LSD= least significant difference ($P\leq0.05$).

Table 4.4 Lignin concentration of *Miscanthus* species and genotypes harvested in winter 2000.

Values are reported in g kg^{-1} on a dry matter basis as determined by the NIRS calibration. The table includes the means, standard deviations and the results of analyses of variance performed on all genotypes within and between countries including levels of significance where identified. Least significant differences (LSD) are reported in g kg^{-1} on a dry matter basis.

Genotype	Denmark	Sweden	England	Germany	Portugal	Mean	SD	df	$P\leq$	LSD
EMI01			97.9	100.0	111.4	103.1	7.3	2	n/s	
EMI02			105.8	105.2	112.6	107.9	4.1	2	n/s	
EMI03			106.6	106.3	113.4	108.8	4.0	2	n/s	
EMI04			102.7	104.5	113.0	106.7	5.5	2	n/s	
EMI05	97.7		106.0	104.5	114.5	105.7	6.9	3	**	8.3
EMI06	100.2	94.9	93.6	90.9	84.5	92.8	5.8	4	**	15.7
EMI07	90.3	101.0	82.8	87.2	95.2	91.3	7.1	4	***	4.9
EMI08	105.7	93.8	75.7	88.9	87.1	90.2	10.9	4	**	30.0
EMI09	82.0	108.6	76.9	81.7	90.0	87.8	12.5	4	***	8.3
EMI10	103.5	98.1	85.5	91.0	87.9	93.2	7.5	4	***	5.5
EMI11	105.6	92.8	92.5	95.2	82.1	93.6	8.4	4	**	10.4
EMI12	104.2	90.2	88.4	90.4	89.6	92.6	6.6	4	**	13.8
EMI13	93.1	88.3	86.8	85.2	83.7	87.4	3.6	4	n/s	
EMI14	98.0	87.4	81.1	88.2	84.2	87.8	6.4	4	***	6.3
EMI15	97.7	93.0	89.8	88.3	89.5	91.7	3.8	4	n/s	
Mean	98.0	94.8	91.5	93.8	95.9					
SD	7.3	6.4	10.5	8.2	12.9					
Df	20	18	28	28	28					
$P\leq$	***	***	***	***	***					
LSD	7.0	10.5	18.3	7.0	13.2					

SD= standard deviation; df = degrees of freedom; *** $P\leq0.001$; ** $P\leq0.05$; n/s = no significant difference ($P\geq0.05$); LSD= least significant difference ($P\leq0.05$).

Table 4.5 Hemicellulose concentration of *Miscanthus* species and genotypes harvested in autumn 1999.

Values are reported in g kg^{-1} on a dry matter basis as determined by the NIRS calibration. The table includes the means, standard deviations and the results of analyses of variance performed on all genotypes within and between countries including levels of significance where identified. Least significant differences (LSD) are reported in g kg^{-1} on a dry matter basis.

Genotype	Denmark	Sweden	England	Germany	Portugal	Mean	SD	df	$P\leq$	LSD
EMI01			273.1	267.7	254.4	265.1	9.6	2	n/s	
EMI02			255.3	244.3	265.5	255.0	10.6	2	n/s	
EMI03			253.8	246.4	265.6	255.3	9.7	2	n/s	
EMI04			267.4	247.7	252.9	256.0	10.2	2	n/s	
EMI05	300.0		276.4	256.6	236.4	267.4	27.2	3	**	23.6
EMI06	283.1	296.5	309.8	321.1	290.7	300.2	15.2	4	**	38.0
EMI07	282.9	324.6	282.8	308.4	273.3	294.4	21.3	4	**	41.7
EMI08	286.6	297.3	344.1	276.4	287.9	298.5	26.6	4	***	46.8
EMI09	324.0	323.5	312.1	319.1	282.3	312.2	17.4	4	***	11.9
EMI10	278.7	309.6	310.7	303.4	281.5	296.8	15.5	4	**	7.3
EMI11	295.3	318.3	322.9	317.2	281.0	306.9	18.0	4	**	36.2
EMI12	297.4	323.4	329.6	315.3	282.8	309.7	19.3	4	n/s	
EMI13	298.1	328.0	325.2	321.8	301.2	314.9	14.1	4	**	29.9
EMI14	303.5	321.3	334.5	316.1	279.0	310.9	21.0	4	***	12.6
EMI15	297.6	314.5	318.0	318.5	281.5	306.0	16.2	4	**	33.0
Mean	295.2	315.7	301.1	292.0	274.40					
SD	12.6	11.2	30.0	31.3	16.8					
Df	20	18	28	28	28					
$P\leq$	***	***	***	***	***					
LSD	13.5	31.6	26.2	32.1	37.8					

SD= standard deviation; df = degrees of freedom; *** $P\leq0.001$; ** $P\leq0.05$; n/s = no significant difference ($P\geq0.05$); LSD= least significant difference ($P\leq0.05$).

Table 4.6 Hemicellulose concentration of *Miscanthus* species and genotypes harvested in winter 2000.

Values are reported in g kg^{-1} on a dry matter basis as determined by the NIRS calibration. The table includes the means, standard deviations and the results of analyses of variance performed on all genotypes within and between countries including levels of significance where identified. Least significant differences (LSD) are reported in g kg^{-1} on a dry matter basis.

Genotype	Denmark	Sweden	England	Germany	Portugal	Mean	SD	df	$P\leq$	LSD
EMI01			269.4	258.9	243.3	257.2	13.1	2	n/s	
EMI02			249.0	247.7	245.7	247.5	1.7	2	n/s	
EMI03			250.7	238.3	237.9	242.3	7.3	2	n/s	
EMI04			251.3	247.0	244.0	247.4	3.7	2	n/s	
EMI05	296.7		265.2	251.8	235.1	262.2	26.1	3	***	30.1
EMI06	292.2	310.7	302.2	312.3	282.5	300.0	12.6	4	n/s	
EMI07	296.3	281.9	294.8	307.1	283.8	292.8	10.3	4	**	10.7
EMI08	271.3	308.0	315.8	282.3	260.6	287.6	23.6	4	***	21.6
EMI09	320.2	253.7	302.1	311.0	274.2	292.2	27.6	4	***	18.1
EMI10	269.7	288.8	308.9	292.8	272.6	286.6	16.0	4	**	20.2
EMI11	281.7	317.0	318.2	311.0	278.4	301.3	19.6	4	n/s	
EMI12	291.3	320.7	324.6	320.9	260.0	303.5	27.8	4	**	33.4
EMI13	305.4	320.7	321.0	326.2	297.8	314.2	12.0	4	n/s	
EMI14	303.9	328.9	338.5	316.6	276.2	312.8	24.3	4	***	9.5
EMI15	304.1	315.8	305.5	316.3	257.9	299.9	24.2	4	**	46.1
Mean	293.9	304.6	294.5	289.4	263.3					
SD	15.2	23.1	29.7	31.8	19.2					
Df	20	18	28	28	28					
$P\leq$	***	***	***	***	***					
LSD	14.5	26.2	36.4	28.1	45.9					

SD= standard deviation; df = degrees of freedom; *** $P\leq0.001$; ** $P\leq0.05$; n/s = no significant difference ($P\geq0.05$); LSD= least significant difference ($P\leq0.05$).

Table 4.7 Cellulose concentration of Miscanthus species and genotypes harvested in autumn 1999.

Values are reported in g kg^{-1} on a dry matter basis as determined by the NIRS calibration. The table includes the means, standard deviations and the results of analyses of variance performed on all genotypes within and between countries including levels of significance where identified. Least significant differences (LSD) are reported in g kg^{-1} on a dry matter basis.

Genotype	Denmark	Sweden	England	Germany	Portugal	Mean	SD	df	$P\leq$	LSD
EMI01			457.0	431.1	390.8	426.3	33.4	2	**	40.3
EMI02			458.2	426.8	404.3	429.8	27.1	2	n/s	
EMI03			444.2	419.4	394.3	419.3	25.0	2	n/s	
EMI04			455.2	414.5	389.6	419.8	33.1	2	**	40.6
EMI05	361.2		427.9	426.9	403.4	404.9	31.2	3	**	42.3
EMI06	423.7	443.5	441.6	410.9	375.1	419.0	28.0	4	***	30.7
EMI07	412.5	422.3	434.6	385.6	406.5	412.3	18.3	4	n/s	
EMI08	381.7	406.6	416.2	398.9	388.4	398.4	13.8	4	n/s	
EMI09	336.0	387.2	371.9	367.1	365.7	365.6	18.6	4	**	21.5
EMI10	384.9	405.1	431.3	421.3	377.8	404.1	22.9	4	**	27.4
EMI11	400.5	413.7	415.5	432.7	349.8	402.4	31.6	4	**	32.3
EMI12	394.5	406.4	409.9	435.1	345.3	398.2	33.1	4	**	49.3
EMI13	405.8	414.8	394.4	422.0	340.3	395.5	32.5	4	**	27.7
EMI14	398.6	433.0	399.0	428.8	350.2	401.9	33.1	4	**	34.6
EMI15	425.0	469.5	433.1	440.1	326.4	418.8	54.3	4	***	8.1
Mean	393.1	420.2	426.0	417.4	373.9					
SD	26.6	23.4	24.9	19.9	26.0					
Df	20	18	28	28	28					
$P\leq$	***	***	***	***	***					
LSD	27.7	25.9	49.9	43.2	66.2					

SD= standard deviation; df = degrees of freedom; *** $P\leq0.001$; ** $P\leq0.05$; n/s = no significant difference ($P\geq0.05$); LSD= least significant difference ($P\leq0.05$).

Table 4.8 Cellulose concentration of *Miscanthus* species and genotypes in winter 2000. Values are reported in g kg^{-1} on a dry matter basis as determined by the NIRS calibration. The table includes the means, standard deviations and the results of analyses of variance performed on all genotypes within and between countries including levels of significance where identified. Least significant differences (LSD) are reported in g kg^{-1} on a dry matter basis.

Genotype	Denmark	Sweden	England	Germany	Portugal	Mean	SD	df	$P\leq$	LSD
EMI01			485.6	448.0	495.1	476.2	24.9	2	n/s	
EMI02			507.8	463.6	485.6	485.7	22.1	2	n/s	
EMI03			498.3	442.9	517.9	486.4	38.9	2	**	55.3
EMI04			509.0	468.8	508.8	495.5	23.2	2	**	39.9
EMI05	444.5		520.3	481.3	529.1	493.8	38.9	3	***	36.8
EMI06	479.1	498.9	464.1	459.7	474.4	475.2	15.3	4	**	19.9
EMI07	457.2	419.8	443.7	443.3	439.3	440.7	13.5	4	**	37.4
EMI08	446.2	484.5	456.3	424.8	445.3	451.4	21.8	4	**	38.3
EMI09	414.2	464.7	413.9	417.5	469.1	435.9	28.4	4	***	4.5
EMI10	449.1	486.6	457.4	444.3	468.3	461.1	16.9	4	**	29.2
EMI11	467.1	492.3	439.1	436.2	449.6	456.9	23.2	4	**	25.2
EMI12	464.8	491.7	437.1	437.6	454.6	457.2	22.6	4	***	17.5
EMI13	466.8	493.2	452.8	458.9	442.7	462.9	19.1	4	**	40.4
EMI14	453.5	487.6	412.4	439.9	472.8	453.2	29.2	4	***	19.3
EMI15	459.3	493.6	484.2	453.5	463.6	470.8	17.2	4	n/s	
Mean	454.7	481.3	465.5	448.0	474.4					
SD	17.0	23.5	34.1	16.7	27.9					
Df	20	18	28	28	28					
$P\leq$	***	***	***	***	***					
LSD	30.0	44.9	48.5	38.9	69.5					

SD= standard deviation; df = degrees of freedom; *** $P\leq0.001$; ** $P\leq0.05$; n/s = no significant difference ($P\geq0.05$); LSD= least significant difference ($P\leq0.05$).

4.3.2. Genotypic and environmental variation in cell wall composition

Interpretation of the data was performed using statistical analyses (3.5) and the results are discussed in terms of their statistical significance. Analysis of the overall genotypic effect on cell wall composition (e.g. analysis of genotypes within each site for each harvest) identified significant genotypic variation in lignin, cellulose, and hemicellulose concentrations ($P\leq0.001$) (Tables 4.3 - 4.8). Analysis of the overall effect of environment on cell wall composition (e.g. analysis of genotypes across all sites for each harvest) identified environment as having a significant effect on concentrations of cellulose and hemicellulose ($P\leq0.001$) but not lignin ($P\geq0.06$) (Table 4.9). This would suggest that lignin concentration is more strongly influenced by genotype rather than environment.

Table 4.9 Results of analyses of variance performed on cell wall compositional data. Results of ANOVAs performed on the cell wall data for all genotypes across all sites in the autumn and winter harvests are presented in the table.

	Autumn harvest					Winter harvest			
	df	ss	ms	vr	*P*=	ss	ms	vr	*P*≤
					Lignin				
Site	4	570.6	142.7	2.1	0.09	904.7	226.2	2.3	0.06
Residual	178	12330.6	69.3			17760.0	99.8		
Total	182	12901.2				18664.7			
					Cellulose				
Site	4	65276.1	16319.0	22.9	<.001	26562.7	6640.7	8.9	<.001
Residual	178	126987.4	713.4			132331.0	743.4		
Total	182	192263.6				158893.8			
					Hemicellulose				
Site	4	27508.0	6877.0	10.9	<.001	29104.8	7276.2	10.0	<.001
Residual	178	112455.2	631.8			129070.3	725.1		
Total	182	139963.3				158175.1			

df = degrees of freedom; ss = sum of squares; ms = mean squares; vr =variance ratio; *P* = significance level.

Across all sites, genotypic means for lignin concentration ranged from 69.9 to 89.9 g kg^{-1} in the autumn harvest and from 87.4 to 108.8 g kg^{-1} the winter harvest. Genotypic means for hemicellulose concentration ranged from 255.0 to 314.9 g kg^{-1} in the autumn and from 242.3 to 314.2 g kg^{-1} in the winter, and mean cellulose concentrations ranged from 365.6 to 429.8 g kg^{-1} in autumn and 435.9 to 495.5 g kg^{-1} in winter.

In sites where the *M. sacchariflorus* (EMI05) and *M. x giganteus* (EMI01-04) successfully established (England, Germany and Portugal), no significant overall genotypic differences in cell wall composition were identified between these genotypes (Table 4.3 – 4.8). This would imply that a smaller degree of genetic variation exists in the cell wall composition of the *M. x giganteus* genotypes. This result is not surprising since the *M. x giganteus* hybrids currently cultivated in Europe probably all derive from the same or similar parental germplasm [82]. As only one genotype of *M. sacchariflorus* was included in the study too much inference should not be drawn about this species as a whole. However, as little significant difference was identified between the cell wall composition of the *M. sacchariflorus* and *M. x giganteus* genotypes it would appear that this genotype and the *M. x giganteus* hybrid share cell wall

characteristics distinctly different from those of the *M. sinensis* (EMI11-15) and *M. sinensis* hybrids (EMI06-10).

At both harvest times the *M. sacchariflorus* and *M. x giganteus* genotypes exhibited a consistently and significantly higher lignin concentration ($P \leq 0.05$) than all the *M. sinensis* genotypes (Table 4.3 and 4.4). The *M. x giganteus* and *M. sacchariflorus* genotypes also exhibited a significantly lower hemicellulose concentration ($P \leq 0.05$) than all the *M. sinensis* genotypes at both harvest times (Table 4.5 and 4.6).

Interestingly in Denmark where *M. sacchariflorus* (EMI05) established and the *M. x giganteus* did not, the same trends in lignin and hemicellulose concentration were not observed. In the winter harvest the *M. sacchariflorus* was identified as having a significantly lower lignin concentration (97.7 g kg^{-1}) than that of the *M. sacchariflorus x sinensis* hybrid EMI08 (105.7 g kg^{-1}) at the $P \leq 0.05$ confidence level. The *M. sacchariflorus x sinensis* hybrids (EMI08 and EMI10) maintained the trend of exhibiting a higher lignin concentration at the winter harvest (Table 4.4) and a lower hemicellulose concentration at both harvest times (Table 4.5 and 4.6). As this trend was not observed at any other site it is not possible to discern whether this is more the result of genetic influence or site specific factors. However it is likely that a different *M. sacchariflorus* genotype (not EMI05) was used to produce these two hybrids.

No clear trend was observed in the mean cellulose concentrations of the different species, hybrids, or genotypes (Table 4.7 and 4.8). However, at both harvests the cellulose concentrations of the *M. x giganteus* genotypes was always within the upper range. At the winter harvest of *M. sacchariflorus* at sites in England, Germany and Portugal cellulose concentration was higher than for any other sample (Table 4.8). This was not observed at the site in Denmark, where *M. sacchariflorus* contained one of the lowest cellulose

concentrations at both harvests, probably as a result of the more limiting environmental conditions found at this site.

There was no clear overall difference in cell wall composition of the 'wild' or hybrid *M. sinensis* genotypes, and no single *M. sinensis* genotype was identified as significantly higher in lignin, cellulose or hemicellulose concentration across all sites. However, when comparing their mean lignin concentrations, EMI11 exhibited the highest lignin concentration at both harvest times (81.6 and 93.6 g kg^{-1} respectively) (Table 4.3 and 4.4). Across most sites at both harvest times the cellulose concentrations of the *M. sinensis* genotypes EMI06 and EMI15 where consistently higher than other *M. sinensis* or *M. sinensis* hybrids and similar to those of the *M. sacchariflorus* and *M. x giganteus* genotypes (Table 4.7 and 4.8). The cellulose concentration of EMI09 was consistently low and therefore a potential parent for a mapping cross with EMI06 or EMI15. Of the *M. sinensis* genotypes EMI13 consistently exhibited high hemicellulose concentration and EMI07 low hemicellulose concentration across most sites, these genotypes would therefore also be potential parents for a mapping population.

4.3.3. Implications of cell wall composition on feedstock quality

Peak dry matter yields for *Miscanthus* are obtained by harvesting in autumn [2, 72], however at that time the above-ground biomass regularly contains higher levels of K, Cl, S, N, and P which can cause slagging, fouling, and corrosion to combustion and pyrolysis systems [3]. Delaying harvest until winter has been shown to reduce the levels of these elements within the harvested biomass [26, 72]. For this reason, at present *Miscanthus* grown commercially for use in direct combustion or co-firing is harvested in late winter/early spring. This study has identified that the lignin and cellulose concentration of all genotypes, as a proportion of the dry weight, was higher in the winter harvest. On this basis it can also be predicted that the calorific value of the winter harvested material would also be significantly increased on the basis of the observed relationship between lignin concentration and heating value [72, 73, 97].

Overall, the *M. x giganteus* and *M. sacchariflorus* genotypes were found to contain the highest concentrations of lignin, and *M. x giganteus* also found to contain the highest concentration of cellulose in all countries where they survived the first winter. This indicates that these genotypes would yield higher heating values in direct combustion, but may cause problems in terms of pyrolysis oil quality/stability [61] and be less suitable to conversion by fermentation or anaerobic digestion processes compared with *M. sinensis* genotypes [36, 98].

Overall, fewer significant differences were observed in cellulose concentrations of the different *Miscanthus* genotypes but two of the *M. sinensis* genotypes (EMI06 and EMI15) exhibited cellulose concentrations comparable if not higher than some *M. x giganteus* genotypes and also contained significantly higher concentrations of hemicellulose at both harvest times. These observations coupled with the high dry-matter yields observed for some of the *M. sinensis* wild and hybrid genotypes [23] indicates potential for breeding *M. sinensis* hybrid genotypes with improved agronomic and feedstock characteristics.

4.4. Chapter conclusions

The NIR calibration models developed for the prediction of lignin, ADF, and NDF concentration in *Miscanthus* samples, were found to predict concentrations with a good degree of accuracy based on the R^2, SE_c, and SE_{cv} values for the 76 sample calibration set.

Across sites, *M. x giganteus* and *M. sacchariflorus* genotypes were identified as being more highly lignified than the *M. sinensis* genotypes, but lower in hemicellulose. No overall significant differences were observed between the cell wall composition of the *M. sinensis* (wild type) or the *M. sinensis* hybrid genotypes. The hemicellulose concentration of *Miscanthus* genotypes displayed an overall decrease between autumn and winter harvests, which is thought to be primarily a result of leaf loss. However, as the samples used for analysis were received as leaf and stem combined, it was not possible to determine the

relative proportions of cell wall components within the leaf and stem fractions separately. The role of leaf loss on total cell wall content of harvested biomass could be a subject for further research.

The higher concentrations of lignin identified in genotypes such as *M. x giganteus* and *M. sacchariflorus*, represent positive and negative feedstock characteristics depending on the intended conversion pathway. Higher lignin concentrations may confer higher heating values, a desirable characteristic in direct combustion and combustion of pyrolysis liquids. However, it has been suggested that higher lignin concentration may have a negative impact on other pyrolysis liquid quality parameters such as viscosity and stability. The extent of this impact will be a subject for further research.

The degree of observed genotypic variation in cell wall composition indicates good potential for dissection of this trait by QTL analysis and also for plant breeding to produce new genotypes with improved feedstock characteristics for energy conversion.

5. INFLUENCE OF NITROGEN AND POTASSIUM FERTILISER ON CELL WALL COMPOSITION OF *MISCANTHUS X GIGANTEUS* AND RESULTANT IMPACTS ON FAST-PYROLYSIS LIQUID QUALITY.

5.1. Introduction

Miscanthus x giganteus is the most widely cultivated *Miscanthus* genotype for commercial production of lignocellulosic biomass. The biomass produced commercially is predominantly used as a feedstock for generation of heat and power via combustion processes such as co-firing with coal. *Miscanthus* also represents a key candidate crop for biomass to liquid conversion to produce liquid fuels and chemicals by processes such as fast-pyrolysis. Little academic research has been undertaken to determine the effects of inorganic fertiliser inputs on the productivity of this commercial genotype, and what impacts this may have on the quality of the harvested biomass in terms of mineral concentration and cell wall composition.

This work represents a collaboration of research undertaken by three institutions under the auspices of the Supergen Bioenergy project. The impacts of inorganic fertiliser inputs were assessed in terms of productivity, cell wall composition, and quality of liquids produced by fast-pyrolysis.

5.2. Materials and methods

5.2.1. Fertiliser application field trials

Field trials were performed at Rothamsted Research (Harpenden, UK) to assess the effects of fertiliser application on the productivity and thermo-chemical conversion characteristics of *M. x giganteus* at five intervals throughout the growing season. Details of field trial experimental methodology are described in section 3.1.2. Yield data presented was measured from the final harvest taken at 19/04/2006.

5.2.2. *Fast pyrolysis trials at Aston University, UK.*

Fast pyrolysis trials were performed by R. Fahmi at Aston University (Birmingham, UK) as part of a PhD research project funded the by the Supergen Bioenergy project [79]. Material from each of the 14 fertiliser treatments was analysed by thermogravimetry (TGA) to determine product yields under pyrolysis conditions, and induced coupled plasma optical emission spectrophotometry (ICPOES) was used to determine inorganic composition. On the basis of results from ICPOES and TGA analyses [79], 5 of the fertiliser treatments were identified as producing biomass with characteristics most suitable to conversion by fast-pyrolysis (e.g. high volatile and low mineral content). Selected treatments are shown in Table 5.1.

Table 5.1 Treatments selected for fast-pyrolysis trials and cell wall composition analysis. The table shows the five fertiliser treatments selected for fast-pyrolysis trials and analysis of cell wall composition. For later reference, selected treatments are listed by their attributed label (T1-T5) including rates of N, KCl, and K_2SO_4 fertilisers applied expressed in kg ha^{-1}. Treatments were selected on the basis of ICPES and TGA analyses of the plant material performed by R. Fahmi [79].

Treatment	N	KCl	K_2SO_4
		kg ha^{-1}	
T1	0	50	0
T2	150	0	0
T3	150	50	0
T4	150	0	50
T5	250	50	0

Fast pyrolysis trials were performed on whole crop (leaf and stem) material harvested at the 3rd sampling period (01/02/2008). Sample material was prepared as described in section 3.1.2 and pyrolysis trials were performed using the same equipment and conditions as described in section 3.3 and [79]. Methodologies used in subsequent analysis of fast-pyrolysis liquids were performed in the same manner as described in sections 3.4.1-3.4.4.

Details of analytical methodologies not performed by the author of this thesis in subsequent experiments have not been presented in this thesis but may be found in: Fahmi, 2007 [79].

5.2.3. Cell wall composition analyses

The lignin, cellulose, and hemicellulose concentrations of sample material from the 5 selected treatments (Table 5.1) was determined using chemometric analysis as described in sections 3.2.3-3.2.7, 4.2.2 and 4.3.1. Moisture and ash concentrations were determined as described in sections 3.2.1 and 3.2.2. Analysis of cell wall composition was performed by the author at the Institute of Grassland and Environmental Research (Aberystwyth, UK).

5.3. Results and discussion

5.3.1. Influence of fertiliser treatment on cell wall composition

Regardless of treatment, mean concentrations of lignin and cellulose in stem and leaf material displayed an overall increase over the growing season (Fig. 5.1 and 5.2). Mean lignin concentrations ranged from 133.8-131.9 g kg^{-1} (stem) and 71.4-77.4 g kg^{-1} (leaf) (Table 5.2) and cellulose concentrations from 437.1-507.8 g kg^{-1} (stem) and 369.1-403.5 g kg^{-1} (leaf) (Table 5.3). Mean hemicellulose concentrations displayed an overall decrease over the growing season (Fig. 5.1 and 5.2), concentrations ranged from 225.1-252.2 g kg^{-1} (stem) and 310.4-338.0 g kg^{-1} (leaf) (Table 5.4). Consistently higher cellulose and lignin concentration was observed in the stem material, and consistently higher hemicellulose concentration was observed in the leaf.

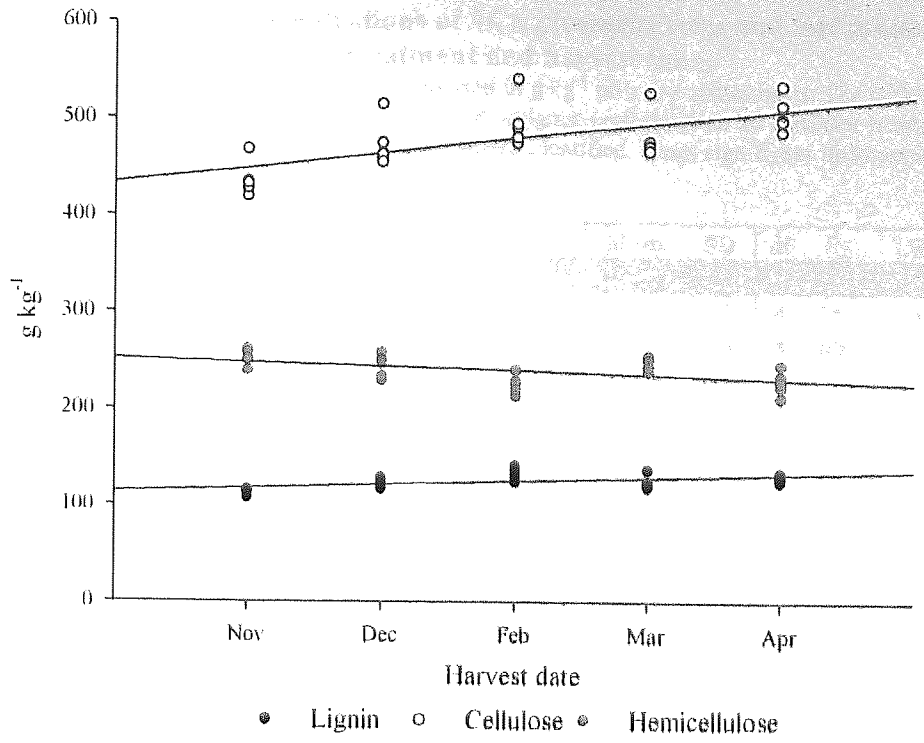

Figure 5.1 Mean concentrations of lignin, cellulose, and hemicellulose in stem material for all treatments over the growing season.

Concentrations of lignin, cellulose and hemicellulose in the stem material produced under all fertiliser treatments are displayed in g kg^{-1} on a dry matter basis as determined by chemometric analysis. Data is reported for all five harvest times over the growing season and includes linear trend lines.

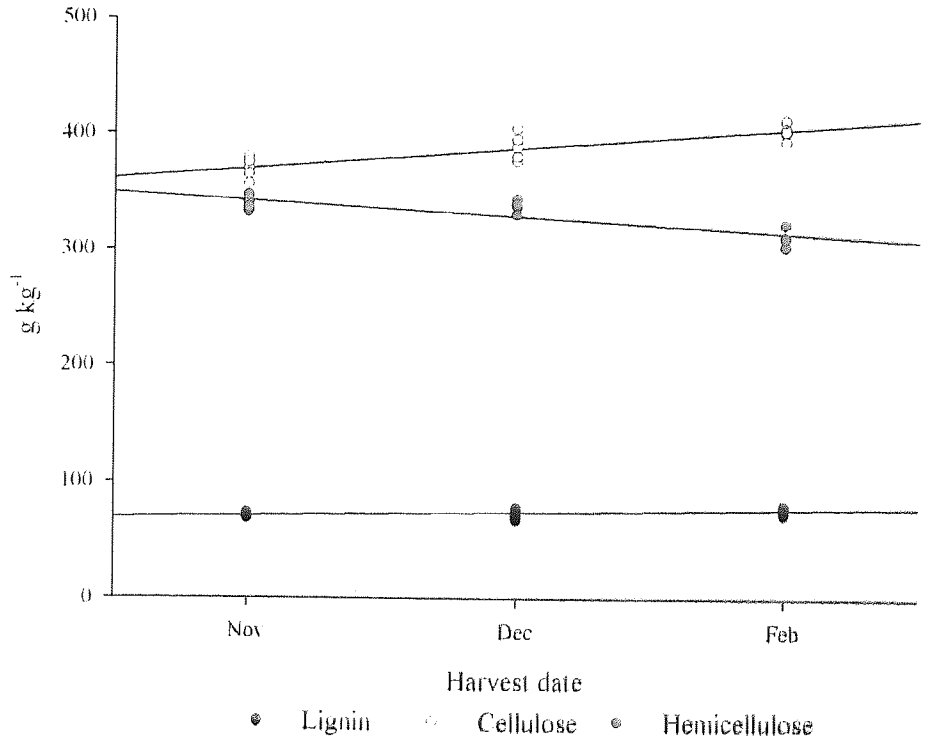

Figure 5.2 Mean concentrations of lignin, cellulose, and hemicellulose (g kg^{-1}) in leaf material for all treatments over the growing season.

Concentrations of lignin, cellulose and hemicellulose in the leaf material produced under all fertiliser treatments are displayed in g kg^{-1} on a dry matter basis as determined by chemometric analysis. Data is reported for the three harvest times over the growing season where leaf material was present, and includes linear trend lines.

Table 5.2 Mean lignin concentrations of *M. x giganteus* stem and leaf material by fertiliser treatment and harvest time.

Mean concentrations in leaf and stem material are reported in g kg^{-1} on a dry matter basis. The table includes the means, standard deviations and the results of analyses of variance performed on all fertiliser treatments within and between harvests including levels of significance where identified. Least significant differences (LSD) are reported in g kg^{-1} on a dry matter basis.

Harvest	T1	T2	T3	T4	T5	Mean	SD	df	$P\leq$	LSD
Stem										
1	114.0	108.2	116.0	116.1	114.5	113.8	3.2	4	**	5.8
2	126.5	117.4	122.8	128.1	121.0	123.2	4.3	4	n/s	
3	140.9	135.9	131.5	124.9	126.5	131.9	6.6	4	**	14.3
4	137.2	124.2	120.1	123.8	122.0	125.5	6.8	4	***	13.0
5	132.2	134.3	129.6	131.7	126.3	130.8	3.0	4	n/s	
Mean	130.2	124.0	124.0	124.9	122.1					
SD	10.5	11.6	6.5	5.8	4.9					
Df	4	4	4	4	4					
$P\leq$	***	***	***	***	***					
LSD	10.6	1.6	6.8	12.0	6.4					
Leaf										
1	73.2	72.9	72.5	69.0	69.6	71.4	2.0	4	n/s	
2	68.0	73.5	70.8	73.0	77.3	72.5	3.5	4	***	2.7
3	73.3	79.3	77.1	79.8	77.7	77.4	2.6	4	**	6.0
Mean	71.5	75.2	73.5	73.9	74.9					
SD	3.0	3.5	3.3	5.4	4.6					
Df	2	2	2	2	2					
$P\leq$	**	**	**	**	***					
LSD	5.2	5.8	4.6	6.7	7.7					

SD= standard deviation; df = degrees of freedom; *** $P\leq0.001$; ** $P\leq0.05$;
n/s = no significant difference ($P\geq0.05$); LSD= least significant difference ($P\leq0.05$).

Overall, lignin, cellulose, and hemicellulose concentrations of stem and leaf material differed significantly between fertiliser treatments and harvest times (Table 5.2-5.4). The overall mean concentrations of lignin, cellulose, and hemicellulose varied between fertiliser treatments by 8.1, 52.7, and 24.3 g kg^{-1} respectively in the stem material, and by 3.7, 19.0, and 2.5 g kg^{-1} respectively in the leaf material. This equates to percentage variations of 6%, 10%, and 10% by weight in the stem material, and 5%, 5% and 1% in the leaf material for concentrations of lignin, cellulose and hemicellulose respectively. It would therefore appear that the fertiliser treatments had a greater impact on the cellulose and hemicellulose concentrations of the stem material compared to the leaf, but that the effect of fertiliser treatment on lignin concentration of the stem and the leaf material was more consistent.

Table 5.3 Mean cellulose concentrations of *M. x giganteus* stem and leaf material by fertiliser treatment and harvest time.

Mean concentrations in leaf and stem material are reported in g kg^{-1} on a dry matter basis. The table includes the means, standard deviations and the results of analyses of variance performed on all fertiliser treatments within and between harvests including levels of significance where identified. Least significant differences (LSD) are reported in g kg^{-1} on a dry matter basis.

Sampling	T1	T2	T3	T4	T5	Mean	SD	df	$P\leq$	LSD
Stem										
1	468.8	419.7	428.4	435.3	433.5	437.1	18.7	4	***	15.5
2	514.6	457.6	474.8	463.3	455.0	473.1	24.4	4	***	39.7
3	540.2	489.5	493.9	474.2	479.7	495.5	26.2	4	***	19.6
4	527.6	476.4	470.7	471.5	466.9	482.6	25.4	4	***	51.1
5	535.5	515.0	501.0	499.3	488.3	507.8	18.2	4	***	20.4
Mean	517.4	471.6	473.8	468.7	464.7					
SD	28.8	35.8	28.4	23.0	21.5					
Df	4	4	4	4	4					
$P\leq$	***	***	***	***	***					
LSD	12.5	13.0	7.2	10.9	8.5					
Leaf										
1	379.5	370.0	375.1	356.3	364.5	369.1	9.1	4	**	18.7
2	404.6	376.5	388.7	380.3	395.1	389.1	11.3	4	***	14.8
3	412.5	402.3	405.5	403.0	394.4	403.5	6.5	4	**	18.0
Mean	398.9	382.9	389.8	379.9	384.7					
SD	17.3	17.1	15.2	23.4	17.5					
Df	2	2	2	2	2					
$P\leq$	***	***	**	**	***					
LSD	7.8	25.7	16.7	23.8	29.8					

SD= standard deviation; df = degrees of freedom; *** $P\leq0.001$; ** $P\leq0.05$;
n/s = no significant difference ($P\geq0.05$); LSD= least significant difference ($P\leq0.05$).

Overall, the concentration of all cell wall components in the stem decreased as rates of nitrogen fertiliser increased (Tables 5.2-5.4). Statistical analysis clearly identified treatment 1, where no nitrogen and 50 kg ha^{-1} of potassium chloride fertiliser was applied, as having the most significant effect on cell wall composition of the stem. Plants grown under treatment 1 had consistently higher concentrations of all cell wall components at all harvest times. Plants grown under treatment 1 also yielded significantly higher concentrations of cellulose in the leaf material but the same was not observed with lignin and hemicellulose.

The cell wall components, as a proportion of the stem dry matter, reduced as rates of nitrogen fertiliser increased (Tables 3-5). However, no apparent relationship was observed regarding the exclusive effect of potassium fertiliser on cell wall composition.

Table 5.4 Mean hemicellulose concentrations of *M. x giganteus* stem and leaf material by fertiliser treatment and harvest time.

Mean concentrations in leaf and stem material are reported in g kg^{-1} on a dry matter basis. The table includes the means, standard deviations and the results of analyses of variance performed on all fertiliser treatments within and between harvests including levels of significance where identified. Least significant differences (LSD) are reported in g kg^{-1} on a dry matter basis.

Sampling	T1	T2	T3	T4	T5	Mean	SD	df	$P\leq$	LSD
Stem										
1	261.7	258.3	250.5	239.0	251.6	252.2	8.7	4	**	19.2
2	257.8	250.6	249.5	229.2	233.4	244.1	12.2	4	**	24.3
3	239.8	225.6	228.2	219.3	212.7	225.1	10.2	4	**	20.4
4	254.2	254.0	250.6	238.3	243.5	248.1	7.0	4	**	12.1
5	246.1	234.7	223.1	212.4	228.8	229.0	12.6	4	***	16.3
Mean	251.9	244.6	240.4	227.7	234.0					
SD	8.9	13.9	13.6	11.7	14.9					
Df	4	4	4	4	4					
$P\leq$	**	***	***	***	***					
LSD	17.0	15.8	5.2	16.7	14.6					
Leaf										
1	340.2	332.1	334.4	336.4	346.7	337.9	5.7	4	n/s	
2	338.0	343.4	338.4	339.9	330.2	338.0	4.9	4	n/s	
3	311.4	303.6	322.6	303.4	311.1	310.4	7.9	4	***	11.1
Mean	329.8	326.4	331.8	326.6	329.3					
SD	16.0	20.6	8.2	20.1	17.8					
Df	2	2	2	2	2					
$P\leq$	***	***	***	***	***					
LSD	26.5	11.2	11.7	32.9	16.4					

SD= standard deviation; df = degrees of freedom; *** $P\leq0.001$; ** $P\leq0.05$;
n/s = no significant difference ($P\geq0.05$); LSD= least significant difference ($P\leq0.05$).

A negative effect of nitrogen fertiliser on the proportion of cell wall components in the biomass dry matter has been observed in other crop species [99-102]. A significant decrease in total cell wall content and increase crude protein and ash has been observed when high rates of N fertiliser have been applied to sweet sorghum and pearl millet [99, 101]. Statistical analysis clearly identified treatment 1, where no nitrogen and 50 kg ha^{-1} of potassium chloride fertiliser was applied, as having the most significant effect on cell wall composition of the stem. Plants grown under treatment 1 had consistently higher concentrations of all cell wall components at all harvest times. Plants grown under treatment 1 also yielded significantly higher concentrations of cellulose in the leaf material but the same was not observed with lignin and hemicellulose.

5.3.2. *Resultant impacts on fast-pyrolysis liquid quality*

Pyrolysis trials were performed by Fahmi, 2007 [79] using whole-crop sample material (stem and leaf) harvested at the third sampling period. In order to compare the results of pyrolysis product yields and characteristics of pyrolysis liquids with results for cell wall composition, only results for the stem material at the third sampling period has been used. The rationale for using the stem data is that the stem material constitutes the greatest component of the harvested biomass in terms of dry weight, therefore values would be more representative of the biomass fed into the fast-pyrolysis reactor. Comparative results of analyses performed on the raw biomass samples and liquids produced by fast-pyrolysis are shown in Table 5.5 and Table 5.6.

Table 5.5 Comparison of the results of cell wall and thermogravimetric analyses, with fast-pyrolysis product yields achieved from *Miscanthus* biomass grown under different fertiliser treatments.

The table compares results from analysis of cell wall composition with the results of thermogravimetric analysis (TGA) and fast-pyrolysis of *M. x giganteus* biomass grown under five fertiliser treatments harvested in February 2006. Results from cell wall analyses are reported in g kg^{-1} on a dry matter basis. Results of TGA and fast-pyrolysis product yields are reported as a percentage of the dry weight.

	T1	T2	T3	T4	T5
Cell wall analysis (g kg^{-1})					
Lignin	140.9	135.9	131.5	124.9	126.5
Cellulose	540.2	489.5	493.9	474.2	479.7
Hemicellulose	239.8	225.6	228.2	219.3	212.7
Ash	12.7	15.7	15.3	18.4	19.1
TGA product yields (% wt)					
Moisture	3.6	3.4	3.4	4.3	2.7
Char	15.5	24.5	23.8	25.0	25.2
Volatiles	84.6	75.5	76.2	75.0	74.8
Fast pyrolysis product yields (% wt)					
Char	19.2	22.8	24.1	27.8	25.6
Gas	11.1	13.7	12.3	16.2	16.0
Reaction water	8.9	13.7	17.0	17.4	15.0
Organics	52.4	43.3	36.6	34.5	39.3
Total liquids	61.3	57.0	53.6	44.9	54.3

Treatment 1, which produced biomass with the highest concentrations of cell wall components, also resulted in higher yields of volatiles in the TGA analysis, the highest proportion of organics in the pyrolysis liquids produced (e.g. the non-water proportion of the pyrolysis liquid considered the desirable product). Treatment 1 also resulted in the lowest

production of non-condensable gases during fast-pyrolysis, and the lowest proportions of char in both TGA analysis and during fast-pyrolysis. Whilst these results appear to be strongly related to the cell wall composition of the biomass produced by treatment 1, these results are also likely to be related to the ash concentration of this sample which was distinctly lower than that of samples from other treatments. Ash is known to have a catalytic effect on thermal decomposition, higher ash concentrations giving rise to higher yields of char and gas and *vice-versa* [63, 67]. This observation was supported by the data reported for treatments 4 and 5 where higher ash concentrations and higher yields of char and gas were reported.

Table 5.6 Comparison of results of cell wall composition analyses with characteristics of fast-pyrolysis liquids produced from *Miscanthus* biomass grown under different fertiliser treatments.

The table compares results from analysis of cell wall composition with the results of molecular weight distribution, viscosity, stability and heating value of liquids produced by fast-pyrolysis of *M. x giganteus* biomass grown under five fertiliser treatments harvested in February 2006. Results from cell wall analyses are reported in g kg^{-1} on a dry matter basis. Molecular weight distribution was determined by gel permeation chromatography (GPC) and is reported in g mol^{-1}. Viscosity was measured using a Rotoviscol viscometer (Gebr Haake GmbH) and the stability of pyrolysis liquids calculated from the degree of change in viscosity after accelerated aging at 80°C for 24 h which equates to storage for 1 year at ambient temperature [94]. Higher and lower heating values (HHV/LHV) of pyrolysis liquids were calculated using equations based on results of the elemental analyses and Karl-Fischer titration and are reported on a 'wet' basis.

	T1	T2	T3	T4	T5
Cell wall analysis (g kg^{-1})					
Lignin	140.9	135.9	131.5	124.9	126.5
Cellulose	540.2	489.5	493.9	474.2	479.7
Hemicellulose	239.8	225.6	228.2	219.3	212.7
Moisture	35.8	33.9	33.8	43.2	27.1
Ash	12.7	15.7	15.3	18.4	19.1
Molecular weight distribution (g mol^{-1})					
Mw (fresh)	440	481	447	436	421
Mn (fresh)	330	338	319	311	303
PD (fresh)	1.3	1.4	1.4	1.4	1.4
Mw (aged)	538	584	580	530	512
Mn (aged)	371	382	370	355	339
PD (aged)	1.5	1.5	1.5	1.5	1.5
Viscosity and heating value					
Viscosity (fresh)	47.4	24.5	31.2	3.7	3.9
Viscosity (aged)	73.5	39.9	71.7	17.5	10.7
Stability	0.6	0.6	1.3	3.8	1.8
Water content	17.7	28.1	35.0	37.4	48.1
HHV (MJ kg^{-1})	20.2	14.8	14.2	9.5	11.7
LHV (MJ kg^{-1})	18.3	12.9	12.2	7.4	9.5

Mw = weight average molecular weight; Mn = number average molecular weight; PD = polydispersity; HHV/LHV = higher/lower heating value.

A comparison of the results of cell wall composition and characteristics of the fast-pyrolysis liquids produced, including molecular weight distribution, viscosity, stability, and heating value is shown in Table 5.6. No clear relationship was observed between the molecular weight distributions of pyrolysis liquids and the variation in cell wall composition resulting from fertiliser treatments applied (Table 5.6). The pyrolysis liquid produced from the high lignin – low ash biomass grown under treatment 1 yielded the highest HHV, LHV, and viscosity, and produced the most stable liquid. The opposite was observed for the pyrolysis liquid produced from the low lignin – high ash biomass produced under treatment 4. The HHV and LHV values reported in Table 5.6 have been corrected for the water content of the pyrolysis liquids. The HHV decreases linearly as water content increases, however the LHV is corrected for the energy that would be required to evaporate the water [59], for this reason the LHV is regarded as the more significant heating value. The water content of pyrolysis liquids is a combination of the moisture content of the feedstock and reaction water formed by catalytic cracking of vapours caused by the presence of metals (ash) [61, 67]. The water content of the pyrolysis liquid did not correlate with the initial moisture content of the feedstocks, but did correlate strongly with the ash concentration (R= 0.93). Therefore, it can be concluded that the water in the pyrolysis liquids was predominantly reaction water formed due to the presence of ash.

An antagonistic relationship has been observed between the lignin and ash concentrations of the feedstocks and the properties of the pyrolysis liquids. High lignin concentrations have been observed to confer high heating value [3, 73, 97] and viscosity [61, 79], whereas high ash concentrations have been observed to confer high reaction water yields which reduce the viscosity and heating value [59, 61, 63, 79]. The lignin and ash concentrations of all treatments were correlated against HHV, LHV, and viscosity of the pyrolysis liquids. Both lignin and ash concentration correlated strongly with HHV and LHV, but a stronger positive correlation was observed with lignin (R= 0.97) compared to the negative correlation observed

with ash (R= -0.94). This indicates that while high ash concentrations lower the heating value of the pyrolysis liquid by increasing the reaction water content, the lignin concentration of the feedstock has the greater overall effect on the heating value of the pyrolysis liquid.

A strong negative correlation was observed between ash concentration and viscosity of both the fresh and aged liquids (R= -0.99 and -0.93 respectively). Positive correlations were also observed between lignin concentration and the viscosity. However, whilst lignin concentration correlated strongly with the viscosity of the fresh liquid (R= 0.93), a weaker correlation was observed with viscosity after aging (R= 0.77). These results indicate that whilst higher lignin concentration does increase the initial viscosity of the pyrolysis liquid, the reduction in viscosity caused by the reaction water resulting from high ash concentration had the greater overall effect.

The degree of change in the viscosity of pyrolysis liquids after aging is expressed by the stability indices (Table 5.6). Higher stability values indicate that a greater degree of change has occurred between the viscosities of the fresh and aged liquids, therefore these liquids are less stable and more likely to phase separate during storage. A relationship was observed between pyrolysis liquid stability and concentrations of lignin and ash in the feedstocks. Correlation of these values identified that lignin had a stronger positive relationship with stability (R= 0.84) than the negative relationship identified with ash (R= -0.72). On the basis of these results, it would appear that while high ash concentration reduces the stability of pyrolysis liquids, higher lignin concentration may counteract the effect of the ash. It has been observed by other researchers that the presence of higher molecular weight compounds derived from lignin reduce the catalytic cracking of volatiles caused by the presence of ash [61]. However, as no relationship between lignin concentration of the feedstocks and the average molecular weights of the pyrolysis liquids was observed in these results it is not possible to confirm this observation.

In summary, fertiliser treatment 1 produced *Miscanthus* biomass with higher concentrations of all cell wall components and lower concentrations of ash. As a result, this biomass produced the highest yield of pyrolysis liquids. The pyrolysis liquids produced from this feedstock had higher heating values and a higher initial viscosity, but was the most stable liquid produced.

5.3.3. Influence of fertiliser treatment on dry matter yield

The mean dry matter yields of *M. x giganteus* grown under the selected fertiliser treatments are shown in Table 5.7.

Table 5.7 Mean dry matter yields of *M. x giganteus* grown under five different fertiliser treatments at Rothamsted Research, Harpenden, UK.

Data is listed by fertiliser treatment number and includes details of N, KCl, and K_2SO_4 treatments applied reported in kg ha^{-1}. Mean dry matter yields and their standard errors are expressed in t ha^{-1} on a dry matter basis as calculated from the final harvest in April 2006.

Treatment	N	KCl	K_2SO_4	Mean yield	SE
		kg ha^{-1}		DM t ha^{-1}	
T1	0	50	0	7.8	1.4
T2	150	0	0	9.5	1.0
T3	150	50	0	11.2	1.1
T4	150	0	50	10.2	0.5
T5	250	50	0	9.9	0.5

An analysis of variance was performed on the yield data attained from the fertiliser application experiment. The results of the analysis identified no significant difference between the dry matter yields of *M. x giganteus* grown under the different fertiliser treatments selected for analysis ($P \leq 0.05$).

5.4. Chapter conclusions

Overall, lignin, cellulose, and hemicellulose concentrations of stem and leaf material differed significantly between fertiliser treatments and harvest times, and the fertiliser treatments appear to have had a greater impact on the cell wall composition of the stem compared to the leaf.

Overall, it would appear that application of nitrogen fertiliser had a negative effect on feedstock quality. Higher rates of nitrogen fertiliser resulted in lower concentrations of cell wall components and higher accumulation of ash within the biomass. The low nitrogen fertiliser treatment produced high quality, low ash - high lignin biomass most suitable as a feedstock for combustion applications.

The *Miscanthus* biomass produced under low fertiliser rates produced a fast-pyrolysis liquid with higher heating value, viscosity, and stability. Lignin concentration of the feedstock had the greatest overall effect on the heating value of the pyrolysis liquid, and the reaction water resulting from the catalytic effect of the ash had the greater overall effect on viscosity.

The results indicate that *Miscanthus* can be used to produce high yields of high quality lignocellulosic biomass without the application of inorganic fertilisers, which would present many environmental and economic benefits which relate to sustainability of crop husbandry and use of *Miscanthus* as a bioenergy feedstock.

6. CHARACTERISATION OF *MISCANTHUS* SPECIES AND GENOTYPES BY THERMOGRAVIMETRY AND PYROLYSIS GAS-CHROMATOGRAPHY MASS-SPECTROMETRY

6.1. Chapter introduction

In this study, fifteen genotypes of *Miscanthus* were screened for lignin, cellulose and hemicellulose content at two intervals within the growing season. The objective was to identify the extent of genetically derived variation in cell wall composition and how this changed over the growing season. Five genotypes of *Miscanthus* which best represented the range of observed variation were selected for further analysis. Pyrolysis-gas chromatography-mass spectrometry (Py-GC-MS) was used to identify key cellulose and lignin markers and to identify whether significant genotypic differences existed between the relative proportions of lignin sub units. Thermo-gravimetric analysis (TGA) was used to examine feedstock properties (moisture, volatiles, char, ash, and fixed carbon content) and apparent first order reaction kinetics.

39 key cellulose and lignin markers were identified in *Miscanthus* genotypes and significant variation in the relative yields of thermal degradation products was observed between genotypes ($P \leq 0.05$). *Miscanthus* lignin was found to be predominantly composed of *p*-hydroxyphenyl units and significant differences in the relative proportions of the lignin sub units were identified between genotypes ($P \leq 0.01$)

6.2. Materials and methods

Analysis of cell wall composition was performed by wet chemistry as described in sections 3.2.3-3.2.6. Thermogravimetric analysis (TGA) and reaction kinetics were performed as described in section 3.2.9, and pyrolysis gas chromatography mass spectrometry (Py-GC-MS) was performed as described in section 3.2.10.

6.3. Results and discussion

6.3.1. Variation in cell wall composition

In all genotypes lignin and cellulose concentrations as a proportion of the dry weight increased between the November and February harvests. Hemicellulose however displayed an overall decrease between November and February. Results of cell wall compositional analyses are shown in Table 6.1.

Table 6.1 Cell wall composition of *Miscanthus* species and genotypes in the November and February harvests.

Mean lignin, cellulose, hemicellulose, holocellulose (cellulose + hemicellulose), and ash concentrations of *Miscanthus* genotypes harvested in November 2005 and February 2006 are reported in g kg^{-1} on a dry matter basis, as determined by wet chemical analyses. The table includes overall means, standard deviations, and results of analyses of variance including levels of significance. Least significant differences (LSD) are reported in g kg^{-1} on a dry matter basis.

Species	Genotype	Lignin	Cellulose	Hemicellulose	Holocellulose	Ash
			November			
M. x giganteus	EMI01	120.2	503.4	248.3	751.7	26.7
M. sacchariflorus	EMI05	121.0	490.6	274.1	764.7	22.9
M. sinensis (hybrid)	EMI08	92.7	430.6	331.4	762.0	34.7
M. sinensis	EMI11	96.9	431.8	339.8	771.6	31.9
M. sinensis	EMI15	92.3	475.9	330.0	805.9	24.4
Mean		104.6	466.5	304.7	771.2	28.1
SD		14.7	33.7	41.0	20.7	5.0
$P\leq$	(df 8)	***	***	***	n/s	***
LSD	(df 8)	4.7	27.6	25.9	54.3	7.5
			February			
M. x giganteus	EMI01	125.8	521.3	257.6	778.9	27.4
M. sacchariflorus	EMI05	121.3	501.8	281.1	782.9	21.6
M. sinensis (hybrid)	EMI08	97.0	453.6	329.9	783.6	27.1
M. sinensis	EMI11	103.2	455.2	338.3	793.5	30.4
M. sinensis	EMI15	93.4	522.0	305.6	827.6	22.2
Mean		108.1	490.8	302.5	793.3	25.7
SD		14.6	34.2	33.6	19.9	3.7
$P\leq$	(df 8)	***	***	**	***	***
LSD	(df 8)	9.9	20.3	32.8	14.7	3.0

SD= standard deviation; df = degrees of freedom; *** $P\leq0.001$; ** $P\leq0.05$;
n/s = no significant difference ($P\geq0.05$); LSD= least significant difference ($P\leq0.05$).

Between the November and February harvests the overall mean concentrations of lignin and cellulose increased, and concentrations of hemicellulose and ash decreased. A similar trend to that observed in previous analyses (4.3.2). The observed reduction of ash concentration as a result of delaying harvest supports findings of previous research [3, 72].

In terms of lignin concentration, in both harvests, *M. x giganteus* and *M. sacchariflorus* were not found to be significantly different from one another but were identified as significantly higher than all of the *M. sinensis* genotypes ($P \leq 0.001$). At both harvests no significant differences were identified between the *M. sinensis* genotypes but EMI15 was consistently the lowest in lignin.

At both harvests *M. x giganteus*, *M. sacchariflorus*, and the wild type *M. sinensis* (EMI15) contained significantly higher concentrations of cellulose than the other genotypes ($P \leq 0.001$). At both harvests the *M. sinensis* genotypes EMI08 and EMI11 contained the lowest concentrations of cellulose and no significant differences were identified between them.

An inverse relationship was observed between lignin and hemicellulose contents, as at both harvest times *M. x giganteus* and *M. sacchariflorus* were identified as significantly lower in hemicellulose than the *M. sinensis* genotypes ($P \leq 0.003$) and the genotypic rank order of concentrations was almost the exact opposite of that found for lignin. One exception was that in the February harvest *M. sacchariflorus* and *M. sinensis* (EMI15) were identified as containing similar concentrations of hemicellulose ($P \leq 0.05$).

Regarding holocellulose concentration (cellulose + hemicellulose), the *M. sinensis* genotype EMI15 was consistently higher and *M. x giganteus* consistently lower than the other genotypes at both harvest times. No significant difference was observed between the holocellulose concentrations of genotypes in the November harvest, but EMI15 was identified as significantly higher than all other genotypes in the February harvest.

The *M. sinensis* genotypes EMI08 and EMI11 contained significantly higher concentrations of ash in the November harvest, EMI11 was also significantly higher than the other genotypes

in February. In both harvests *M. sacchariflorus* (EMI05) and the *M. sinensis* genotype EMI15 contained significantly lower concentrations of ash.

The higher lignin concentrations observed in the *M. x giganteus* and *M. sacchariflorus* genotypes is in keeping with previous results [103] (section 4.3.2) which identified these genotypes as being similar in cell wall composition. An interesting feature arising from these results is the similarity between *M. sinensis* EMI15 and *M. x sacchariflorus*. Both displayed very similar cellulose, hemicellulose, and ash concentrations but EMI15 was consistently lower in lignin at both harvest times and significantly higher in holocellulose in February.

6.3.2. Thermogravimetric analysis

The pyrolysis product yields and apparent activation energies calculated from thermogravimetric analysis (TGA) of *Miscanthus* species and genotypes harvested in November 2005 and February 2006 are shown in Table 6.2.

The observed yields of volatiles and char (Table 6.2) are within the ranges observed in previous studies of *Miscanthus* genotypes [104, 105]. Statistical analysis of the results from the TGA analysis identified *M. sinensis* EMI15 as having significantly greater volatile content and lower char content than all other genotypes at both harvest times ($P \leq 0.001$). *M. x giganteus* and *M. sacchariflorus* were consistently lowest in volatile content and highest in char content in both harvests, significantly so in February ($P \leq 0.05$).

Pyrolysis yields determined by TGA were correlated against the cell wall data determined by wet chemistry. As expected, holocellulose concentration correlated strongly with yields of volatiles (R=0.94 in November and R=0.88 in February), and lignin correlated strongly with char (R=0.88 in November and R=0.95 in February). A relationship between ash concentration and yields of volatiles and char was not identified. These observations indicate

that as lignin concentration increased yields of char increased and yields of volatiles decreased.

Table 6.2 Thermogravimetric analysis and apparent activation energies of *Miscanthus* species and genotypes in the November and February harvests.

Pyrolysis product yields of *Miscanthus* species and genotypes as determined by thermogravimetric analysis (TGA) reported as a percentage of the initial weight. Apparent activation energies (*Ea*) determined from reaction kinetics are reported in kJ mol^{-1}. Results include overall means, standard deviations, and results of analyses of variance including levels of significance. Least significant differences (LSD) are reported in corresponding units.

Species	Genotype	Moisture	Volatiles	Char	Ash	*Ea*
		% wt	% wt	% wt	% wt	(kJ mol^{-1})
			November			
M. x giganteus	EMI01	4.2	73.9	19.3	2.7	76.3
M. sacchariflorus	EMI05	3.8	73.6	20.3	2.3	69.3
M. sinensis (hybrid)	EMI08	4.3	74.8	17.4	3.5	65.9
M. sinensis	EMI11	4.2	74.7	17.9	3.2	64.6
M. sinensis	EMI15	4.2	78.2	15.1	2.4	66.3
Mean		4.2	75.1	18.0	2.8	68.5
SD		0.2	1.9	2.0	0.5	4.7
$P\leq$	(df 8)	n/s	***	***	***	**
LSD	(df 8)	0.5	1.3	1.4	0.7	4.7
			February			
M. x giganteus	EMI01	4.9	72.6	19.8	2.7	76.7
M. sacchariflorus	EMI05	4.1	73.4	20.4	2.2	69.0
M. sinensis (hybrid)	EMI08	4.5	75.6	17.2	2.7	67.7
M. sinensis	EMI11	4.4	74.9	17.7	3.0	65.7
M. sinensis	EMI15	4.5	77.7	15.6	2.2	70.4
Mean		4.5	74.8	18.1	2.6	69.9
SD		0.3	2.0	2.0	0.4	4.2
$P\leq$	(df 8)	n/s	***	***	***	***
LSD	(df 8)	0.8	0.8	1.7	0.1	3.3

SD= standard deviation; df = degrees of freedom; *** $P\leq0.001$; ** $P\leq0.05$;
n/s = no significant difference ($P\geq0.05$); LSD= least significant difference ($P\leq0.05$).

Statistical analysis of the activation energies calculated for all genotypes and heating rates (Table 6.2) revealed that at both harvest times the activation energy required for decomposition of *M. x giganteus* was significantly higher than all other genotypes ($P\leq0.004$) and no differences were observed between the activation energies of *M. sacchariflorus* and the *M. sinensis* ($P\leq0.05$). The first instinct would be to suggest that the high lignin and cellulose content of *M. x giganteus* would be the main reason for the higher activation energy required for its decomposition, however no significant differences were observed between the total lignin and cellulose content of *M. x giganteus* and *M. sacchariflorus* which had a significantly lower activation energy more similar to the *M. sinensis* genotypes. This suggests

that the higher activation energy of *M. x giganteus* could be related to the composition of the lignin and the manner in which it binds the holocellulose rather than total content. It could be possible that differences in the architecture of the lignin-holocellulose matrix such as different composition/deposition of lignin or cross-linkages between cell wall polymers, may affect the rate of volatile release and the activation energy required to initiate that release.

6.3.3. Py-GC-MS characterisation

Py-GC-MS analysis was performed on all genotypes from both harvest times in triplicate. From the resulting spectra, 39 key marker compounds were selected which represented the most abundant compounds present in the biomass. The key marker compounds identified are shown in Figure 6.1 and Table 6.2.

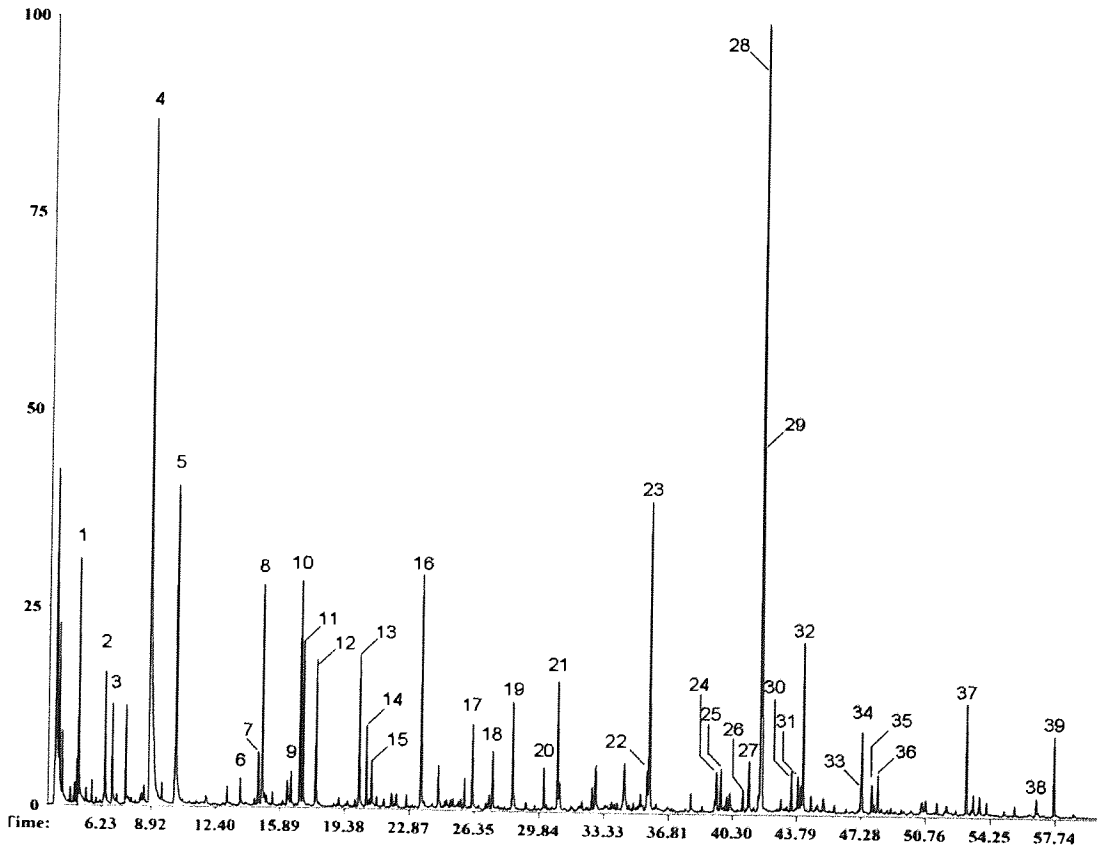

Figure 6.1 Example chromatogram of *M. x giganteus* from PY-GC-MS analysis.
The figure shows an example chromatogram produced from Py-GC-MS of the *M. x giganteus* genotype EMI01. Figure includes key marker compounds labelled by peak numbers (1-39) as listed in Table 6.3.

Table 6.3 Key marker compounds identified by Py-GC-MS analysis of *Miscanthus* species and genotypes.

Details of the 39 key marker compounds identified in *Miscanthus* species and genotypes by Py-GC-MS analysis are listed by peak number corresponding to retention time (min). Compound names, origins, molecular weights (Mw), and *m/z* values listed in order of relative abundance.

Peak	RT	Compound name	Origin	Mw	*m/z*
1	4.98	propanal-2-one	C	72	43/42/72/44
2	6.40	2,3-butanedione	C	86	43/86/42/44
3	6.79	3-pentanone	C	86	57/42/86/39
4	8.77	acetic acid	C	60	45/43/60/42
5	10.22	hydroxypropanone	C	74	43/74/42/45
6	13.72	2-propenoic acid methyl ester	C	86	55/58/57/86
7	14.69	1-hydroxy-2-butanone	C	88	57/56/88/42
8	14.91	3-hydroxypropanal (isomer of 5)	C	74	43/42/73/74
9	16.27	(2H)-furan-3-one	C	84	54/84/55/42
10	16.92	butanedial	C	86	58/57/43/44
11	17.12	2-hydroxy-3-oxobutanal	C	102	43/42/102/44
12	17.78	2-furaldehyde (furfural)	C	96	96/95/39/38
13	20.00	3-furfural alcohol	C	98	98/41/39/42
14	20.51	1-acetyloxypropane-2-one	C	116	43/86/42/116
15	20.80	tetrahydro-4-methyl-3-furanone	C	100	43/72/57/42
16	23.40	dihydro-methyl-furanone	C	98	98/55/42/41
17	26.22	(5H)-furan-2-one	C	84	55/84/54/39
18	27.29	4-hydroxy-5,6-dihydro-(2H)-pyran-2-one	C	114	58/114/57/42
19	28.34	2-hydroxy-1-methyl-1-cyclopentene-3-one	C	112	112/55/69/41
20	29.98	phenol	H	94	94/66/65/39
21	30.79	guaiacol	G	124	109/81/124/53
22	35.54	guaiacol, 4-methyl	G	138	123/138/95/73
23	35.78	anhydrosugar (unknown)	C	132	44/57/43/41
24	39.33	guaiacol, 4-ethyl	G	152	137/43/41/152
25	39.65	3-methyl-2,4-furandione	C	114	56/42/114/84
26	40.79	1,4:3,6-dianhydro-glucopyranose	C	144	69/57/41/70
27	41.18	1,5-anhydro-arabinofuranose	C	132	57/43/73/44
28	41.79	phenol, 4-vinyl	H	120	120/91/65/39
29	41.88	guaiacol, 4-vinyl	G	150	150/135/77/107
30	43.47	5-hydroxymethyl-2-furaldehyde	C	126	41/97/39/126
31	43.83	catechol	H	110	110/64/63/81
32	44.12	syringol	S	154	154/139/96/93
33	47.08	1,5-anhydro-β-D-xylofuranose	C	132	57/73/43/44
34	47.33	isoeugenol (trans)	G	164	164/77/103/91
35	47.83	syringol, 4-methyl	S	168	168/153/125/53
36	48.17	vanillin	G	162	151/152/81/109
37	52.99	syringol, 4-vinyl	S	180	180/165/137/77
38	56.83	1,6-anhydro-β-D-glucopyranose (levoglucosan)	C	162	60/57/73/43
39	57.67	syringol, 4-propenyl (cis)	S	194	194/91/77/119

Origin: C = holocellulose; H = *p*-hydroxyphenyl; G = Guaiacyl; S = Syringyl.

Of the 39 key marker compounds identified, 26 were holocellulose derived and 13 were lignin derived. The holocellulose fraction (cellulose + hemicellulose) comprises the major proportion of the biomass, therefore holocellulose derivatives would be expected to yield the greater proportion of pyrolysis products. However, it is known that at pyrolysis temperatures of 500°C complete pyrolysis of lignin does not occur [71, 106-113]. Pyrolysis experiments performed on purified Kraft lignin at 500°C have reported that 50-60% of the lignin was retained in the char [110]. However, the key lignin markers identified in this research represent the main pyrolysis products observed to result from pyrolysis of lignin at temperatures between 400-600°C [113].

In order to get an overall picture of the major compositional differences between genotypes, the overall mean amounts (%TIC) of the 39 key markers were added and grouped according to whether they were holocellulose or lignin derived and expressed as a percentage of the total. The lignin derived compounds subsequently grouped according to their sub unit origin (*p*-hydroxyphenyl, guaiacyl, syringyl). Analyses of variance performed on grouped data revealed no significant genotypic differences in the total amounts of holocellulose derived compounds at either harvest time, and no significant difference between relative proportions of lignin sub-units in the November harvest. However, in the February harvested material significant genotypic differences were identified between the relative proportions of lignin sub-units. *M. x giganteus* was identified as significantly higher in syringyl ($P \leq 0.002$) and *M. sacchariflorus* significantly higher in *p*-hydroxyphenyl ($P \leq 0.004$) than all other genotypes. No overall significant differences were identified between the *M. sinensis* genotypes at either harvest time, but in February the *M. sinensis* genotype EMI15 and *M. sacchariflorus* were found to contain similar amounts of syringyl derived compounds ($P \leq 0.05$).

The overall mean amounts (%TIC) of key marker compounds and genotypic standard deviations are shown for both harvest times in Figure 6.2. At both harvest times, of all key

marker compounds identified, *Miscanthus* genotypes were highest in acetic acid (4), 4-vinyl-phenol (28) and the unknown anhydrosugar (23) compound [90, 91].

Whilst no significant differences were observed between genotypes in the total amount of holocellulose derived compounds, significant differences were observed between genotypes in the relative proportions of individual compounds. An analysis of variance was performed on the relative amounts of individual key marker compounds identified in each genotype at both harvest times. Significant differences were observed between genotypes at both harvest times ($P \leq 0.05$) and genotypes differed significantly in amounts of 16 of the 39 key marker compounds in the November harvest, and 24 in February.

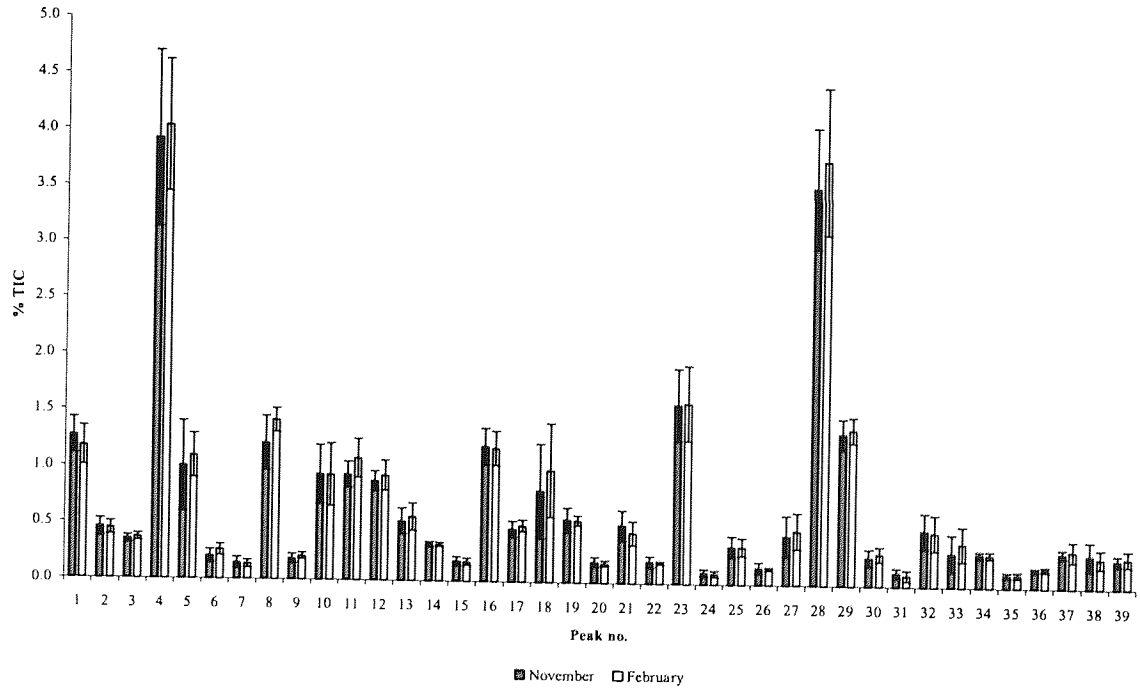

Figure 6.2 Mean amounts and standard deviations of key markers identified in *Miscanthus* genotypes at both harvest times

The overall mean amounts (%TIC) of the 39 key marker compounds in the November and February harvested *Miscanthus* biomass are displayed in the graph. The error bars represent the genotypic standard deviations for amounts of each compound.

In November the most salient results were that *M. sacchariflorus* was identified as significantly higher than all other genotypes in compounds 15, 20, 21, 23, and 26 ($P \leq 0.04$) and *M. x giganteus* significantly lower than all genotypes in compounds 9, 22, and 38 (levoglucosan) ($P \leq 0.03$). All *M. sinensis* genotypes were significantly higher in compound 27 ($P \leq 0.001$), and EMI15 also significantly higher in compounds 8, 18, and 33 ($P \leq 0.05$) but lower than all other genotypes in compound 10 ($P \leq 0.01$).

In February *M. x giganteus* and *M. sacchariflorus* displayed a greater degree of similarity and were identified as being significantly higher than the *M. sinensis* genotypes in amounts of 2, 10, 13, 21, 23, and 32. All the *M. sinensis* genotypes were significantly higher in compounds 18, 25, and 27 ($P \leq 0.004$). EMI11 was significantly higher in compound 16 ($P \leq 0.04$), and EMI11 and EMI15 significantly higher than all other genotypes in amounts of compounds 8 and 38 ($P \leq 0.002$). In addition, EMI15 displayed the most distinct differences and was higher than all other genotypes in amounts of compounds 9, 11, 30, and 33 ($P \leq 0.03$).

The most interesting feature of these results is the extent of genotypic variation in types and amounts of compounds produced during pyrolysis. It is evident that the *M. sinensis* genotypes share characteristics distinctly different to those of *M. x giganteus* and *M. sacchariflorus* particularly in holocellulose compounds. A smaller degree of variation was observed between genotypes in the amounts of lignin derived compounds but this is expected as a substantial proportion of the lignin is un-pyrolysed at 500°C and is retained in the char.

Of all genotypes, EMI15 seems to display the most interesting characteristics, low in lignin and char, high in holocellulose and volatiles, and higher in valuable products such as levoglucosan and 5-hydroxy-methyl-2-furaldehyde which can be converted to the high value chemicals levulinic and formic acid [114].

6.4. Chapter conclusions

Significant genotypic variation in cell wall composition was identified by both wet chemical and Py-GC-MS techniques. TGA analysis revealed that cell wall composition of genotypes had a significant effect on yields of char and volatiles and also in terms of apparent activation energy. How the observed variation in composition will affect the quality of liquids produced by fast-pyrolysis will be investigated in the following chapter.

Py-GC-MS analysis revealed significant genotypic differences in the range of products which may be derived via pyrolysis processing and indicated that genotypes other than the currently commercially cultivated *M. x giganteus* have great potential for use in energy conversion processes and as feedstocks for the bio-refining of chemicals.

The method of analysis used to assess the results of Py-GC-MS (%TIC) only provided semi-quantification of the yields of pyrolysis products. However, as all analyses were performed under the same conditions this method was adequate for statistical assessment of the major genotypic differences. Full quantification should be performed in further research to provide more accurate data regarding the amounts of pyrolysis products produced from *Miscanthus*, and to more accurately assess the variation in cell wall composition between species and genotypes.

The results have identified several genotypes which present excellent candidates for the generation of genetic mapping families and the breeding of new genotypes which may be matched to a range of conversion pathways.

7. INFLUENCE OF GENOTYPIC VARIATION IN CELL WALL COMPOSITION OF *MISCANTHUS* ON THE QUALITY OF PYROLYSIS LIQUIDS PRODUCED UNDER FAST-PYROLYSIS CONDITIONS.

7.1. Introduction

The aim of this experiment was to determine whether genotypically derived variation in cell wall composition of *Miscanthus* had any major effects on the product yields or properties of the pyrolysis liquids produced through fast-pyrolysis. The *Miscanthus* biomass used was grown at the European *Miscanthus* Improvement (EMI) [2, 3] project trial site at Rothamsted Research (Harpenden, UK) and produced without application of inorganic fertilisers.

The key criteria used to assess *Miscanthus* as a fast-pyrolysis feedstock included the yields of fast-pyrolysis products (liquids, gases, and char) and properties of the liquid product in terms of heating value, stability, total organic content, and chemical composition. These results were then compared with those of other potential biomass crop species and agricultural residues.

Feedstocks for fast-pyrolysis experiments were selected primarily on the basis of lignin concentration due to the previously observed relationship between lignin concentration and quality parameters of pyrolysis liquids such as heating value, stability and viscosity [61, 79]. Three *Miscanthus* genotypes which were distinctly different in their cell wall composition were selected for use as fast-pyrolysis feedstocks.

7.2. Materials and methods

7.2.1. Feedstock selection and characterisation

The selected genotypes were harvested from the EMI field trial site at Rothamsted research (Harpenden, UK) in February 2005. All fifteen EMI genotypes were screened for cell wall composition and ash concentration as described in sections 3.2.1 - 3.2.6. Three *Miscanthus*

types were selected for use as feedstocks in fast-pyrolysis experiments: *M. x giganteus* (EMI02), *M. sacchariflorus* (EMI05), and *M. sinensis* (EMI12). These genotypes were selected on the basis of lignin concentration, species, and the harvested material available for use e.g. in sufficient quantity for respectable yields of pyrolysis liquids to be achieved (Table 7.1).

Table 7.1 Species, genotype, and lignin concentration of EMI genotypes harvested in February 2006 showing genotypes selected for fast-pyrolysis experiments

Species	Genotype	Lignin ($g\ kg^{-1}$)
M. x giganteus	EMI 01	128.2
	EMI 02	**121.6**
	EMI 03	125.9
M. sacchariflorus	EMI 04	131.2
	EMI 05	**106.5**
	EMI 06	101.4
M. sinensis (hybrid)	EMI 07	100.8
	EMI 08	98.8
	EMI 09	97.4
	EMI 10	98.8
	EMI 11	110.4
M. sinensis (wild)	**EMI 12**	**84.6**
	EMI 13	103.5
	EMI 14	107.4
	EMI 15	102.6

7.2.2. Fast-pyrolysis experiments

Fast-pyrolysis was performed using a bench scale 150 $g\ hr^{-1}$ experimental rig with a fluidised bed reactor, an overview of the rig construction is illustrated in Figure 7.1. The reactor consisted of a stainless steel cylinder 26 cm in length and 4 cm in diameter. The fluidising and heat transfer medium used was quartz sand in a particle size range of 355-500 μm, approximately 150 g of which was used in the fluidised bed. A schematic diagram of the reactor is illustrated in Figure 7.2.

The reactor was placed inside a furnace and all exposed parts of the reactor including the transition pipe were wrapped in insulating material. The furnace was set to maintain a constant reactor operating temperature of approximately 500°C. The transition pipe, connecting the reactor outlet to the condenser, was wrapped with trace heating tape and maintained at a temperature of 420°C to prevent vapours from cooling and condensing prior

to entering the primary condenser. The temperature was monitored at several points within the reactor to ensure optimal temperature conditions were maintained throughout the pyrolysis process.

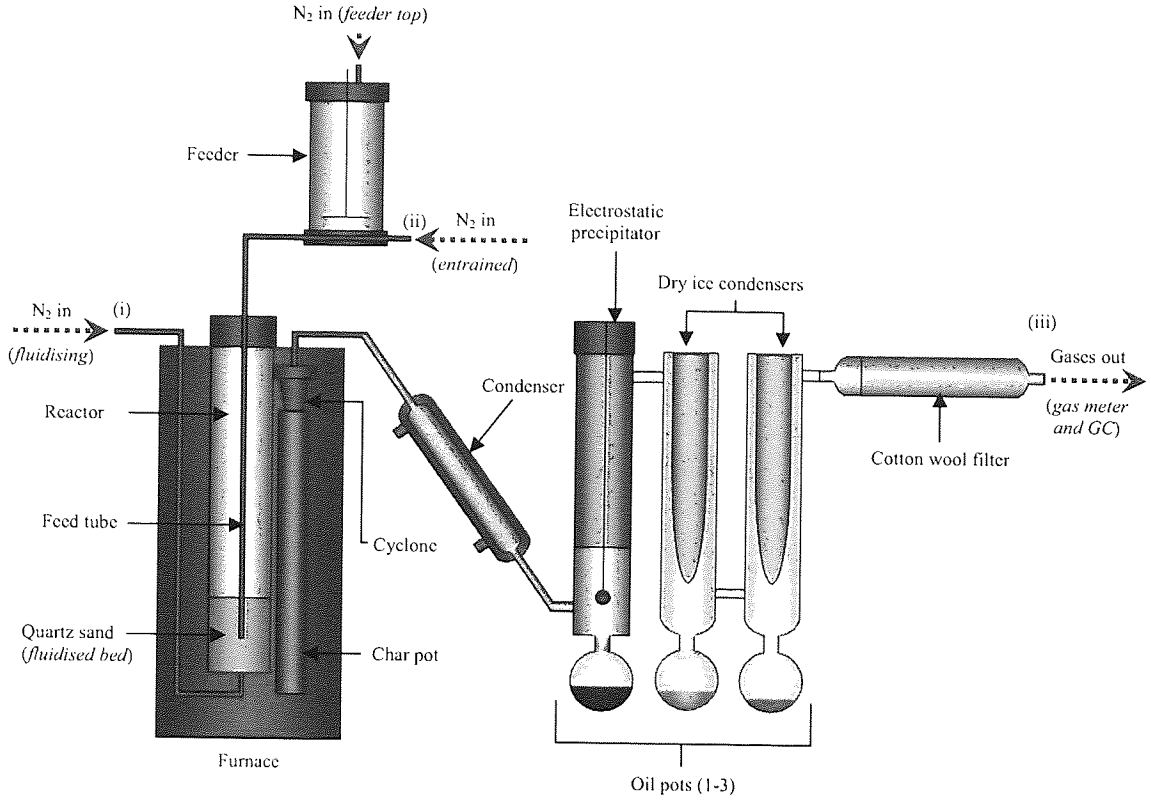

Figure 7.1 Schematic diagram of the bench scale rig used for fast-pyrolysis of *Miscanthus* biomass.

The diagram details composition and organisation of the bench scale fast-pyrolysis rig used in experiments carried out at Aston University (Birmingham, UK), including application of fluidising and entrained N_2.

Thermocouples were positioned to measure temperature in the fluidised bed (a), reactor freeboard (b), feeding tube outlet (c), and the transfer pipe (d) (Figure 7.2). Biomass feeding commenced once readings from all thermocouples had stabilized at approximately 20°C above the optimum pyrolysis temperature. This slightly higher initial temperature was used to compensate for the temperature reduction which occurs when feeding commences. This reduction is due to the endothermic reaction when lignocellulosic biomass is pyrolysed, the degree of reduction depending on the rate of feeding and flow rate of entrainment and fluidising nitrogen. The initial temperature used in this research was based on preliminary trials and observations by previous researchers [63, 115].

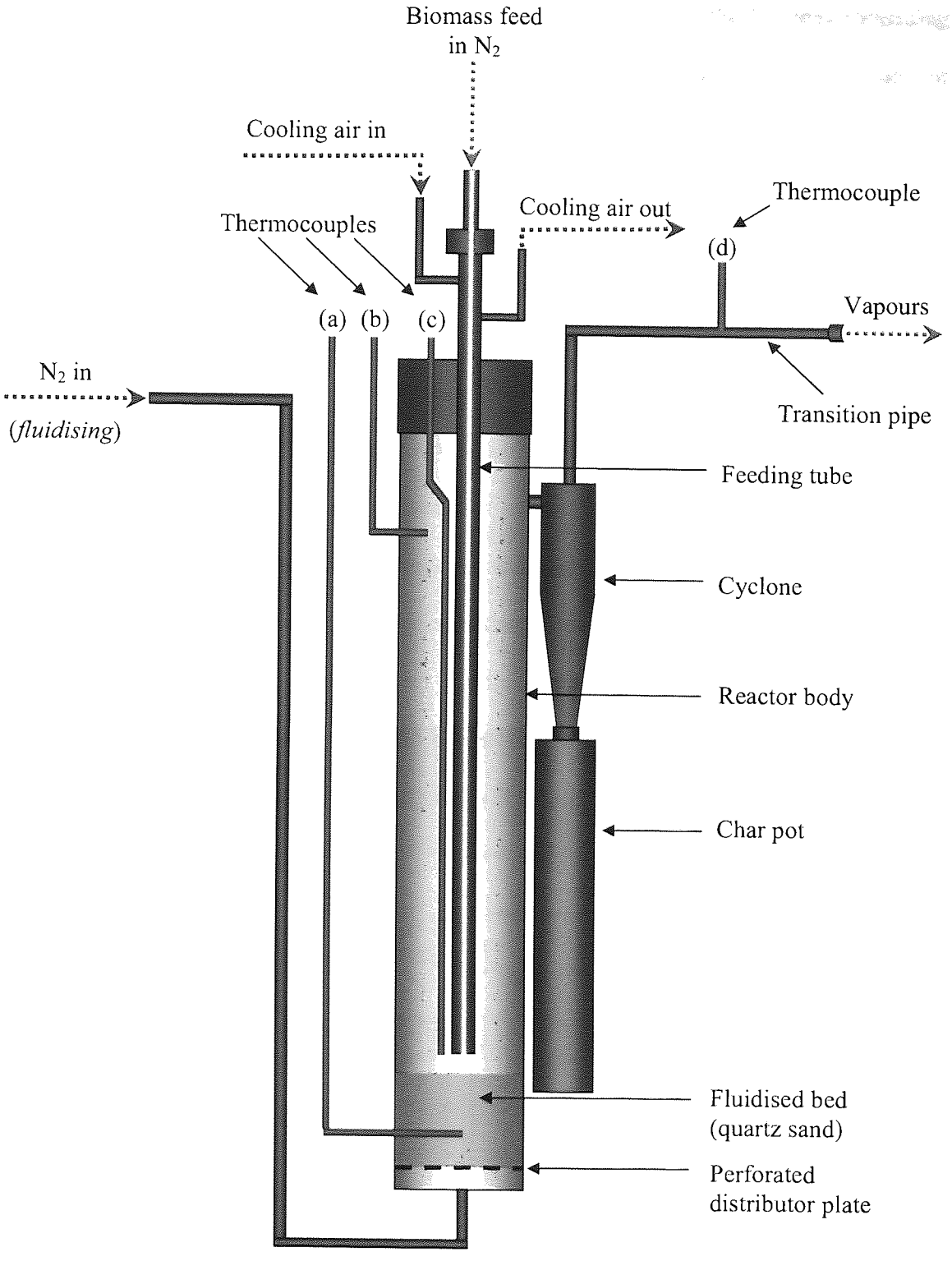

Figure 7.2 Schematic diagram of the bench scale reactor unit used for fast-pyrolysis of *Miscanthus* biomass.

The diagram details the composition and organisation of the bench scale fast-pyrolysis reactor unit used in experiments carried out at Aston University (Birmingham, UK), including application of fluidising and entrained N_2, cooling air, and location of thermocouples used for measurement of temperature within the reactor unit.

The system was flooded with nitrogen and on-line GC measurements commenced at least 15 min before biomass feeding to ensure the system was air-tight and the GC was measuring correctly. During pyrolysis processing of all samples, a nitrogen gas flow rate of approximately 6 L min^{-1} was used and pressure measurements were recorded at the fluidising and entrainment gas inlets (i, ii) and at the gas outlet between the cotton wool filter and the gas meter (iii) (Figure 7.1).

The feeder was filled with approximately 100 g of milled *Miscanthus* with a 250-355 μm particle size range. This particle size range was determined as optimal for this feeding system and feedstock by preliminary trials and the results of previous researchers [115] as it provided the most consistent feeding and minimised risk of blockage. The feeding system used an entrained flow of nitrogen, whereby nitrogen was introduced to the feeder from above and below the biomass material to aid feeding consistency during pyrolysis. The biomass sample was agitated using a variable speed rotary paddle and nitrogen flow from the top and the bottom of the feeder was used to draw the biomass particles through the feeder tube into the reactor. A schematic diagram of the feeder unit is illustrated in Figure 7.3.

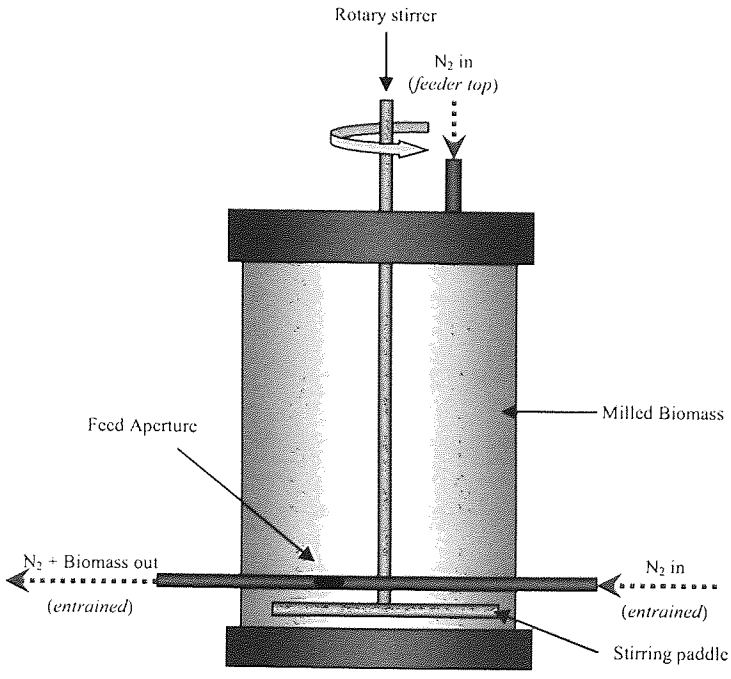

Figure 7.3 Schematic diagram of the biomass feeder unit.

Prior to connecting the feeder to the reactor, the feeding rate was measured and adjusted so that biomass was fed into the reactor at a rate of approximately 1 g min^{-1} for each sample. Biomass particles were carried though the feeding tube by the nitrogen flow and injected into the middle of the fluidised bed. The feeding tube was internally cooled by a flow of air to prevent blockages that might be caused by pyrolysis of biomass particles inside the feeding tube. Biomass particles were pyrolysed on contact with the fluidising medium producing a product mixture of volatiles, aerosols, char, water, and non-condensable gases. The product mixture was carried out of the reactor and through the cyclone where solid char was separated from the mixture and collected in the char pot. Vapours plus any un-separated char fines then passed through the transition pipe and into the condensation system comprising of a water-cooled condenser, an electrostatic precipitator (ESP), and two dry ice and acetone-cooled condensers (Figure 7.1).

In the water-cooled condenser the majority of the pyrolysis vapours were condensed, non-condensed vapours, aerosols, and char fines were carried into the ESP headspace where they were precipitated by an electrostatic charge (15 kV, 0.5 mA) and the liquid product collected in a 100 ml spherical flask beneath the ESP (oil pot 1). Residual uncondensed vapours, predominantly water and light volatiles, passed out of the ESP and were subsequently condensed by the series of dry ice condensers maintained at an estimated temperature of -30°C [63, 115]. Vapours condensed by the dry ice condensers were collected in two 50 ml spherical collection flasks (oil pots 2 and 3). Any un-condensed volatiles were prevented from exiting the system by a cotton wool filter and accounted for in the mass balance calculation. Non-condensable gases passed through the cotton wool filter and into the gas meter where the total volume of gases produced over the run was measured. A proportion of the gas was sent to the on-line GC for analysis and the remainder was vented.

All subsequent analyses, pertaining to mass balance calculation and characterisation of the pyrolysis products are described in section 3.4. Statistical analysis of data was performed as described in section 3.5.

7.3. Results and discussion

7.3.1. Dry matter yields of selected genotypes

Final harvest of the EMI trial site in February 2006 reported mean dry matter yields of 12.20, 10.77, and 8.34 t ha^{-1} for EMI02, EMI05, and EMI12 respectively.

7.3.2. Feedstock characterisation

To address problems associated with feeding biomass into the fast-pyrolysis reactor, the particle size range of the milled (<1 mm) *Miscanthus* biomass was restricted to a particle size range of 250-355 µm. To ensure direct comparison could be made between data from cell wall composition analyses and fast-pyrolysis product data, compositional analyses were performed again using this particle size fraction. Particle size has been observed to affect results of wet chemical analyses [116]. A small degree of variation was observed between the results of cell wall composition analyses performed on the fractionated and un-fractionated *Miscanthus* biomass (data not shown), however the genotypic rank order of cell wall component concentrations remained unchanged. It was decided that the results of analyses performed on the fractionated biomass used in fast-pyrolysis provided the more suitable data set for comparison with pyrolysis product yields and liquid composition.

The concentrations of cell wall components, moisture, and ash (g kg^{-1}) for the selected samples are shown in Table 7.2. The feedstock composition data presented is from analyses performed on the 250-355 µm particle size fraction used in fast-pyrolysis experiments.

Table 7.2 Cell wall composition and ash concentration of genotypes selected for fast-pyrolysis.

Data reported includes mean concentrations of lignin, cellulose, and hemicellulose of selected genotypes as determined by wet chemical analyses, and ash concentrations determined gravimetrically by loss on ignition. All values are reported for the 250-355 μm particle size fraction and are presented in g kg^{-1} on a dry matter basis. The results of analysis of variance have also been included with least significant differences (LSD) ($P \leq 0.05$) expressed in g kg^{-1} on a dry matter basis.

Genotype	Code	Lignin	Cellulose	Hemicellulose	Ash
M. x giganteus	EMI02	121.6	519.1	278.5	21.9
M. sacchariflorus	EMI05	106.5	511.7	291.1	20.6
M. sinensis	EMI12	84.6	438.6	361.3	32.2
df		2	2	2	2
$P \leq$		**	**	***	***
LSD		21.8	73.1	70.2	13.8

df = degrees of freedom; *** $P \leq 0.001$; ** $P \leq 0.05$; LSD= least significant difference ($P \leq 0.05$).

Analysis of variance identified significant genotypic differences between concentrations of all cell wall components ($P \geq 0.05$). The *M. x giganteus* genotype contained the highest concentrations of lignin and cellulose, and the *M. sinensis* genotype the lowest. The opposite rank order was observed for hemicellulose concentration. No significant difference was observed between the lignin, cellulose, and ash concentrations of *M. x giganteus* and *M. sacchariflorus*, however, both genotypes were identified as being significantly higher in lignin and cellulose, and lower in ash than *M. sinensis*. This supports previous observations that *M. x giganteus* and *M. sacchariflorus* display greater similarity when compared with *M. sinensis* [103]. The hemicellulose concentrations of all genotypes were identified as significantly different from one another.

7.3.3. Fast-pyrolysis products

The pyrolysis temperatures for all runs were consistent differing by a maximum of 4°C overall. The mass balance and run data are shown in Table 7.3. The mass balance closure for all runs was greater than 90% which is acceptable for the pyrolysis rig used [63, 79]. The shard-like nature of the milled *Miscanthus* feedstocks caused frequent blockage of the reactor feeding tube in preliminary trials (data not shown), restricting the particle size range to 250-355 μm significantly reduced incidences of blockage. In addition, the speed of the rotary paddle stirrer and rate of N_2 flow into the feeder-top was adjusted when necessary during runs

to avoid blockages occurring. These adjustments were responsible for the differences in the amounts of biomass dry matter fed and the feed rates seen in Table 7.3. During the fast-pyrolysis of the *M. sinensis* genotype (EMI12) blockages were a persistent problem and led to a proportion of un-pyrolysed biomass being retained in the feed tube and reactor on stopping the run. The weight of this un-pyrolysed biomass was measured and subtracted from the total weight fed. However it is likely that not all of the biomass was accounted for, and would explain the lower mass balance closure calculated for this genotype.

Table 7.3 Feedstock characteristics, operating conditions, product yields and mass balances achieved in the fast-pyrolysis of *Miscanthus* genotypes.

Data is reported by species and genotype. Feedstock characteristics include particle size range (μm) and total weight of biomass fed, including moisture, lignin, and ash concentration on a dry matter (DM) basis. Operating conditions reported include the mean pyrolysis temperature (°C) calculated from measurements taken at time points throughout the run, and feed rate calculated as the total amount of biomass fed over the whole run expressed in g hr^{-1}. Product yields and mass balances were calculated as the sum of the differences in weight of all rig components pre and post pyrolysis plus the calculated weight of non-condensable gases. Reaction water content was determined using the Karl-Fischer titration method. Mass balance values were expressed as a percentage of the total amount of biomass fed on a dry matter basis.

Feedstock		***M. x giganteus***	***M. sacchariflorus***	***M. sinensis***
Genotype		EMI02	EMI05	EMI12
Particle size	(μm)	250-355	250-355	250-355
Weight Fed	(g DM)	61.7	56.9	57.5
Moisture content	(g kg^{-1} DM)	58.0	72.1	59.7
Lignin	(g kg^{-1} DM)	121.6	106.5	84.6
Ash content	(g kg^{-1} DM)	21.9	20.6	32.2
Operating conditions				
Pyrolysis temperature	(°C)	494.6	493.9	497.9
Feed rate	(g hr^{-1})	87.3	51.1	61.7
Product yields and mass balances (% DM fed)				
Char		17.7	15.9	15.9
Liquids:		68.8	70.8	64.3
	Organics	46.7	48.5	49.9
	Reaction water	22.1	22.3	14.4
Gases:		10.2	9.0	10.3
Hydrogen	H_2	0.0	0.0	0.0
Carbon monoxide	CO	2.0	0.0	2.1
Methane	CH_4	0.6	0.7	0.6
Carbon dioxide	CO_2	7.4	8.0	7.3
Ethene	C_2H_4	0.1	0.1	0.1
Ethane	C_2H_6	0.1	0.2	0.1
Propene	C_3H_6	0.1	0.1	0.0
Propane	C_3H_8	0.0	0.0	0.0
n-Butane	C_4H_{10}	0.0	0.0	0.0
Closure:		**96.7**	**95.7**	**90.5**

Comparison of fast-pyrolysis product yields and cell wall composition of the *Miscanthus* genotypes, several relationships were apparent. The char yields ranged from 15.9-17.7% between genotypes, with *M. x giganteus* producing the highest yield and *M. sinensis* the lowest. It is known that lignin comprises a substantial proportion of the char produced at fast-pyrolysis temperatures (500°C) [107, 110, 113]. The char yields did share the same genotypic rank order as the lignin concentrations, but were not proportional to the variation observed in the lignin concentrations of the genotypes as determined by wet chemistry.

Characterisation of the char was not performed in this research, however it was possible that differences in lignin composition (S, G, and H sub unit ratios) had an influence on the proportion of lignin which was volatilised or retained in the char and would be a suitable topic for further research. However, char yields are also influenced by the ash content of the biomass [61, 67, 79] which has been observed to have a catalytic effect on thermal decomposition. Higher ash concentrations gave rise to higher yields of char and gas, which was observed in previous experiments discussed in sections 5.3.2 and 6.3.2. The *M. sacchariflorus* genotype (EMI05) contained the least amount of ash and also produced the lowest yield of gas, however the variation in ash concentration between genotypes was relatively small and no significant impact of total ash concentration on pyrolysis product yields can be discerned from these results. However, it is possible that significant genotypic differences may exist in the composition of the ash itself. If this was the case, it would undoubtedly alter the effect the catalysis had on the thermal decomposition of the biomass. The non-condensable gases produced by fast-pyrolysis of *M. x giganteus* and *M. sinensis* were mainly composed of CO_2 and CO. CO_2 was also the main non-condensable gas produced by *M. sacchariflorus* but no CO was detected.

The yields of liquid organics correlated strongly with the concentrations of holocellulose determined from the wet chemical analyses (R=0.96). The fast-pyrolysis liquid produced from

M. sinensis (EMI12) had a much lower reaction water content than the other genotypes which is not proportional to the moisture content of the feed and is not explained by any other variables or analyses.

The variation in cell wall composition between genotypes was relative subtle, as was the variation in product yields produced from fast-pyrolysis. In addition, it was likely that a certain proportion of the observed variation was related to differences in the operating conditions of the pyrolysis rig such as temperature, feed rate, and the rate of entrained nitrogen flow which had to be altered during fast-pyrolysis experiments to prevent blockages from occurring. In order to further assess the influence of cell wall composition, it was necessary to examine the properties of the fast-pyrolysis liquids produced from the different *Miscanthus* genotypes.

7.3.4. Molecular weight distribution and stability of pyrolysis liquids

The molecular weight distribution of the fast-pyrolysis liquids produced was analysed using gel permeation chromatography (GPC). The liquid collected in oil pot 1 constituted around 95% of the total organic liquid yield, with the remaining 5% collected in oil pots 2 and 3. The inclusion of multiple liquid collection vessels is a feature of the bench-scale fast-pyrolysis unit used and is included in the design to account for limitations in the condensation system. In industrial scale fast-pyrolysis facilities with more efficient condensation systems multiple collection vessels are not included in the design [54]. For these reasons, the liquid collected in oil pot 1 was regarded as the main fast-pyrolysis product and an in-depth analysis of the liquids collected in oil pots 2 and 3 was not performed.

GPC analysis was performed on the pyrolysis liquids collected in oil pot 1 before and after accelerated aging at 80°C for 24 h. The weight average molecular weight (Mw), the number average molecular weight (Mn), and the polydispersity (PD) of pyrolysis liquids produced

from different genotypes are reported in Table 7.4 and expressed in g mol^{-1}. The stability indices represent the degree of change observed in the Mw of pyrolysis liquids before and after accelerated aging (section 3.4.5). Higher stability values indicate greater instability and increased likelihood of phase separation during storage. The Mw of pyrolysis liquids produced ranged from 420-438 g mol^{-1} in the fresh liquid and from 541-564 g mol^{-1} after aging. The Mn of the fresh liquid ranged from 259-276 g mol^{-1} and 315-324 g mol^{-1} after aging. The PD value represents the ratio of Mw to Mn (Mw/Mn) and ranged from 1.59-1.62 in the fresh liquid and from 1.72-1.75 after aging. The Mw, Mn, and PD values were all significantly higher in the aged liquids, which implies that a certain degree of polymerisation did occur during accelerated aging of pyrolysis liquids produced from all genotypes.

Table 7.4 Molecular weight distribution of pyrolysis liquid before and after aging as determined by gel permeation chromatography.

Results show the weight average molecular weight (Mw), the number average molecular weight (Mn), and the polydispersity (PD) of pyrolysis liquids produced from different genotypes both fresh and after accelerated aging by incubating sub-samples of pyrolysis liquid for 24 h at 80°C. Values are reported in g mol^{-1}. Stability was calculated from the difference in Mw before and after aging. The results of the analysis of variance and levels of significance difference are also included.

Feedstock	***M. x giganteus***	***M. sacchariflorus***	***M. sinensis***	
Genotype	EMI02	EMI05	EMI12	
		Fresh		$P\leq$
Mw	421	438	420	**
Mn	264	276	259	***
PD	1.6	1.6	1.6	
		Aged		$P\leq$
Mw	541	564	558	**
Mn	315	323	324	**
PD	1.7	1.8	1.7	
Stability index	0.3	0.3	0.3	**

**$P\leq0.05$; ***$P\leq0.001$

Significant genotypic differences were identified between the Mw and Mn values of the pyrolysis liquids produced ($P\leq0.05$). The fresh pyrolysis liquid produced from *M. sacchariflorus* had significantly higher Mw than that produced from *M. x giganteus* and *M. sinensis* ($P\leq0.01$). The Mn values of pyrolysis liquids produced from all genotypes were found to be significantly different from one another ($P\leq0.001$), highest for *M. sacchariflorus*

and lowest for *M. sinensis*. However, whilst the Mw of the pyrolysis liquid produced from *M. sinensis* was significantly lower than that from *M. sacchariflorus*, it was likely to have produced the most viscous liquid as the reaction water content was nearly half that of the other two genotypes.

After accelerated aging, the Mw and Mn values of pyrolysis liquids produced from *M. sacchariflorus* and *M. sinensis* were significantly higher than that produced from *M. x giganteus* ($P \leq 0.03$). As the Mw of the pyrolysis liquid produced from *M. x giganteus* displayed the smallest increase after aging, it can be surmised that this liquid was the most stable, as reflected in the calculated stability value (Table 7.4). However the analysis of variance did not identify a significant difference between the stability of the pyrolysis liquid produced from *M. x giganteus* and *M. sacchariflorus*. Conversely, the liquid produced from *M. sinensis* was identified as significantly less stable than that produced from the other genotypes. No significant genotypic differences were observed in the poly-dispersity (PD) values indicating the pyrolysis liquids produced from all genotypes displayed a similar degree of molecular homogeneity both before and after aging.

From these results, the influence of cell wall composition on molecular weight distribution of the produced liquids cannot be discerned. It would be expected that higher lignin concentrations would confer higher Mw to the liquid product but this relationship was not identified in this study. This may be due to differences in the proportions of lignin retained in the char but this was not possible to substantiate from these results. However, the presence of higher ash concentrations in the *M. sinensis* biomass does appear to be related to the greater instability of the liquid product.

7.3.5. Pyrolysis liquid composition

In order to further assess the influence of feedstock composition on the composition of the fast-pyrolysis liquid product, all liquids produced were analysed using liquid injection GC-MS and the data analysed as described in section 3.4.6. Analysis of the GC-MS data identified that the most abundant compounds present in the fast-pyrolysis liquids corresponded closely to the key marker compounds identified by the Py-GC-MS characterisation (section 6.3.3). For this reason, and for ease of comparison, the peak numbers used in this section (1-39) are the same as those used in the Py-GC-MS characterisation performed in the previous chapter (section 6.3.3).

As described in the previous section (7.3.4), the liquid collected in oil pot 1 was regarded as the main fast-pyrolysis product. GC-MS analysis of the combined liquids collected in oil pots 2 and 3 identified them as predominantly composed of acetic acid (4), furfural (12), 2,3-butanedione (2), and hydroxypropanone (5), respectively. However, as this fraction represented less than 5% of the total organic liquid yield it was not subjected to further in-depth statistical analysis. Analysis of the pyrolysis liquid collected in oil pot 1 identified acetic acid (4) and levoglucosan (38) as the most abundant compounds present in pyrolysis liquids produced from all the *Miscanthus* genotypes. The results of the GC-MS analysis of oil pot 1 are reported in Table 7.5.

Of the 39 key markers identified by analytical Py-GC-MS (6.3.3) several compounds could not be accurately characterised in the fast-pyrolysis liquid collected in oil pot 1, namely propanal-2-one (1), 2-propanoic acid methyl ester (6), and 1,5-anhydro-β-D-xylofuranose (33). Accurate identification of these compounds could not be performed due to co-elution of compounds which produced overlapping spectra which could not be separated by deconvolution. On the whole, the types and amounts of compounds identified in the pyrolysis liquids produced from the different genotypes displayed a great degree of uniformity.

Table 7.5 Key marker compounds identified by GC-MS analysis of fast-pyrolysis liquids produced from *Miscanthus* genotypes.

Results shown are from the GC-MS analysis of pyrolysis liquids collected in oil pot 1. Compounds are listed by peak number relative to retention time (RT min^{-1}) and include compound name and origin. Mean compound amounts are expressed in terms of peak area as a percentage of the total ion chromatograph (TIC). Significant genotypic differences and level of significance have been included where identified by analysis of variance.

Peak	RT	Compound name	Origin	EMI 02	EMI 05	EMI 12	$P\leq$
1	-	propanal-2-one	C	-	-	-	
2	6.69	2,3-butanedione	C	0.1	0.1	0.1	ns
3	7.06	3-pentanone	C	<0.0	<0.0	<0.0	ns
4	9.06	acetic acid	C	1.0	1.2	0.8	ns
5	10.41	hydroxypropanone	C	0.4	0.3	0.4	ns
6	-	2-propenoic acid methyl ester	C	-	-	-	
7	14.35	1-hydroxy-2-butanone	C	0.2	0.1	0.1	***
8	14.78	3-hydroxypropanal (isomer of 5)	C	0.4	0.4	0.6	ns
9	15.75	(2H)-furan-3-one	C	0.1	0.1	0.1	ns
10	16.83	Butanedial	C	0.3	0.2	0.2	ns
11	16.98	2-hydroxy-3-oxobutanal	C	0.1	0.2	0.2	**
12	17.70	2-furaldehyde (furfural)	C	0.6	0.5	0.6	ns
13	19.99	3-furfural alcohol	C	0.1	<0.0	0.1	ns
14	20.35	1-acetyloxypropane-2-one	C	0.3	0.3	0.4	ns
15	20.62	Tetrahydro-4-methyl-3-furanone	C	0.1	0.1	0.1	ns
16	23.32	dihydro-methyl-furanone	C	0.6	0.6	0.6	ns
17	26.00	(5H)-furan-2-one	C	0.4	0.4	0.4	ns
18	27.13	4-hydroxy-5,6-dihydro-(2H)-pyran-2-one	C	0.2	0.4	0.7	**
19	28.21	2-hydroxy-1-methyl-1-cyclopentene-3-one	C	0.7	0.5	0.5	***
20	29.85	Phenol	H	0.3	0.3	0.3	**
21	30.57	Guaiacol	G	0.6	0.5	0.4	***
22	35.36	4-methyl-guaiacol	G	0.2	0.2	0.2	ns
23	35.46	anhydrosugar (unknown)	C	0.3	0.3	0.3	ns
24	39.11	4-ethyl-guaiacol	G	0.1	0.1	<0.0	ns
25	39.32	3-methyl-2,4-furandione	C	<0.0	<0.0	<0.0	ns
26	40.58	1,4:3,6-dianhydro-glucopyranose	C	0.1	0.1	0.1	***
27	40.92	1,5-anhydro-arabinofuranose	C	0.2	0.2	0.3	ns
28	41.54	4-vinyl-phenol	H	0.5	0.6	0.5	ns
29	41.57	4-vinyl-guaiacol	G	0.1	0.2	0.2	ns
30	43.20	5-hydroxymethyl-2-furaldehyde	C	0.1	0.1	0.2	**
31	43.62	Catechol	H	<0.0	<0.0	<0.0	ns
32	43.82	Syringol	S	0.5	0.3	0.2	***
33	-	1,5-anhydro-β-D-xylofuranose	C	-	-	-	
34	47.01	Isoeugenol	G	0.4	0.3	0.4	ns
35	47.53	4-methyl-syringol	S	0.1	0.1	0.1	ns
36	47.87	Vanillin	G	0.2	0.2	0.2	ns
37	52.62	4-vinyl-syringol	S	0.1	0.1	<0.0	ns
38	56.54	levoglucosan	C	1.0	0.9	1.1	ns
39	57.32	syringol, 4-propenyl (cis)	S	0.2	0.1	0.1	ns

Origin: C = holocellulose; H = *p*-hydroxyphenyl; G = Guaiacyl; S = Syringyl. *** $P\leq0.001$; ** $P\leq0.05$; n/s = no significant difference ($P\geq0.05$).

However, statistical analysis did identify significant genotypic differences in the amounts of 8 of the 39 key marker compounds identified in the liquid collected in oil pot 1. Significant genotypic differences were identified in amounts of 5 holocellulose derived and 3 lignin derived compounds. Amongst the holocellulose derived compounds, the liquid produced from *M. x giganteus* contained significantly higher amounts of compounds 8, 19 and 26, and significantly lower amounts of compound 11 than that produced from the other genotypes, whereas the *M. sinensis* liquid contained significantly higher amounts of compounds 18 and 30 than the other genotypes. Amongst the lignin derived compounds, the pyrolysis liquid produced from *M. x giganteus* was significantly higher in compound 20 than all other genotypes, and the *M. sinensis* liquid contained significantly lower amounts of compounds 21 and 32 than that produced from *M. x giganteus* and *M. sacchariflorus*.

Comparing these results with those of the analytical pyrolysis experiments carried out in the previous chapter (6.3.3), a degree of similarity was observed regarding where significant genotypic differences were identified within the two data sets. With the exception of *M. x sacchariflorus* (EMI05), different genotypes of *M. x giganteus* and *M. sinensis* were used in the analytical pyrolysis and fast-pyrolysis experiments. However, similar within species trends were observed within material harvested at the same time. In both experiments *M. x giganteus* and *M. sacchariflorus* were identified as containing significantly higher concentrations of guaiacol and syringol (compounds 21 and 32) compared to *M. sinensis*. In all cell wall analyses performed in this thesis, the *M. x giganteus* and *M. sacchariflorus* clones used displayed cell wall characteristics similar to one another and distinctly different to those of *M. sinensis*. The results of both the Py-GC-MS and GC-MS analysis of the fast pyrolysis liquids indicated that differences may exist in the lignin composition of these species, but further analysis would be required to substantiate this. The pyrolysis liquid produced from the *M. sinensis* genotype (EMI12) was significantly higher in the holocellulose derived compounds 11, 18, and 30. A similar trend was observed in the *M. sinensis* genotypes

analysed by Py-GC-MS and suggests a similarity may exist between the EMI12 and EMI15 genotypes.

Overall, a high degree of uniformity was observed in the composition of the fast-pyrolysis liquids produced from the different *Miscanthus* species and genotypes. However, significant genotypic differences were observed in the amounts (%TIC) of several compounds which can be linked to differences in cell wall composition of the feedstock. In both the analytical pyrolysis experiments and the GC-MS analysis of the fast-pyrolysis liquids similar compositional trends were observed between *Miscanthus* species which indicates a potential for breeding to improve the pyrolysis product yields of high value compounds such as levoglucosan and 5-hydroxymethyl-2-furaldehyde, provided a clear link between yields of these compounds and cell wall compositional traits can be determined.

7.3.6. Comparison of pyrolysis liquids produced from Miscanthus and other feedstocks

In order to assess the suitability of *Miscanthus* as a feedstock for fast-pyrolysis it is necessary to compare the results with those attained using other feedstocks. The results in Table 7.6 compare feedstock and fast-pyrolysis product characteristics of *Miscanthus* with published data of other potential feedstocks, short rotation coppice (SRC) willow and wheat straw [61]. Fast-pyrolysis of all feedstocks was performed using the same equipment and conditions.

Comparing the composition of the feedstocks, as expected, willow SRC had a much higher concentration of lignin than the grasses and a positive relationship was observed between lignin concentration the HHV of the raw biomass (R=0.74) which supports observations made previously [73, 97]. However, no significant difference was observed between the HHV or LHV of the *Miscanthus* biomass used in this study. The holocellulose concentration of the *Miscanthus* genotypes was considerably higher than the other feedstocks by approximately 130-170 g kg^{-1}. Wheat straw contained a significantly higher moisture content (13-34 g kg^{-1})

and was significantly higher in ash by 30-50 g kg^{-1} [79], almost double that of *M. sinensis* which contained the second highest ash concentration.

Table 7.6 Influence of feedstock type and composition on fast-pyrolysis product yields and characteristics of the liquid product.

Feedstock composition and fast-pyrolysis products of *Miscanthus* genotypes were compared with wheat straw and short rotation coppice (SRC) willow as determined by Fahmi *et al.*, 2008 [61]. Mean concentrations of lignin, holocellulose, moisture, and ash are reported in g kg^{-1} on a dry matter basis. All fast-pyrolysis experiments were conducted using a bench-scale (150 g h^{-1}) pyrolysis rig and performed under the same experimental conditions. Product yields are reported as a percentage of the total amount of biomass fed on a dry matter basis. Reaction water content was determined using the Karl-Fischer titration method and reported in weight percent. Higher heating values (HHV) and lower heating values (LHV) of raw biomass and pyrolysis liquids were calculated using equations based on results of the elemental analyses and expressed in MJ kg^{-1}. Analyses of the fast-pyrolysis liquids were performed on the liquids collected in oil pot 1.

		Miscanthus genotypes				
		EMI 02	EMI 05	EMI 12	Wheat straw	Willow SRC
		Feedstock characteristics				
Lignin	g kg^{-1}	121.6	106.5	84.6	73.6	196.2
Holocellulose	g kg^{-1}	797.6	802.8	799.9	671.4	624.1
Ash	g kg^{-1}	21.9	20.6	32.2	62.9	13.4
Moisture	g kg^{-1}	58.0	72.1	59.7	91.4	77.6
HHV	MJ kg^{-1}	16.6	16.7	16.7	17.3	18.9
LHV	MJ kg^{-1}	15.5	15.5	15.6		
		Fast-pyrolysis product yields				
Char	% DM	17.7	15.9	15.9	31.9	20.9
Gases:	% DM	10.2	9.0	10.3	15.6	9.3
Total liquids:	% DM	68.8	70.8	64.3	50.6	68.8
Organics	% DM	46.7	48.5	49.9	24.9	52.9
Reaction water	% DM	22.1	22.3	14.4	25.7	15.9
		Fast-pyrolysis liquid characteristics				
Carbon	% wt	44.1	45.6	44.8	28.2	43.2
Hydrogen	% wt	7.1	7.0	7.1	8.8	7.2
Nitrogen	% wt	-	-	-	-	-
Sulphur	% wt	-	-	-	-	-
Oxygen	% wt	48.0	46.5	47.4	62.8	49.5
Water	% wt	22.1	18.3	16.5	47.4	17.4
HHV	MJ kg^{-1}	14.6	15.7	15.8	7.2	15.2
LHV	MJ kg^{-1}	12.9	14.0	14.1	5.0	13.5
Stability*		Single phase	Single phase	Single phase	Separated	Single phase

*Stability: based on homogeneity of liquids after three months storage at ambient temperature.

The high ash concentration clearly influenced the yields of gas and char as is evident from the product yields observed for wheat straw [79], which produced higher yields of char and gas, and lower yields of liquid compared to all other feedstocks. Ash concentration correlated strongly with yields of char and gas (R=0.81 and 0.97 respectively). The higher lignin concentration of willow SRC did appear to contribute to the char yield of this feedstock which was higher than the *Miscanthus* despite having a lower ash concentration. Differences

observed between the fast-pyrolysis product yields of *Miscanthus* genotypes and willow SRC which are not explained by cell wall composition may be related to differences in operating conditions during fast-pyrolysis processing due to the occurrence of blockage during fast-pyrolysis of the *Miscanthus* genotypes using the lab scale rig (section 7.3.3).

Characterisation of the pyrolysis liquid produced from all *Miscanthus* feedstocks was performed using the pyrolysis liquid collected in oil pot 1 as it accounted for approximately 95% of the organic liquid yield. Higher and lower heating values (HHV and LHV) of the pyrolysis liquids were calculated using equations based on the results of the elemental analysis and were corrected for their water content [86, 87]. The HHV and LHV of the pyrolysis liquids produced from the *M. sacchariflorus* and *M. sinensis* genotypes were significantly higher than that produced from *M. x giganteus* ($P \leq 0.01$), and were also higher than that produced from the other feedstocks. Variation in heating values was predominantly related to reaction water and ash concentration, and not to lignin. A strong relationship between lignin concentration and the heating values of the pyrolysis liquids was not observed, however a strong negative relationship was observed between ash concentration and the heating values (R= -0.91). This relationship was observed as the ash concentration had the greatest effect on yields of reaction water in pyrolysis liquids (R=0.92).

In previous research a relationship was observed between the lignin content of the biomass feedstock and its heating value [3, 73, 97, 117]. Whilst a relationship was observed between lignin concentration and HHV of the raw biomass (Table 7.6), this relationship was not observed in the heating values of the pyrolysis liquids. The HHV and LHV of the pyrolysis liquid produced from willow SRC was lower than that of the *M. sacchariflorus* and *M. sinensis* genotypes despite having a significantly higher lignin concentration (Table 7.6). The results of these experiments indicate that ash concentration had the greatest impact on the heating values of the pyrolysis liquids due to the relationship observed between ash

concentration and reaction water. However, it has been reported that a substantial proportion of the lignin is retained in the char at pyrolysis temperatures below 550°C [110]. Therefore the lignin concentration of the raw feedstock may not provide a proportional representation of the pyrolytic lignin content of the liquids produced from fast-pyrolysis.

Comparison of fast-pyrolysis liquid stability between *Miscanthus* and other feedstocks was based on visual assessment of phase stability after storage at ambient temperature for three months. After storage, phase separation was visible in the pyrolysis liquid produced from wheat straw but not in the liquids produced from *Miscanthus* and willow. Furthermore, phase separation had also not visibly occurred in the *Miscanthus* pyrolysis liquids after accelerated aging at 80°C for 24 h which suggests that the liquids would still be in a single phase after storage for one year [94]. These results indicate that ash concentration had the greatest effect on pyrolysis liquid stability which supports observations made previously [61, 67, 94]. The high ash concentration of wheat straw appeared to be responsible for the instability and phase separation of the produced liquid after storage. The high ash *M. sinensis* genotype was also identified as producing the least stable pyrolysis liquid of the *Miscanthus* feedstocks on the basis of stability indices calculated from the Mw averages before and after accelerated aging. However as no visible phase separation had occurred in the *M. sinensis* pyrolysis liquid after storage or accelerated aging, it can be assumed that the ash concentration of this genotype was not high enough to greatly influence the stability of the pyrolysis liquid.

Viscosity analysis was not performed on the pyrolysis liquids produced from the *Miscanthus* genotypes. The pyrolysis liquids produced from the *Miscanthus* genotypes were not in sufficient quantity to perform an accurate analysis of viscosity.

7.4. Chapter conclusions

Significant genotypic differences were observed in the dry matter yields, cell wall composition, and ash concentrations of the *Miscanthus* genotypes. *M. x giganteus* (EMI02) had the highest dry matter yield and also the highest concentrations of lignin and cellulose and the lowest concentration of hemicellulose. The opposite was observed for the *M. sinensis* genotype (EMI12).

Little overall genotypic difference was observed between the yields of fast-pyrolysis products. The total liquid yield observed for all genotypes ranged from 64-70%, with char yields ranging from 15-18%, and gas yields ranging from 9-10%.

The HHV and LHV of the pyrolysis liquids produced from the *M. sacchariflorus* and *M. sinensis* genotypes were higher than that produced from *M. x giganteus*, and variation in heating value was predominantly related to reaction water and ash concentration, and not to lignin. The heating values of *Miscanthus* genotypes compared favourably with those of pyrolysis liquids produced from wheat straw and willow SRC.

Ash concentration was observed to have the greatest effect on yields of reaction water, heating value and stability. The pyrolysis liquids produced from *Miscanthus* genotypes had high stability and did not phase-separate during storage.

A high degree of uniformity was observed in the composition of the fast-pyrolysis liquids produced from the different *Miscanthus* species and genotypes. However, significant genotypic differences were observed in the amounts of several compounds which can be linked to differences in cell wall composition.

The elemental analysis identified oxygen as the most abundant element in the pyrolysis liquids produced from all feedstocks. This is a common feature of biomass derived pyrolysis liquid and represents a major limiting factor in its utilisation as a fuel due to the reduction of heating value [49, 52, 54, 59]. However, the oxygen content can be reduced through upgrading processes such as hydrogenation or zeolite cracking [48, 49, 52, 63]. The nitrogen and sulphur content of the pyrolysis liquids produced from all feedstocks were negligible (<0.1%) which indicates that combustion of these liquids would not result in high emissions of pollutant gases such as NO_x and SO_2.

Overall, *Miscanthus* biomass appears to provide a good feedstock for fast-pyrolysis. The yields and quality parameters of the pyrolysis liquids produced from *Miscanthus* compared favourably with that produced from willow SRC and resulted in a liquid with a higher LHV.

8. SUMMARY OF CONCLUSIONS

A significant range of variation in cell wall composition has been identified between the *Miscanthus* species and genotypes investigated in this study. Overall, genotype had a more significant effect on cell wall composition than environment. This indicates good potential for dissection of this trait by QTL analysis and also for plant breeding to produce new genotypes with improved feedstock characteristics for energy conversion.

The NIRS calibration models developed for the prediction of cell wall composition from sample spectra was found to predict concentrations with a good degree of accuracy. The technique provided a suitable high-throughput screening method for the analysis of *Miscanthus* biomass, and has potential to be further developed to assess other energy crop species and/or other compositional features of interest.

Application of nitrogen and potassium fertiliser had a negative effect on feedstock quality. Higher rates of nitrogen fertiliser resulted in lower concentrations of cell wall components and higher accumulation of ash within the biomass. The results indicate that *Miscanthus* can be used to produce high yields of high quality lignocellulosic biomass without the application of inorganic fertilisers. This presents considerable environmental and economic benefit, and reflects positively on the sustainability of crop and its use as a bioenergy feedstock.

Overall, *Miscanthus* biomass appears to provide a good feedstock for fast-pyrolysis. The yields and quality parameters of the pyrolysis liquids produced from *Miscanthus* compared favourably with that produced from willow SRC and resulted in a liquid with a higher LHV. A high degree of uniformity was observed in the composition of the fast-pyrolysis liquids produced from the different *Miscanthus* species and genotypes. However, significant genotypic differences were observed in the amounts of several compounds which can be linked to differences in cell wall composition. Py-GC-MS analysis revealed significant

genotypic differences in the range of products which may be derived via pyrolysis processing and indicated that genotypes other than the currently commercially cultivated *M. x giganteus* have great potential for use in energy conversion processes and as feedstocks for the bio-refining of chemicals.

Concentrations of ash were identified as having a stronger effect on the yields of volatiles and char than lignin. However, lignin concentration was also identified as a key factor. Variation in heating value and stability of pyrolysis liquids was predominantly related to reaction water and ash concentration, and not to lignin. The pyrolysis liquids produced from *Miscanthus* genotypes were more stable than that produced from wheat straw and SRC willow and did not phase-separate during storage.

9. RECOMMENDATIONS FOR FURTHER RESEARCH

Development/adaptation of more reliable and descriptive analytical methods which can provide more in-depth and reliable data on which to develop chemometric calibrations and to better inform *Miscanthus* breeding programmes. Proposed research would include the investigation of existing and novel methods of analysis by both wet-chemical, enzymatic, and mass spectral techniques to more effectively characterise cell wall composition and secondary metabolites. In particular, methods for quantifying relative proportions of lignin sub-units (S, G, H) and hemicelluloses would provide higher resolution data for assessing genetic and environmental variation, and also how this variation could best be exploited in a bio-refinery system.

Results of this study, and the findings of previous research, have highlighted the improvement of *Miscanthus* biomass quality by delaying crop harvesting until after senescence occurs. Senescence has been linked to flowering time which has been observed to differ significantly between genotypes. Further study of genetic and environmental influence on senescence and the relationship between maturity and cell wall composition would provide useful information for optimising harvest times and additional information for use in breeding programmes.

In this study the inorganic components of the biomass were simply determined as 'total ash' and as such it was difficult to identify and attribute potential genotypic differences in the retention of inorganics within the biomass. Analysis of the elemental composition of the ash, particularly the alkali metal fraction, could possibly allow better explanation of the catalytic influence the ash component of the biomass had on thermal decomposition and thermal stability of the pyrolysis liquids.

Fast-pyrolysis experiments conducted in this study were performed using a bench scale rig (150 g h^{-1}), as a result relatively small amounts of biomass were processed. Utilisation of a

larger scale rig (5 kg h^{-1}) would allow conversion of larger amounts of *Miscanthus* biomass and provide an improved representation of the commercial potential of *Miscanthus* as a feedstock for fast-pyrolysis. Inclusion of a full characterisation of pyrolysis products (liquids, gases and chars) would provide improved data on conversion efficiency, product yields and characteristics, and would also provide an additional indirect method for assessing variation in cell wall composition of the biomass used. Full characterisation of pyrolysis products from *Miscanthus* would also provide information necessary for life-cycle assessment of this conversion pathway, and also the potential for utilisation of process residues.

In this study, emphasis was placed on the thermo-chemical conversion pathway. Investigation of potential for utilisation of *Miscanthus* in bio-chemical conversion processes such as anaerobic digestion and fermentation would provide useful information regarding the potential and suitability of the crop to these conversion processes. In addition, characterisation of residues from bio-chemical conversion would provide useful information regarding the potential for additional/sequential conversion and utilisation of these residues as part of a bio-refinery system.

10. BIBLIOGRAPHY

1. Powlson, D.S., A.B. Riche, and I. Shield, *Biofuels and other approaches for decreasing fossil fuel emmissions from agriculture.* Annals of Applied Biology, 2005. **146**: p. 193-201.
2. Clifton-Brown, J.C., I. Lewandowski, B. Andersson, G. Basch, D.G. Christian, J.B. Kjeldsen, U. Jorgensen, J.V. Mortensen, A.B. Riche, K.U. Schwarz, K. Tayebi, and F. Teixeira, *Performance of 15 Miscanthus genotypes at five sites in Europe.* Agronomy (U.S), 2001. **93**(5): p. 1013-1019.
3. Lewandowski, I., J.C. Clifton-Brown, B. Andersson, G. Basch, D.G. Christian, U. Jorgensen, M.B. Jones, A.B. Riche, K.U. Schwarz, K. Tayebi, and F. Teixeira, *Biofuels: environment and harvest time affects the combustion qualities of Miscanthus genotypes.* Agronomy (U.S), 2003. **95**: p. 1274-1280.
4. Stampfl, P.F., J.C. Clifton-Brown, and M.B. Jones, *Europe-wide GIS-based modelling system for quantifying the feedstock from Miscanthus and the potential contribution to renewable energy targets.* Global Change Biology, 2007. **13**: p. 2283-2295.
5. Houghton, J.T., Y. GDing, D.J. Griggs, M. Noguer, P.J. Van der Linden, X. Dai, K. Maskel, and C.J. Johnson, *Intergovernmental Panel on Climate Change: Third assessment report; Working group 1 - The scientific basis*. 2001, UNEP. WMO. IPCC.
6. Stern, *The Stern Review: Economics of climate change*, H.M.T. Office, Editor. 2007.
7. Marland, G., T.A. Boden, and R.J. Andres, *Global, Regional, and National CO2 Emmissions: A compendium of data on global change.*, O.R.N.L. Carbon dioxide information centre, Tennessee, U.S.A., Editor. 2005.
8. UNFCCC, *The first ten years*. 2004, United Nations Framework Convention on Climate Change Secretariat.
9. DTI, *A white paper on energy: Meeting the energy challenge*, D.o.T.a. Industry, Editor. 2007, TSO.
10. DTI, *Energy White Paper: Our energy future: Creating a low carbon economy*, D.o.T.a. Industry, Editor. 2003, TSO.
11. BERR, *The Energy White Paper: Updated energy and carbon emissions projections*, D.f.B.E.a.R. Reform, Editor. 2008, TSO.
12. McKendry, P., *Energy production from biomass (part 1): overview of biomass.* Bioresource Technology, 2002. **83**(1): p. 37-46.
13. Demirbas, A., *Biomass resource facilities and biomass conversion processing for fuels and chemicals.* Energy Conversion and Management, 2001. **42**(11): p. 1357-1378.

14. Scurlock, J.M.O., *Biofuels for transport in the UK: What is feasible?* Energy and Environment., 2005. **16**: p. 273-282.

15. RCEP, *Biomass as a renewable energy source*, in *Royal Commission on Environmental Pollution*. 2004.

16. DEFRA, *UK Biomass Strategy*, DEFRA, Editor. 2007, TSO.

17. Venturi, P. and G. Venturi, *Analysis of energy comparison for crops in European agricultural systems.* Biomass and Bioenergy, 2003. **25**(3): p. 235-255.

18. Green, N.P.O., G.W. Stout, and D.J. Taylor, *Biological Science: Organisms, Energy and Environment* ed. R. Soper. 1984, Cambridge, UK: Cambridge University Press.

19. Furbank, R.T. and W.C. Taylor, *Regulation of photosynthesis in C_3 and C_4 plants: A molecular approach.* The Plant Cell, 1995. **7**: p. 797-807.

20. Long, S.P., *C_4 photosynthesis at low temperatures.* Plant Cell and Environment, 1983. **6**: p. 345-363.

21. Monteith, J.L., *Light distribution and photosynthesis in field crops.* Journal of Experimental Biology, 1978. **29**: p. 17-37.

22. Beale, C.V., J.I.L. Morison, and S.P. Long, *Water use efficiency of C_4 perennial grasses in a temperate climate.* Agricultural and Forest Meteorology, 1999. **96**(1-3): p. 103-115.

23. Christian, D.G. and E. Haase, *Agronomy of Miscanthus*, in *Miscanthus for energy and fibre*, M.B. Jones and M. Walsh, Editors. 2001, James & James science Publishers Ltd. Cromwell Press.

24. Styles, D., F. Thorne, and M.B. Jones, *Energy crops in Ireland: An economic comparison of willow and Miscanthus production with conventional farming systems.* Biomass and Bioenergy, 2008. **32**(5): p. 407-421.

25. Venturi, P., J.K. Gigler, and W. Huisman, *Economical and technical comparison between herbaceous (Miscanthus x giganteus) and woody energy crops (Salix viminalis).* Renewable Energy, 1999. **16**(1-4): p. 1023-1026.

26. Gullu, D. and A. Demirbas, *Biomass to methanol via pyrolysis process.* Energy Conversion and Management, 2001. **42**(11): p. 1349-1356.

27. Sanderson, M.A., F. Agblevor, M. Collins, and D.K. Johnson, *Compositional analysis of biomass feedstocks by near infrared reflectance spectroscopy.* Biomass & Bioenergy, 1996. **11**(5): p. 365-370.

28. Dey, P.K. and K. Brinson, *Plant cell walls.* Advances in crabohydrate chemistry and biochemistry, 1984. **42**: p. 265-382.

29. Northcote, D.H., *Chemistry of the plant cell wall.* Annual Review of Plant Physiology, 1972. **23**: p. 113-132.

30. Popper, Z.A., *Evolution and diversity of green plant cell walls.* Current Opinion in Plant Biology, 2008. **11**: p. 286-292.

31. Salmen, L., *Micromechanical understanding of the cell wall structure.* Comptes Rendus Biologies, 2004. **327**: p. 873-880.

32. Brett, C. and K. Waldron, *Physiology and biochemistry of the plant cell wall.* Second ed. 1996, London, UK: Chapman and Hall.

33. McCann, M.C. and N.C. Carpita, *Designing the deconstruction of plant cell walls.* Current Opinion in Plant Biology, 2008. **11**: p. 314-320.

34. Vogel, J., *Unique aspects of the grass cell wall.* Current Opinion in Plant Biology, 2008. **11**: p. 301-307.

35. DOE, *Breaking the biological barriers to cellulosic ethanol: A joint research agenda. DOE/SC/EE-0095.* 2006, U.S. Department of Energy: Office of Science & Office of Energy Efficiency and Renewable Energy.

36. Dixon, R.A., F. Chen, D. Guo, and K. Parvathi, *The biosynthesis of monolignols: a 'metabolic gid', or independent pathways to guaiacyl and syringyl units?* Phytochemistry, 2001. **57**: p. 1069-1084.

37. Del Rio, J.C., A.T. Martinez, and A. Gutierrez, *Presence of 5-hydroxyguaiacyl units as native lignin constituents in plants as seen by Py-GC/MS.* Journal of Analytical and Applied Pyrolysis, 2006.

38. Boudet, A.M., S. Kajita, J. Grima-Pettenati, and D. Goffner, *Lignins and lignocellulosics: a better control of synthesis for new and improved uses.* Trends in plant science, 2003. **8**: p. 576-581.

39. Donaldson, L.A., *Lignification and lignin topochemistry - an ultrastructural view.* Phytochemistry, 2001. **57**: p. 859-873.

40. Whetten, R. and R. Sederoff, *Lignin biosynthesis.* The Plant Cell, 1995. **7**: p. 1001-1013.

41. Ishii, T., *Structure and functions of feruloyated polysaccharides.* Plant Science, 1997. **127**: p. 111-127.

42. Ralph, J., S. Guillaumie, J.H. Grabber, C. Lapierre, and Y. Barriere, *Genetic and molecular basis of grass cell-wall biosynthesis and degradability. III. Towards a forage grass ideotype.* Comptes Rendus Biologies, 2004. **327**: p. 467-479.

43. Lewandowski, I., J.C. Clifton-Brown, J.M.O. Scurlock, and W. Huisman, *Miscanthus: European experience with a novel energy crop.* Biomass and Bioenergy, 2000. **19**(4): p. 209-227.

44. Scally, L., T.R. Hodgkinson, and M.B. Jones, *Origins and taxonomy of Miscanthus*, in *Miscanthus for energy and fibre*, M.B. Jones and M. Walsh, Editors. 2001, James & James Science Publishers Ltd. Cromwell Press.

45. Greef, J.M. and M. Deuter, *Syntaxonomy of Miscanthus x giganteus Greef et Deu.* Angewandte Botanik, 1993. **67**(3/4): p. 87-90.

46. Jones, M.B. and M. Walsh, eds. *Miscanthus for energy and fibre.* 2001, James & James Science publishers Ltd. Cromwell Press.

47. Hotz, A., W. Kuhn, and S. Jodl, *Screening of different miscanthus cultivars in respect of their productivity and usability as a raw material for energy and industry.*, in *Miscanthus for energy and fibre.*, M.B. Jones and M. Walsh, Editors. 1996, James & James Science Publishers Ltd. Cromwell Press.

48. McKendry, P., *Energy production from biomass (part 2): conversion technologies.* Bioresource Technology, 2002. **83**(1): p. 47-54.

49. Bridgwater, A.V., *The production of biofuels and renewable chemicals by fast pyrolysis of biomass.* International Journal of Global Energy Issues, 2007. **27**: p. 160-202.

50. Demirbas, A., *Carbonization ranking of selected biomass for charcoal, liquid and gaseous products.* Energy Conversion and Management, 2001. **42**(10): p. 1229-1238.

51. Faaij, A.P.C., *Bio-energy in Europe: changing technology choices.* Energy Policy, 2006. **34**: p. 322-342.

52. Bridgwater, A.V., *Renewable fuels and chemicals by thermal processing of biomass.* Chemical Engineering Journal, 2003. **91**(2-3): p. 87-102.

53. DTI, *Renewable Energy: Reform of the Renewables Obligation*, T.a. Industry, Editor. 2007, TSO.

54. Bridgwater, A.V., *An introduction to fast pyrolysis of biomass for fuels and chemicals*, in *Fast pyrolysis of biomass: a handbook*, A.V. Bridgwater, et al., Editors. 1999, CPL Scientific publishing services Ltd: Newbury, UK. p. 1-13.

55. Brammer, J.G., M. Lauer, and A.V. Bridgwater, *Opportunities for biomass-derived "bio-oil" in European heat and power markets.* Energy Policy, 2006. **34**: p. 2871-2880.

56. Chiaramonti, D., A. Oasmaa, and Y. Solantausta, *Power generation using fast pyrolysis liquids from biomass.* Renewable and Sustainable Energy Reviews, 2007. **11**: p. 1056-1086.

57. Oasmaa, A. and S. Czernik, *Fuel oil quality of biomass pyrolysis oils - state of the art for end users.* Energy and Fuels, 1999. **13**: p. 914-921.

58. Bridgwater, A.V., A.J. Toft, and J.G. Brammer, *A techno-economic comparison of power production by biomass fast pyrolysis with gasification and combustion.* Renewable and Sustainable Energy Reviews, 2002. **6**(3): p. 181-246.

59. Diebold, J.P., *Overview of fast pyrolysis of biomass for the production of liquid fuels*, in *Fast pyrolysis of biomass: a handbook*, A.V. Bridgwater, et al., Editors. 1999, CPL Scientific Publishing Services Ltd.: Newbury, UK. p. 14-32.

60. Oasmaa, A. and E. Kuoppala, *Fast pyrolysis of forest residue. 3. Storage stability of liquid fuel.* Energy & Fuels, 2003. **17**: p. 1075-1084.

61. Fahmi, R., A.V. Bridgwater, I. Donnison, N. Yates, and J.M. Jones, *The effect of lignin and inorganic species in biomass on pyrolysis oil yields, quality and stability.* Fuel, 2008. **87**(7): p. 1230-1240.

62. Oasmaa, A., K. Sipila, Y. Solantausta, and E. Kuoppala, *Quality improvement of pyrolysis liquids: effect of light volatiles on the stability of pyrolysis liquids.* Energy and Fuels, 2005. **19**: p. 2556-2561.

63. Pattiya, A., *Catalytic pyrolysis of agricultural resudues for bio-oil production. PhD Thesis*. 2007, Aston University. School of Chemical Engineering and Applied Chemistry: Birmingham, UK.

64. Pattiya, A., J.O. Titiloye, and A.V. Bridgwater, *Fast pyrolysis of cassava rhizome in the presence of catalysts.* Journal of Analytical and Applied Pyrolysis, 2008. **81**: p. 72-79.

65. Chiaramonti, D., A. Oasmaa, and Y. Solantausta, *Power generation using fast pyrolysis liquids from biomass.* Renewable and Sustainable Energy Reviews, 2005. **11**: p. 1056-1086.

66. Radlein, D., *The production of chemicals from fast pyrolysis bio-oils*, in *Fast pyrolysis of biomass: a handbook*, A.V. Bridgwater, et al., Editors. 1999, CPL Scientific Publishing Services Ltd.: Newbury, UK. p. 164-188.

67. Fahmi, R., A.V. Bridgwater, L.I. Darvell, J.M. Jones, N. Yates, S. Thain, and I.S. Donnison, *The effect of alkali metals on combustion and pyrolysis of Lolium and Festuca grasses, switchgrass and willow.* Fuel, 2007. **86**(10-11): p. 1560-1569.

68. Amen-Chen, C., H. Pakdel, and C. Roy, *Production of monomeric phenols by thermochemical conversion of biomass: a review.* Bioresource Technology, 2001. **79**(3): p. 277-299.

69. Boateng, A.A., K.B. Hicks, and K.P. Vogel, *Pyrolysis of switchgrass (Panicum virgatum) harvested at several stages of maturity.* Journal of Analytical and Applied Pyrolysis, 2006. **75**(2): p. 55-64.

70. Di Blasi, C., *Comparison of semi-global mechanisms for primary pyrolysis of lignocellulosic fuels.* Journal of Analytical and Applied Pyrolysis, 1998. **47**(1): p. 43-64.

71. Yanik, J., C. Kornmayer, M. Saglam, and M. Yüksel, *Fast pyrolysis of agricultural wastes: Characterization of pyrolysis products.* Fuel Processing Technology, 2007. **88**(10): p. 942-947.

72. Lewandowski, I. and A. Kicherer, *Combustion quality of biomass: practical relevance and experiments to modify the biomass quality of Miscanthus x giganteus.* European Journal of Agronomy, 1997. **6**(3-4): p. 163-177.

73. Demirbas, A., *Calculation of higher heating values of biomass fuels.* Fuel, 1997. **76**(5): p. 431-434.

74. Friedl, A., E. Padouvas, H. Rotter, and K. Varmuza, *Prediction of heating values of biomass fuel from elemental composition.* Analytica Chimica Acta, 2005. **544**(1-2): p. 191-198.

75. Oasmaa, A., E. Kuoppala, and Y. Solantausta, *Fast pyrolysis of forestry residue. 2. Physiochemical composition of product liquid.* Energy & Fuels, 2002. **17**: p. 433-443.

76. Yang, H., R. Yan, H. Chen, D.H. Lee, and C. Zheng, *Characteristics of hemicellulose, cellulose, and lignin pyrolysis.* Fuel, 2007. **86**: p. 1781-1788.

77. Zabaniotou, A., O. Ioannidou, E. Antonakou, and A. Lappas, *Experimental study of pyrolysis for potential energy, hydrogen and carbon material production from lignocellulosic biomass.* International Journal of Hydrogen Energy, 2008. **33**: p. 2433-2444.

78. Effendi, A., H. Gerhauser, and A.V. Bridgwater, *Production of renewable phenolic resins by thermochemical conversion of biomass: a review.* Renewable and Sustainable Energy Reviews, 2008. **12**: p. 2092-2116.

79. Fahmi, R., *The characterisation and optimisation of modified herbaceous grasses for identifying pyrolysis-oil quality traits. PhD Thesis.* 2007, Aston University. School of Chemical Engineering and Applied Chemistry: Birmingham, UK.

80. Landau, S., T. Glasser, and L. Dvash, *Monitoring nutrition in small ruminants with the aid of near infrared reflectance spectroscopy (NIRS) technology: A review.* Small Ruminant Research, 2006. **61**(1): p. 1-11.

81. Atienza, S.G., Z. Satovic, K.K. Petersen, O. Dolstra, and A. Martin, *Identification of QTLs influencing agronomic traits in Miscanthus sinensis Anderss. I. Total height, flag-leaf height and stem diameter.* Theoretical and Applied Genetics, 2003. **107**(1): p. 123-129.

82. Greef, J.M., M. Deuter, C. Jung, and J. Schondelmaier, *Genetic diversity of European Miscanthus species revealed by AFLP fingerprinting.* Genetic Resources and Crop Evolution, 1997. **44**(2): p. 185-195.

83. Vansoest, P.J. and R.H. Wine, *Determination of Lignin and Cellulose in Acid-Detergent Fiber with Permanganate.* Journal of the Association of Official Analytical Chemists, 1968. **51**(4): p. 780-&.

84. Anon., *Neutral detergent fibre and NCGD. Gerhardt Guideline Methodology, Method No. GMFC2. 20th Oct., 1998.* 1998a.

85. Anon., *Acid detergent fibre. Gerhardt Guideline Methodology, Method No. GMFC3. 20th Oct., 1998.* 1998b.

86. Channiwala, S.A. and P.P. Parikh, *A unified correlation for estimating HHV of solid, liquid and gaseous fuels.* Fuel, 2002. **81**: p. 1051-1063.

87. ECN, *Phyllis database: Determination of lower heating value (LHV).* 2008, Energy Research Centre of the Netherlands.

88. Friedman, H.L., *Kinetics of thermal degradation of char-forming plastics from thermogravimetry. Application to a phenolic plastic.* Journal of Polymer Science, 1965. **6**: p. 183-195.

89. Fahmi, R., A.V. Bridgwater, S.C. Thain, I.S. Donnison, P.M. Morris, and N. Yates, *Prediction of Klason lignin and lignin thermal degradation products by Py-GC/MS in a collection of Lolium and Festuca grasses.* Journal of Analytical and Applied Pyrolysis, 2007. **80**(1): p. 16-23.

90. Faix, O., I. Fortmann, J. Bremer, and D. Meier, *Thermal degradation products of wood: Gas chromatographic separation and mass spectral characterisation of polysaccharide derived products.* Holz Als Roh-Und Werkstoff, 1991. **49**: p. 213-219.

91. Faix, O., I. Fortmann, J. Bremer, and D. Meier, *Thermal degradation products of wood: A collection of electron-impact (EI) mass spectra of polysaccharide derived products.* Holz Als Roh-Und Werkstoff, 1991. **49**: p. 209-304.

92. Faix, O., D. Meier, and I. Fortmann, *Thermal degradation products of wood: Gas chromatographic separation and mass spectrometric characterisation of monomeric lignin derived compounds.* Holz Als Roh-Und Werkstoff, 1990. **48**: p. 281-285.

93. Faix, O., D. Meier, and I. Fortmann, *Thermal degradation products of wood: A collection of electron-impact (EI) mass spectra of monomeric lignin derived products.* Holz Als Roh-Und Werkstoff, 1990. **48**: p. 351-354.

94. Oasmaa, A. and E. Kuoppala, *Fast pyrolysis of forest residue. 3. Storage stability of liquid fuel.* Energy & Fuels, 2004. **17**: p. 1075-1084.

95. Barnes, R.J., *Near infra-red spectra of ammonia-treated straw and of isolated cell walls.* Animal Feed Science and Technology, 1988. **21**(2-4): p. 209-218.

96. Stone, M., *Cross-validatory choice and assessment of statistical predictions.* Journal of the Royal Statistical Society B, 1974. **36**: p. 111-147.

97. Demirbas, A., *Relationships between lignin contents and heating values of biomass.* Energy Conversion and Management, 2001. **42**(2): p. 183-188.

98. Esteghlalian, A., A.G. Hashimoto, J.J. Fenske, and M.H. Penner, *Modelling and optimisation of the dilute suphuric acid pre-treatment of corn stover, poplar, and switchgrass.* Bioresource Technology, 1996. **59**: p. 129-136.

99. Blummel, M., E. Zerbini, B.V.S. Reddy, C.T. Hash, F. Bidinger, and D. Ravi, *Improving production and utilization of sorghum and pearl millet as livestock feed: methodological problems and possible solutions.* Field Crops Research, 2003. **84**: p. 123-142.

100. Van Herwaarden, A.F., J.F. Angus, R.A. Richards, and G.D. Farquhar, *'Haying-off', the negative grain yield response of dryland wheat to nitrogen fertiliser. II. Carbohydrate and protein dynamics.* Australian Journal of Agricultural Research, 1998. **49**: p. 1083-1094.

101. Reddy, B.V.S., P.S. Reddy, F. Bidinger, and M. Blummel, *Crop management factors influencing yield and quality of crop residues.* Field Crops Research, 2003. **84**: p. 57-77.

102. Powell, J.M. and L.K. Fussell, *Nutrient and structural carbohydrate partitioning in pearl-millet.* Agronomy Journal, 1993. **85**(4): p. 862-866.

103. Hodgson, E.M., S.J. Lister, A.V. Bridgwater, J.C. Clifton-Brown, and I. Donnison, *Genotypic and environmentally derived variation in the cell wall composition of Miscanthus in relation to its use as a biomass feedstock.* Biomass and Bioenergy, Submitted April 2008.

104. de Jong, W., A. Pirone, and M.A. Wojtowicz, *Pyrolysis of Miscanthus Giganteus and wood pellets: TG-FTIR analysis and reaction kinetics*.* Fuel, 2003. **82**(9): p. 1139-1147.

105. Szabo, P., G. Varhegyi, F. Till, and O. Faix, *Thermogravimetric/mass spectrometric characterisation of two energy crops, Arundo donax and Miscanthus sinensis.* Journal of Analytical and Applied Pyrolysis, 1996. **36**: p. 179-190.

106. Alves, A., M. Schwanninger, H. Pereira, and J. Rodrigues, *Analytical pyrolysis as a direct method to determine the lignin content in wood - Part 1: Comparison of pyrolysis lignin with Klason lignin.* Journal of Analytical and Applied Pyrolysis, 2006. **76**(1-2): p. 209-213.

107. Caballero, J.A., R. Font, and A. Marcilla, *Study of the primary pyrolysis of Kraft lignin at high heating rates: yields and kinetics.* Journal of Analytical and Applied Pyrolysis, 1996. **39**: p. 159-178.

108. Del Rio, J.C., A. Gutierrez, J. Romero, M.J. Martinez, and A.T. Martinez, *Identification of residual lignin markers in eucalypt kraft pulps by Py-GC/MS.* Journal of Analytical and Applied Pyrolysis, 2001. **58-59**: p. 425-439.

109. Nonier, M.F., N. Vivas, N. Vivas de Gaulejac, C. Absalon, P. Soulie, and E. Fouquet, *Pyrolysis-gas chromatography/mass spectrometry of Quercus sp. wood: Application to structural elucidation of macromolecules and aromatic profiles of different species.* Journal of Analytical and Applied Pyrolysis, 2006. **75**(2): p. 181-193.

110. Sharma, R.K., J.B. Wooten, V.L. Baliga, X. Lin, W. Geoffrey Chan, and M.R. Hajaligol, *Characterization of chars from pyrolysis of lignin.* Fuel, 2004. **83**(11-12): p. 1469-1482.

111. Kleen, M. and G. Gellerstedt, *Influence of inorganic species on the formation of polysaccharide and lignin degradation products in the analytical pyrolysis of pulps.* Journal of Analytical and Applied Pyrolysis, 1995. **35**(1): p. 15-41.

112. Reeves, J.B. and B.A. Francis, *Pyrolysis-gas-chromatography-mass-spectrometry for the analysis of forages and by-products.* Journal of Analytical and Applied Pyrolysis, 1997. **40-41**: p. 243-266.

113. Alen, R., E. Kuoppala, and P. Oesch, *Formation of the main degradation compound groups from wood and its components during pyrolysis.* Journal of Analytical and Applied Pyrolysis, 1996. **36**: p. 137-148.

114. Girisuta, B., L.P.B.M. Janssen, and H.J. Heeres, *Green chemicals. A kinetic study on the conversion of glucose to levulinic acid.* Chemical Engineering Research and Design, 2006. **84(A5)**: p. 339-349.

115. Fahmi, R., *The characterisation and optimisation of modified herbacious grasses for identifying pyrolysis-oil quality traits. PhD Thesis.* 2007, Aston University. School of Chemical Engineering and Applied Chemistry: Birmingham, UK.

116. Bridgeman, T.G., L.I. Darvell, J.M. Jones, P.T. Williams, R. Fahmi, A.V. Bridgwater, T. Barraclough, I. Shield, N. Yates, S.C. Thain, and I.S. Donnison, *Influence of particle size on the analytical and chemical properties of two energy crops.* Fuel, 2007. **86**(1-2): p. 60-72.

117. Jung, H.J.G., V.H. Varel, P.J. Weimer, and J. Ralph, *Accuracy of Klason lignin and acid detergent lignin methods as assessed by bomb calorimetry.* Journal of Agricultural and Food Chemistry, 1999. **47**(5): p. 2005-2008.